7

Iron and Aluminum Hydroxysulfates from Acid Sulfate Waters

J. M. Bigham

School of Natural Resources
2021 Coffey Road
The Ohio State University
Columbus, Ohio 43210

D. Kirk Nordstrom

U. S. Geological Survey
3215 Marine Street
Boulder, Colorado 80303

Acid sulfate waters are produced mostly by the oxidation of common sulfide minerals such as pyrite, chalcopyrite, pyrrhotite, and marcasite in rocks, soils, sediments, and industrial wastes. This spontaneous process of mineral weathering plays a fundamental role in the supergene alteration of ore deposits, the formation of acid sulfate soils, and the mobilization and release of acidity and metals to surface and ground waters. The purely natural process of "acid rock drainage" is often intensified by human activities related to mining, mineral processing, construction, soil drainage, and dredging. Geochemical reaction rates are accelerated because physical disturbance gives greater exposure of mineral surfaces to air and water, and to microbes that catalyze the reaction process. Large quantities of reactive sulfides are also concentrated and exposed to air as a result of mining and mineral processing. Acid sulfate waters produce a number of fairly insoluble hydroxysulfate and oxyhydroxide minerals that precipitate during oxidation, hydrolysis, and neutralization. The objective of this chapter is to describe the formation, properties, fate, and environmental implications of the nano- to microphase hydroxy-sulfates of Fe and Al that are precipitated from acid sulfate waters. These minerals are commonly of poor crystallinity and difficult to characterize. Much remains to be learned about their occurrence, formation, and properties.

INTRODUCTION TO ACID SULFATE ENVIRONMENTS

Mine drainage

The best known examples of acid sulfate waters are those released from mines where coal and metallic sulfide ores have been exploited (Ash et al. 1951, Barton 1978, Nordstrom 1982a, Rose and Cravotta 1998, Nordstrom and Alpers 1999). There may be as many as 500,000 inactive or abandoned mine sites in the United States alone (Lyon et al. 1993). Although most of these pose no immediate water-quality problem, Kleinmann (1989) estimated that about 19,300 km of streams and more than 72,000 ha of lakes and reservoirs have been seriously damaged by mine effluents. Contamination of natural waters by mine drainage has killed enormous numbers of fish and other aquatic organisms, destroyed natural vegetation, induced massive erosion and sedimentation, caused widespread corrosion of bridge abutments, culverts, roads, and other structures, and made many streams and lakes so turbid as to be unfit for recreational activities.

Most acid mine waters have pH values in the range of 2 to 4 (Nordstrom 1991,

1529-6466/00/0040-0007$05.00 DOI: 10.2138/rmg.2000.40.7

Plumlee et al. 1999). Acid mine drainage occurs when acid production exceeds the buffering capacity of the host rock or the surrounding spoil and soil. In areas where carbonate rocks are available to neutralize acidity, higher pH drainage may be common. Cravotta et al. (1999), for example, reported a bimodal frequency distribution for the pH of a large number of mine drainage waters from the eastern U.S. coal province (Fig. 1). Most samples were either distinctly acidic (pH 2-4) or near neutral (pH 6–7), with relatively few samples having pH values in the range of 4 to 6. A similar distribution is apparent in the data of Plumlee et al. (1999). Neutralization promotes the removal of Fe, Al, and other metals from solution but has a much less noticeable effect on the concentrations of SO_4.

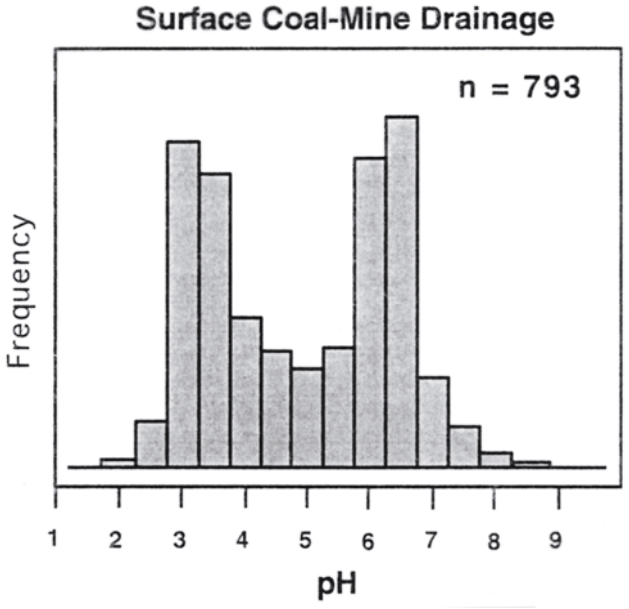

Figure 1. The pH of mine drainage from 793 sites in the eastern U.S. coal province showing a strong bimodal distribution of acid mine drainage and neutral to alkaline mine drainage. (modified from Cravotta et al. 1999).

Precipitates of Fe, Al, and sometimes Mn provide a highly visible means of identifying mine-impacted waters. Those precipitates composed primarily of Fe compounds are yellow-to-red-to-brown in color and have long been referred to as "yellow boy" by North American miners. Acid mine waters rich in Al, on the other hand, typically produce a milky-white precipitate that may be more abundant than is commonly recognized because its color can be masked by associated Fe compounds. These chemical precipitates are environmentally significant because they (1) add to the suspended sediment and bed load of receiving streams, (2) decrease the effective life of wetlands, limestone drains, and ponds constructed for mine drainage abatement, and (3) play a major role in the binding and transport of toxic elements. There have been relatively few quantitative measurements of deposition rates, and published results obviously vary with the chemistry and hydrology of the drainage system. Letterman and Mitsch (1978) observed particulate Fe accumulations of up to 3 g m^{-2} d^{-1} in a Pennsylvania stream receiving mine drainage. Typical Fe loading rates for constructed wetlands range from 0.4 to 250 g· $m^{-2}d^{-1}$ (Brodie et al. 1988, Fennessy and Mitsch 1989). Kirby et al. (1999) noted that a drainage of 10^6 L d^{-1} with an Fe concentration of 25 mg L^{-1} will yield 17 tonnes of "$Fe(OH)_3$" per year. The ability of these precipitates to scavenge metals and oxyanions from solution has been documented in numerous studies (see Singh et al. 1997 for a recent review). This process is so efficient that most contaminant species are transported in particulate form (e.g. Kimball et al. 1995) and any factor influencing the stability of the colloidal precipitates (photoreduction, pH changes, and composition changes) must also have an impact on the availability of sorbed trace elements (McKnight et al. 1988, Fuller and Davis 1989).

Residues from mineral extraction and ore processing

Mineral mining and processing usually result in the production of an extremely large volume of unwanted material. For example, an average metal mine immediately rejects 42% of the total mined material as waste rock (spoil), 52% of the ore is separated at the mill as tailings, 4% leaves the smelter as slag, and only 2% is retained as the commodity for which the ore was extracted (Godin 1991). The unwanted by-products represent a problem not just because of their volume, but because many of them contain chemically reactive sulfide minerals that have a high potential for producing acid sulfate drainage.

Tailings contain large volumes of sand- and silt-sized particles and are usually disposed of by slurry-pumping to an impoundment constructed close to the mill. As mining progresses, the impoundment is commonly increased in height by the construction of retaining dams. Elevated impoundments result in hydraulic loading and water-table mounding so that the impoundments become areas of ground-water recharge unless the impoundment areas are prepared with impermeable liners and dams are constructed from low-conductivity materials. Maintaining water-table depth is a concern because oxygen penetration can lead to accelerated sulfide oxidation and acid generation. Analyses of pore waters in the vadose zone of several Canadian tailings impoundments have shown high concentrations of Fe, Al and trace metals (Blowes and Jambor 1990, Blowes et al. 1998). Chemical discontinuities in the tailings may also give rise to cemented layers or "hardpans" composed of a variety of solid phases. Hardpans or "ferricretes" have formed naturally as well as in mining-impacted areas, commonly where an acid stream reacts with oxygenated soil or sediments. At some sites, these precipitated layers have suppressed the movement of oxygen and dissolved metals through the tailings and have thereby moderated the environmental impact of sulfide oxidation (Blowes et al. 1991).

Waste-rock dumps and tailings impoundments have properties in common; however, important differences also exist. Most waste-rock dumps usually have a much greater height-to-base ratio and contain coarser materials than associated tailings deposits (Ritchie 1994). Moreover, waste rock has not been subject to the processes of ore beneficiation that typically include crushing, sizing, and concentration of the desired ore mineral(s) through flotation, magnetic, and gravity processes. Waste-rock dumps are frequently unsaturated systems, so the chemical environment is heterogeneous and wide ranges in temperature, gas composition, and solution chemistry are common. The oxidation of iron sulfides is the primary mechanism for generating pollution in both tailings and waste rock environments, but drainage from the toe of a waste-rock dump provides only an integrated estimate of processes occurring within the pile (Ritchie 1994). Pyrite and pyrrhotite oxidize by an exothermic reaction that can generate air temperatures of 50 to 65° C in waste-rock piles (Cathles 1994). Higher temperatures of more than 220° C in underground massive sulfide mines (Wright 1906), and more than 530° C at nearly 300-m depth at the Mt. Isa sulfide deposits, Australia, have been documented (Ninteman 1978). Thermal gradients from heat generation cause convective air flow which can then become an important oxygen-supply mechanism (Ritchie 1994).

Rock weathering

Sulfide oxidation occurs in the absence of mining or land disturbance and numerous instances of naturally acidic waters containing high concentrations of sulfate and metals have been documented (Runnells et al. 1992, Posey et al. 2000, Mast et al. 2000, Yager et al. 2000). Other examples include streams (Theobald et al. 1963, Schwertmann et al. 1995) and lakes (Childs et al. 1997) receiving drainage from sulfide-bearing rocks, as well as craters (Rowe et al. 1992), fumaroles, and hot springs in active geothermal areas (Tkachenko and Zotov 1982). The H_2SO_4 associated with volcanic activity may be

derived by oxidation of magmatic gases (H_2S and SO_2) or elemental sulfur oxidation (Nordstrom et al. 1997) rather than metal sulfides. Not all acid rock drainage is recent in origin. For example, ancient deposits of ferricretes in the Rocky Mountains indicate that the discharge of acidic, metal-bearing waters has occurred over thousands of years in response to the weathering and oxidation of exposed sulfide ore bodies (Furniss et al. 1999). The ferricrete is cemented by iron oxyhydroxide and hydroxysulfate minerals and occurs as aprons around acidic springs and as remnants of ancient stream terraces.

The existence of gossans and related ferricretes on Earth as aqueous weathering products has been used as evidence for similar episodes of weathering on Mars under an earlier climatic regime that was presumably both warmer and wetter (Burns 1988). Spectroscopic analyses, coupled with data from the Viking and Pathfinder missions, have provided much information about the surface materials on Mars (Morris et al. 2000). The data suggest that many of the Martian bright regions are covered by ferricretes and fine-grained "soil" rich in sili cates and nanophase Fe minerals. The LANDER data (Clark et al. 1982, Rieder et al. 1997) have also revealed relatively high concentrations of S (7% SO_3) in Martian soil as compared to local rocks (<1% SO_3). Burns (1994) suggested that permafrost exists beneath the martian regolith and that iron oxides and hydroxysulfates were precipitated in equatorial regions of Mars where seepages of saline meltwaters were once exposed to the atmosphere. These meltwaters are generally thought to have been acidic (Clark and Van Hart 1981) and might therefore have been similar to acid sulfate waters on Earth. The proposed iron hydroxysulfate precipitates also have spectral characteristics comparable to those of terrestrial analogs that can be formed both by biotic and abiotic processes (Bishop and Murad 1996). The possible existence of water and biominerals on Mars has been used as a logical indicator of exobiology (Bishop 1998).

Acid sulfate soils (cat clays)

Wet, sulfidic soils that become hyperacid with drainage have been recognized for many years (Bloomfield and Coulter 1973, Van Mensvoort and Dent 1998). The famous plant taxonomist, Linnaeus (1735), described *argilla vitriolacea* (clay with sulfuric acid) in European swamps and developed a classification system for Dutch soils that included *argilla mixta fusca, vitriolica salsa* (mixed brown clays with the taste of salts from sulfuric acid). Areas of acid sulfate soils were produced by drainage of the great Haarlemmermeer polder in 1852, and such areas came to be known as katteklei (cat clay) (Pons 1973, Bloomfield 1972). "Cat" was used in the Dutch vernacular to indicate harmful, mysterious qualities (Fanning and Burch 1997), and "cat clay" was associated with the excrement of cats (Westerveld and van Holst 1973). Dent and Pons (1995) succinctly described acid sulfate soils as "the nastiest soils in the world" and noted that their evil reputation is derived from an unusual combination of properties, including odd colors, foul odors, stunted vegetation, and rapid chemical deterioration following drainage (Fig. 2). Modern drainage systems designed to reclaim swamps and wetlands to exploit their anticipated fertility for agricultural production have, in some cases, laid waste large areas underlain by sulfidic materials. Not only have local farmers suffered from the development of acid sulfate conditions but water pollution and damage to fisheries have also occurred over wide areas in some coastal regions. Ochre from the oxidation products of acid sulfate weathering often reduces the capacity of drain lines (Bloomfield 1972, Trafford et al. 1973, Fanning et al. 1993) and may inadvertently slow the acidification process by halting efficient drainage.

Most acid sulfate soils have developed from sulfidic deposits accumulated under mangroves and reedswamps in tidal areas where abundant organic matter and the

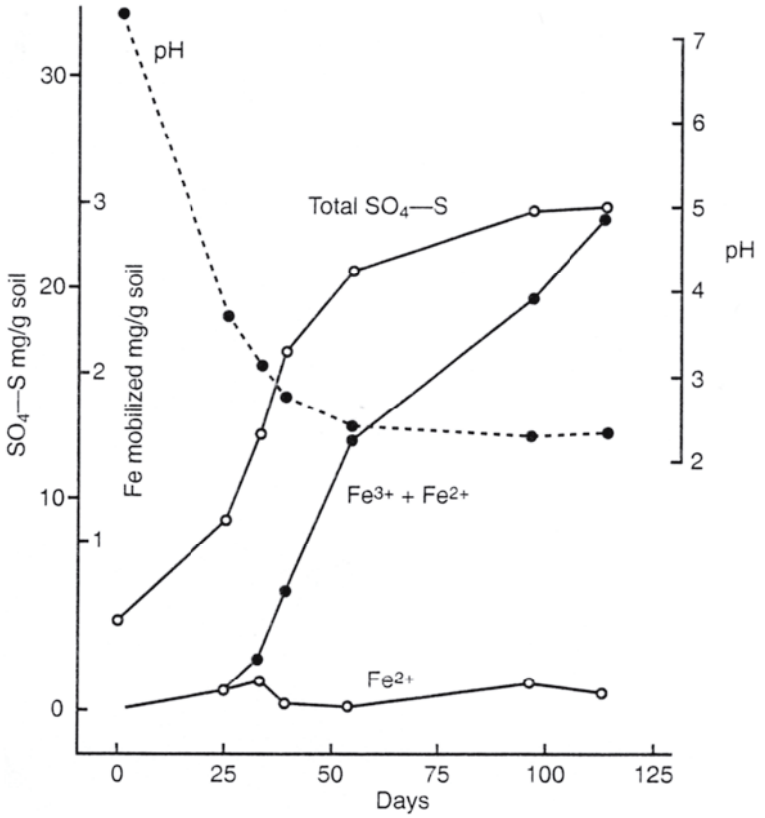

Figure 2. Changes in pH and the concentrations of SO_4^{2-} and Fe in the pore-waters of a green-colored soil containing pyrite after exposure to oxidation (modified from Trafford et al. 1973).

constant accretion of sulfate from seawater stimulate the activity of sulfate-reducing bacteria to produce FeS and FeS_2. Concentrations of up to 15 wt % FeS_2 have been reported. Extensive areas of such sediments are found in Indonesia, Indochina, the Guyanas, the Orinoco Delta, west Africa, and northern Australia (Dent and Pons 1995). It has been estimated that there are some 12-14 million ha of soils in Holocene coastal plains and tidal swamps where the topsoil is severely acid or will become so if drained (van Breeman 1980). There may be twice this area of sulfidic materials covered by thin veneers of alluvium or peat that could easily be removed through erosion or oxidation. Some Holocene sediments have been drained naturally by isostatic rebound, tectonic uplift, or through changes in delta distribution systems; however, most acid sulfate soils are clearly the result of artificial drainage.

Unusual but significant areas of saline-sulfidic soils have formed in the rolling uplands of South and West Australia in response to rising saline ground waters from the extensive removal of native *Eucalyptus* forests over the past century (Fitzpatrick et al. 1992, 1996; Fitzpatrick and Self 1997). Waterlogging and the formation of sulfidic materials occur during the wet winter months and are followed by oxidation and acidification during the dry summer months. The result is a cancerous growth of barren, red scalds across the landscape.

Much has been written about soil formation in mine spoils, rock tailings, and dredged materials around the globe. Many of these constructed soils may qualify as acid sulfate depending on the character of the waste material. Numerous studies have been dedicated to halting the acidification process and modifying root-zone chemistry to

enable the establishment of higher plants for erosion control and agronomic production. Efforts include re-soiling with borrowed soil material, treatment with bactericides, and the addition of alkaline amendments (agricultural limestone, alkaline coal-combustion by-products, cement-kiln dusts) or organic wastes (yard waste compost, sewage sludge, paper-mill sludge, etc.). The reader is referred to a comprehensive review by Barnhisel et al. (2000) of current technology for managing disturbed lands.

Because of their ability to create extreme agricultural and environmental problems, acid sulfate soils are given special recognition in many soil classification systems. Soils containing sulfide minerals that can oxidize to form sulfuric acid under appropriate conditions are commonly referred to, in the U.S., as potential acid sulfate soils (Fanning and Burch 1997) or in Europe as "unripe" sulfidic soils (Dent and Pons 1995). Active or "raw" acid sulfate soils are recognized by acid drainage waters and by the appearance of straw-yellow accumulations of jarosite in the soil profile (Schwertmann 1961, van Breemen and Harmsen 1975, Öborn and Berggren 1995), both of which indicate active oxidation of sulfides above the local ground water. Materials in which the sulfides have been completely oxidized may be described as post-active or "ripe" acid sulfate soils. Most of these soils have conspicuous red mottles and may still be very acid with high concentrations of soluble Al.

FORMATION OF ACID SULFATE WATERS AND ASSOCIATED WEATHERING PRODUCTS OF FE AND AL

Pyrite (cubic FeS_2) and pyrrhotite or other ferrous sulfide phases such as chalcopyrite, arsenopyrite, greigite, and mackinawite are the most abundant Fe sulfide minerals in nature, and their decomposition is essential to obtain the conditions and products needed for the formation of iron and aluminum weathering compounds, including hydroxysulfate minerals. Pyrrhotite and ferrous sulfide phases are more reactive than pyrite (Bhatti et al. 1993, 1994; Jambor 1994). Reactivity, however, largely depends on grain size. Field and laboratory studies have largely focused on pyrite oxidation to understand the mechanism by which acid sulfate waters are generated. The weathering of pyrite is commonly described by the single, incongruent reaction given in Equation (1); however, this reaction is a gross oversimplification. As has been noted by Nordstrom (1982a, 2000) and Nordstrom and Alpers (1999), pyrite decomposition is a complex biogeochemical process involving hydration, hydrolysis, and oxidation reactions as well as microbial catalysis. Oxidation rates are dependent on temperature, pH, Eh, relative humidity, and the surface area of reactant pyrite.

$$\underset{\text{(pyrite)}}{FeS_{2(aq)}} + 3.75\ O_{2(g)} + 3.5\ H_2O_{(l)} \leftrightarrow Fe(OH)_{3(s)} + 2\ H_2SO_{4(aq)} \qquad (1)$$

The Fe system

Reaction (1) demonstrates that oxygen and water provide the ultimate driving force for pyrite oxidation, that both the sulfur and the ferrous iron in pyrite are subject to oxidation, and that final products include an insoluble form of oxidized Fe and sulfuric acid. However, the complexity of possible solid-phase weathering products represented generically by $Fe(OH)_3$ is not depicted. Nor does the reaction indicate the important role of chemolithotrophic Fe- and S-oxidizing bacteria, the effect of the semi-conducting pyrite surface on intermediate reactions, or the role of intermediate sulfoxyanions.

The best known of the chemoautotrophic bacteria catalyzing pyrite oxidation, *Thiobacillus ferrooxidans*, oxidizes both Fe and S over the pH range 1.0 to 3.5. *Leptospirillum ferrooxidans*, an Fe-oxidizer, is now thought to play an important role in the oxidative dissolution of iron sulfide minerals at very low pH (Sand et al. 1992,

Schrenk et al. 1998, Rawlings et al. 1999). A third species, *Thiobacillus thiooxidans*, oxidizes S only. These acidophilic bacteria require only O_2, CO_2, a reduced form of Fe and/or S, and minor N and P for their metabolism. They produce enzymes that catalyze the oxidation reactions and use the energy released from these processes to transform inorganic carbon into cellular material (Gould et al. 1994). A newly described Fe-oxidizing Archaeon, *Ferroplasma acidarmanus*, has been found at Iron Mountain at elevated temperatures (40° C) and low pH (0.7, Edwards et al. 2000). Microbial diversity probably enhances the oxidation of pyrite relative to that accomplished by a single species.

The importance of bacterial oxidation becomes apparent when Reaction (1) is considered as the composite of a sequence of reactions (Fig. 3). It is thought that pyrite weathering is initiated by oxygen and water (Eqn. 1.1 of Fig. 3) because circumneutral pH values are not conducive to the activity of acidophilic microorganisms; however, the literature also indicates controversy regarding the role of bacteria in propagating this reaction. In complex natural systems, it seems logical that an interplay of chemical and biological processes may occur on a microscale (Nordstrom and Alpers 1999). Thus, it is entirely possible that extremely acid conditions might develop adjacent to pyrite grain surfaces before changes in pore water chemistry are detected. Under such conditions, measurements of bulk-water chemistry are highly unlikely to reflect the chemistry at the surface of the pyrite. It is also possible that neutrophilic *Thiobacilli* may catalyze the initial stage of pyrite oxidation (Blowes et al. 1995, 1998).

Nordstrom and Alpers (1999) summarized available data from McKibben and

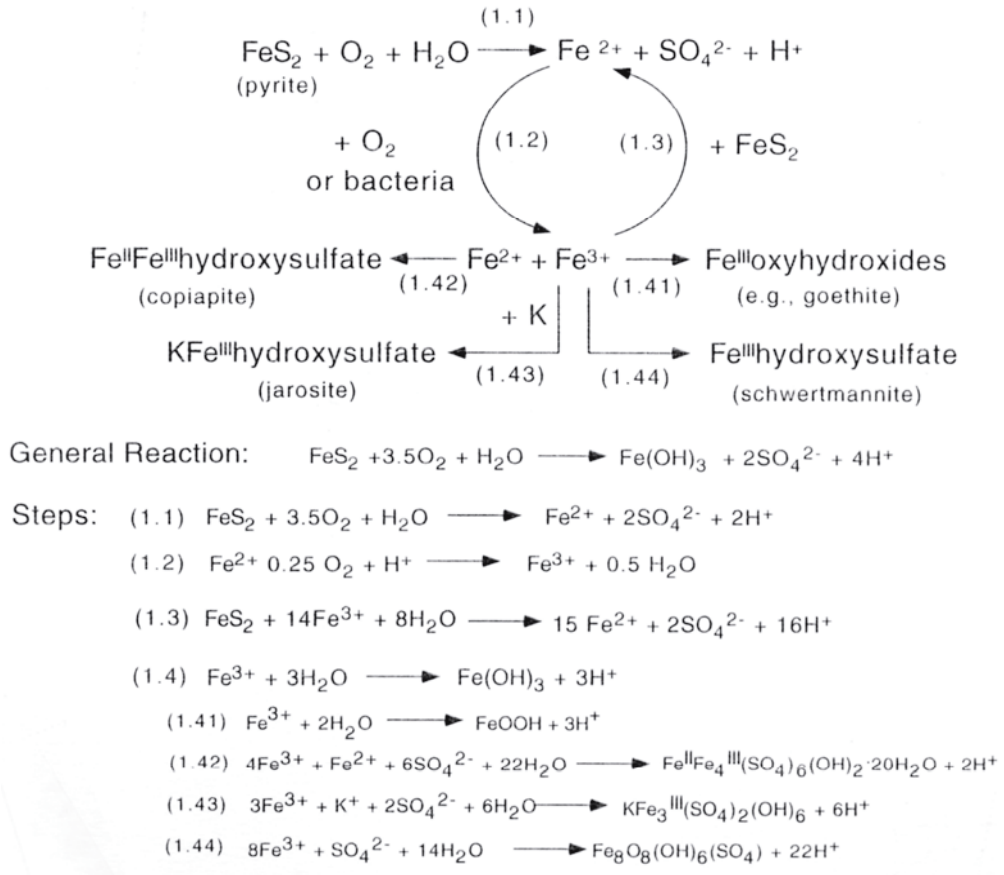

Figure 3. Schematic diagram showing the "steps" in pyrite oxidation and possible secondary Fe minerals that may form as weathering products (modified from Rose and Cravotta 1998).

Barnes (1986) and Olson (1991) for abiotic vs. microbial rates of pyrite oxidation under comparable conditions and concluded that the rates are similar at about 10^{-8} mol m^{-2} s^{-1}. As suggested by these units, oxidation rates are dependent on the surface area of pyrite exposed to solution as well as the crystallinity and structure of the pyrite surface (McKibben and Barnes 1986). The high surface area of the raspberry-like clusters of pyrite grains (framboidal pyrite) found in many sedimentary rocks at least partly accounts for their observed reactivity (Carrucio 1975). Hammack et al. (1988) observed that sedimentary pyrite was more reactive than could be explained by surface area alone, and suggested that the cause was a difference in crystal structure or the frequency of surface defects.

The S moiety in pyrite oxidizes more quickly than Fe giving rise to aqueous solutions enriched with SO_4^{2-}, H^+, and Fe^{2+}. Intermediate sulfoxyanions of lower oxidation state, such as sulfite (SO_3^{2-}), thiosulfate ($S_2O_3^{-}$), and polythionates ($S_nO_6^{2-}$), may also form but are subject to rapid oxidation by pyrite (Xu and Schoonen 1995), ferric iron (Williamson and Rimstidt 1993), or biodegradation (Luther 1990, Gould et al. 1994). A summary of the current research on the catalytic effect of the pyrite surface and of Fe^{3+} on intermediate sulfoxyanions (thiosulfate, polythionates, sulfite) formed during pyrite oxidation can be found in Nordstrom (2000). Several studies have confirmed that these highly efficient catalysts rapidly degrade intermediate sulfoxyanions to sulfate and that these species are not likely to be detected in acid mine waters.

Ferrous iron released in the initial stage of pyrite decomposition is also subject to oxidation (Eqn. 1.2 of Fig. 3). It is well known that the abiotic oxidation of Fe^{2+} proceeds rapidly above pH 4 and that the rate is pH dependent (Fig. 4). At lower pH values, the rate becomes very slow and is independent of pH. Singer and Stumm (1968), for example, calculated a rate of 2.7×10^{-12} mol L^{-1} s^{-1} at pH values below 4. They found that acidophilic, Fe-oxidizing bacteria increased the oxidation rate by 10^5 to about 3×10^{-7} mol L^{-1} sec^{-1} (Singer and Stumm 1970). The importance of this difference in reaction rates at low pH is related to the fact that dissolved Fe^{3+} rapidly oxidizes pyrite according to the stoichiometry shown in Equation 1.3 of Figure 3. The reaction is considerably faster than when oxygen is the oxidant (Fig. 4); however, significant concentrations of Fe^{3+} only occur at low pH due to the low solubility of hydrolyzed ferric iron at pH > 4. Without active bacterial populations to ensure the production of Fe^{3+}, the process of pyrite oxidation would proceed very slowly because the abiotic rate of Fe^{2+} oxidation at low pH is substantially slower than the rate of pyrite oxidation by Fe^{3+} (Fig. 4). For this

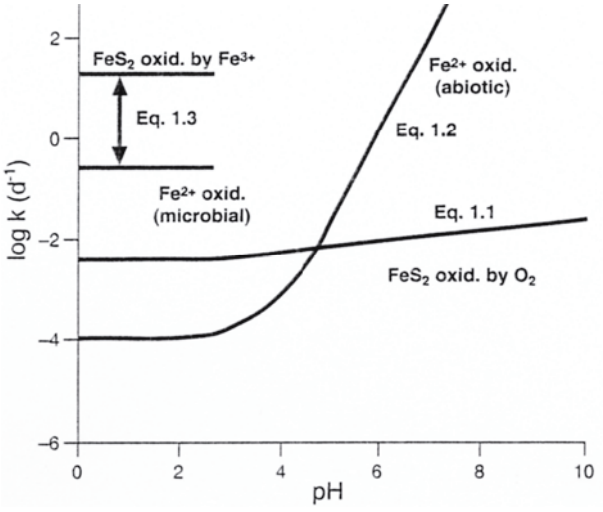

Figure 4. Comparison of rate constants for pyrite oxidation by O_2 (Eqn. 1.1 in Fig. 3) and Fe^{3+} (Eqn. 1.3 in Fig. 3) and the abiotic (Eqn. 1.2 in Fig. 3) and biotic oxidation of Fe^{2+} (modified from Nordstrom 1982a).

reason, Equation (1.2) of Figure 3 has frequently been described as the rate-limiting step in pyrite oxidation (Singer and Stumm 1970). When pyrite oxidation reaches an advanced stage, Fe is aggressively cycled between reduced and oxidized forms as a result of pyrite oxidation by Fe^{3+} and bacterial oxidation of Fe^{2+} (Fig. 3) (Kleinmann et al. 1981). The system approaches a steady state unless pyrite is consumed or the cycle of Fe oxidation-reduction is somehow broken.

Natural systems are "leaky" and Fe is eventu ally released to the environment either in reduced or oxidized form depending on the local pH and Eh. Equation (1.4) of Figure 3 suggests that the final repository for Fe is as an insoluble form of iron oxide or oxyhydroxide. Equation (1.4) does not reflect the multitude of possible intermediates that may be produced (Table 1; Alpers et al 1994). For example, soluble iron-sulfate minerals may precipitate directly from acid sulfate waters in virtually all climates during dry periods, especially at the interface between saturated and unsaturated zones, at which evaporation leads to an accumulation of dissolved species (Eqn. 1.1 of Fig. 3). As these waters become progressively more concentrated, salts accumulate in surface efflorescences reminiscent of those formed in closed drainage basins in arid environments. Melanterite ($FeSO_4 \cdot 7H_2O$), rozenite ($FeSO_4 \cdot 4H_2O$), and szomolnokite ($FeSO_4 \cdot H_2O$) are probably the most common of the efflorescent Fe sulfate minerals. With partial oxidation, they may be converted to soluble hydroxysulfates such as copiapite [$Fe^{II}(Fe^{III})_4(SO_4)_6(OH)_2 \cdot 20H_2O$]. Copiapite may also precipitate directly from acid sulfate

Table 1. Selected sulfates and hydroxysulfates of Fe and Al

Fe Mineral	*Formula*	*Al Mineral*	*Formula*
	Soluble		
melanterite	$Fe^{II}SO_4 \cdot 7H_2O$		
siderotil	$Fe^{II}SO_4 \cdot 5H_2O$		
rozenite	$Fe^{II}SO_4 \cdot 4H_2O$		
szomolnokite	$Fe_{II}SO_4 \cdot H_2O$		
copiapite	$Fe^{II}Fe_4^{III}(SO_4)_6(OH)_2 \cdot 20H_2O$	aluminocopiapite	$Al_{2/3}Fe^{III}_4(SO_4)_6(OH)_2 \cdot 20H_2O$
römerite	$Fe^{II}Fe_2^{III}(SO_4)_4 \cdot 14H_2O$	halotrichite	$Fe^{II}Al_2(SO_4)_4 \cdot 22H_2O$
coquimbite	$Fe_2^{III}(SO_4)_3 \cdot 9H_2O$	pickeringite	$MgAl_2(SO_4)_4 \cdot 22H_2O$
rhomboclase	$(H_3O)Fe^{III}(SO_4)_2 \cdot 3H_2O$	alunogen	$Al_2(SO_4)_3 \cdot 17H_2O$
fibroferrite	$Fe^{III}(SO_4)(OH) \cdot 5H_2O$	jurbanite	$Al(SO_4)(OH) \cdot 5H_2O$
amarantite	$Fe^{III}(SO_4)(OH) \cdot 3H_2O$		
butlerite	$Fe^{III}(SO_4)(OH) \cdot 2H_2O$		
	Less Soluble		
jarosite	$KFe_3^{III}(SO_4)_2(OH)_6$	alunite	$KAl_3(SO_4)_2(OH)_6$
natrojarosite	$NaFe_3^{III}(SO_4)_2(OH)_6$	natroalunite	$NaAl_3(SO_4)_2(OH)_6$
hydronium jarosite	$(H_3O)Fe_3^{III}(SO_4)_2(OH)_6$		
schwertmannite	$Fe_8^{III}O_8(SO_4)(OH)_6$	basaluminite	$Al_4(SO_4)(OH)_{10} \cdot 4H_2O$
		aluminite	$Al_2(SO_4)(OH)_4 \cdot 7H_2O$

waters as suggested by Equation (1.42) of Figure 3; however, there appears to be little field evidence for this mechanism of formation (Jambor et al., this volume). Rapid dissolution of accumulated soluble salts during subsequent rainfall events may release stored acidity and produce major "pulses" of contaminants, often with severe consequences for downstream ecosystems.

As the Fe in acid sulfate waters becomes fully oxidized, it eventually reaches saturation with respect to a variety of less soluble oxides, oxyhydroxides, and hydroxysulfate minerals that comprise the ochreous precipitates found in many streams and lakes impacted by mine drainage. The hydrolysis reactions giving rise to these minerals generate additional acidity (Eqns. 1.41–1.44 of Fig. 3) and are often responsible for suppressing the pH even after acid sulfate solutions are mixed with waters of higher alkalinity. The most common oxides and oxyhydroxides include goethite (α-FeOOH), lepidocrocite (γ-FeOOH) and ferrihydrite (nominally $Fe_5HO_8 \cdot H_2O$), each of which seems to occupy a specific geochemical niche (Bigham 1994). A comprehensive treatment of the structure, properties, and occurrence of these minerals was reported by Cornell and Schwertmann (1996) and Jambor and Dutrizac (1998).

Jarosite, $[K,H_3O,Na]Fe_3(SO_4)_2(OH)_6$ (Eqn. 1.43), is a straw-yellow mineral that is common in the weathered zone of sulfide ore deposits and in acid sulfate soils. Speciation-saturation analyses of low-pH surface waters high in sulfate commonly indicate supersaturation with respect to this mineral (e.g. Chapman et al. 1983, Filipek et al. 1987). Supersaturation and the infrequent detection of jarosite suggest that kinetic barriers may prevent its rapid precipitation from most surface waters. More details concerning the properties and geochemistry of the jarosite-group minerals are presented by Dutrizac and Jambor (this volume) and by Stoffregen et al. (this volume). Schwertmannite $[Fe_8O_8(OH)_6SO_4]$ is a less soluble hydroxysulfate mineral that is a much more common phase than jarosite in ochre deposits from acid sulfate solutions. Later sections of this chapter include descriptions of schwertmannite and its Al analog(s).

The Al system

The primary source of soluble Al in acid sulfate waters is the same as in most natural weathering environments, namely, various aluminosilicates that are subject to proton attack and dissolution as typified by Reaction (2) for K-feldspar:

$$\underset{\text{(K-feldspar)}}{KAlSi_3O_{8(s)}} + 4\,H^+_{(aq)} + 4\,H_2O_{(l)} \leftrightarrow Al^{3+}_{(aq)} + 3\,Si(OH)_4{}^0_{(aq)} + K^+_{(aq)} \quad (2)$$

Such minerals occur in spoil and tailing deposits as gangue material and also comprise the matrix of most soils and sediments. The release of Al and Si from host aluminosilicates is not directly mediated by bacterial processes; however, leaching studies of ore samples have shown that rates are clearly enhanced in inoculated specimens due to the accelerated generation of sulfuric acid by microbially-mediated pyrite oxidation (Bhatti et al. 1994) (Fig. 5).

Because monosilicic acid (Reaction 2) is a very weak acid, it can be removed from the system by simple leaching. The Al component, on the other hand, is usually conserved as a solid phase through the formation of gibbsite or kaolinite.

$$KAlSi_3O_{8(s)} + H^+_{(aq)} + 7\,H_2O_{(l)} \leftrightarrow \underset{\text{(gibbsite)}}{Al(OH)_{3(s)}} + 3\,Si(OH)_4{}^o_{(aq)} + K^+_{(aq)} \quad (3)$$

$$KAlSi_3O_{8(s)} + H^+_{(aq)} + 4.5\,H_2O_{(l)} \leftrightarrow 0.5\,\underset{\text{(kaolinite)}}{Al_2Si_2O_5(OH)_{4(s)}} + 2\,Si(OH)_4{}^o_{(aq)} + K^+_{(aq)} \quad (4)$$

Due to Reactions (3) and (4), the concentration of dissolved Al in most natural

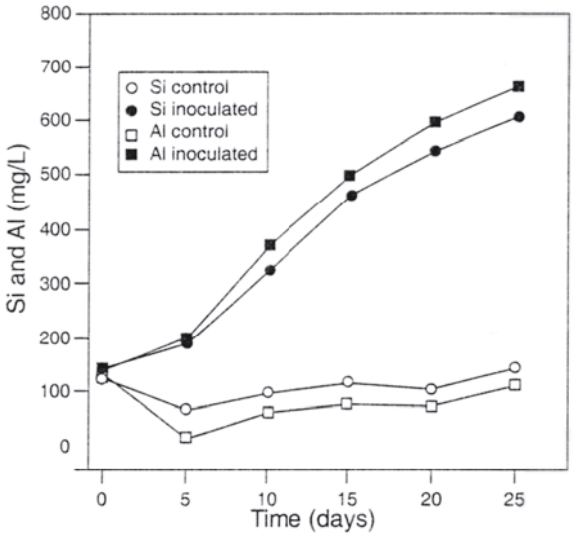

Figure 5. Changes in soluble Al and Si concentrations during the oxidative dissolution of a black schist ore by a mixed culture of Fe- and S-oxidizing thiobacilli as compared to non-inoculated controls (modified from Bhatti et al. 1994).

waters is low (10^{-5} to 10^{-8} M) so long as the pH is near neutral and the concentration of strong complexing agents, such as organic acids, is not significant (Nordstrom 1982b). In most acid systems, such as highly weathered soils, the activity of soluble Al is controlled by the solubilities of gibbsite and kaolinite. In acid sulfate waters, however, the geochemistry of Al is significantly modified by sulfate so that gibbsite and kaolinite are probably not the most stable phases. Instead, a variety of soluble sulfate and insoluble hydoxysulfate minerals may form. Studies of efflorescences from coal deposits and dumps have identified halotrichite [$Fe^{II}Al_2(SO_4)_4 \cdot 22H_2O$], pickeringtite [$MgAl_2(SO_4)_4 \cdot 22H_2O$], aluminocopiapite [$Al_{2/3}Fe^{III}_4(SO_4)_6(OH)_2 \cdot 20H_2O$], and alunogen [$Al_2(SO_4)_3 \cdot 17H_2O$] as common alteration products from pyrite oxidation (Zodrow and McCandlish 1978) (Table 1). When acid sulfate solutions containing dissolved Al are mixed with waters of higher pH, or are buffered to higher pH by carbonate minerals, insoluble hydroxysulfates form by reactions analagous to those in the Fe^{III} system (Reactions 5 and 6).

$$3\ Al^{3+}_{(aq)} + K^{+}_{(aq)} + 2\ SO_4^{2-}{}_{(aq)} + 6\ H_2O_{(l)} \leftrightarrow \underset{\text{(alunite)}}{KAl_3(SO_4)_2(OH)_{6(s)}} + 6\ H^{+}_{(aq)} \qquad (5)$$

$$4\ Al^{3+}_{(aq)} + SO_4^{2-}{}_{(aq)} + 14\ H_2O_{(l)} \leftrightarrow \underset{\text{(basaluminite)}}{Al_4(SO_4)(OH)_{10} \cdot 4H_2O_{(s)}} + 10\ H^{+}_{(aq)} \qquad (6)$$

Alunite has been observed in naturally acidic, hypersaline lakes (Alpers et al. 1992, Long et al. 1992), and it is commonly found in volcanic regions where hydrothermal alteration has occurred (Hemley et al. 1969, Raymahashay 1968). Alunite does not appear to be a major component of the white precipitates that are formed at some localities by mixing and dilution of acid sulfate waters at low temperature (e.g. Theobald et al. 1963) but it has been found in a mixing zone at Doughty Springs, Colorado (Nordstrom et al. 1984). Most aluminous precipitates have the composition of basaluminite (Nordstrom et al. 1984, Alpers et al. 1994) but are very poorly crystalline so that structural details are lacking. The precipitates, however, do not form unless the pH is nearly 5.0 or higher because the pK_1 for Al hydrolysis is 5.0 (Nordstrom and May 1996). For pH values much less than 5.0, dissolved Al behaves as a conservative constituent, whereas above a pH of 5.0 Al becomes highly insoluble and maintains an apparent solubility corresponding to that of microcrystalline to amorphous gibbsite in surface water (Nordstrom and Ball 1986, Nordstrom and Alpers 1999) even though the precipitate is an apparently amorphous basaluminite.

FE AND AL HYDROXYSULFATES OF LOW CRYSTALLINITY

Schwertmannite [$Fe_8O_8(OH)_6SO_4 \cdot nH_2O$]

Schwertmannite, first described from an occurrence at Pyhä salmi, Finland (Bigham et al. 1994), is probably the most common direct precipitate of Fe from acid sulfate waters in the pH range of 2 to 4 (Bigham et al. 1992); however, its existence has been viewed with caution because it is poorly crystalline, is metastable, and is commonly admixed with other nanophase Fe minerals. The mineralogical history of schwertmannite is interesting and reflects the difficulties encountered when attempting to define the properties of materials with short-range structural order (Murad et al. 1994). A brief summary follows.

Mineralogical history. E.F. Glocker (1853) published a report characterizing a "new ferric sinter" that was rich in sulfate and derived from dripstones in the medieval Alt-Hackelsberg silver and gold mine near Zlaté Hory, The Czech Republic. The morphology of the dripstones, some reaching over 1 m in length, was described in a succeeding paper (Glocker 1858). Glocker (1853) suggested the material was a new hydrous ferric sulfate, and it was subsequently named glockerite by Naumann (1855). Cornu (1909) expressed the view that glockerite was not a new mineral but rather limonite with adsorbed sulfate. Glockerite was given the approximate formula $Fe_4^{III}(SO_4)(OH)_{10} \cdot 1\text{-}3H_2O$ by Palache et al. (1951). Fojt (1975) revisited the type location identified by Glocker, photographed the dripstones, and obtained new samples for chemical and mineralogical analysis. He noted that the dripstones always originated from portions of the ore that were rich in pyrite and that the infiltrating water was strongly acid (pH 1.5-4.5). Chemical analyses of five samples yielded Fe/S ratios in the range of 5.4 to 8.2 and infrared spectra showed clear evidence of SO_4 absorption features. X-ray diffraction patterns gave no measurable peaks, but thermal analyses produced an exothermic effect thought to indicate recrystallization of lepidocrocite to maghemite. Fojt (1975) concluded that glockerite was cryptocrystalline lepidocrocite with variable amounts of water and "unstable" sulfate content, and the name glockerite was discredited by the IMA. At about the same time, Margulis et al. (1975, 1976) prepared and characterized an "amorphous" basic sulfate by the hydrolytic precipitation of Fe^{III} from the $Fe_2(SO_4)_3$–KOH–H_2O system at various temperatures. The amorphous precipitate had the approximate composition $2Fe_2O_3 \cdot SO_3 \cdot nH_2O$ and, depending on the synthesis conditions, was associated with jarosite or goethite. Its thermal and infrared properties were similar to those reported by Fojt (1975). Flynn (1990) prepared a "dense amorphous basic ferric sulfate," or DABS, by neutralizing a ferric sulfate solution with a sodium bicarbonate solution. He found that the material, when carefully washed, gave a consistent formula of $Fe_4(OH)_{10}SO_4 \cdot 2\text{-}3H_2O$ and converted to goethite in 8 to 12 days at 25° C. He observed, like Bigham et al. (1996b) when dissolving schwertmannite, that Fe(III) concentrations first increased then decreased during the conversion to goethite. Spectroscopic data, however, were either lacking or inadequate to further characterize this material.

Lazaroff et al. (1982, 1985) conducted infrared (IR) and scanning electron microscope (SEM) studies of ferruginous sediments that had formed through the oxidation of acid, ferrous sulfate solutions by resting suspensions of *T. ferrooxidans* in the laboratory. Jarosites were produced when the $FeSO_4$ solutions contained Na, K, or NH_4 and an excess of sulfate at pH 2.5. Without these cations, an "amorphous" ferric hydroxysulfate was produced that was indistinguishable from precipitates collected from acid mine waters. Mössbauer analyses of similar synthetic precipitates led Murad (1988a) to conclude that the "amorphous" material was a well-crystallized ferrihydrite. Brady et al. (1986) studied the mineralogy of an ochreous sediment isolated from a stream receiving

acid mine drainage and determined that it consisted of nanophase goethite and another poorly crystalline phase that yielded an X-ray diffraction profile with characteristics of both ferrihydrite and feroxyhite (δ′-FeOOH). Precipitates from other localities were collected and characterized (Bigham et al. 1990), and data from the purest specimens of this "mine drainage mineral" were used to support the recognition of schwertmannite as a new mineral. The proposal was submitted without knowledge of the prior work by Glocker (1853, 1858) or Fojt (1975) which had been responsible for the recognition and discrediting, respectively, of glockerite as a mineral. Eventually, samples of "glockerite" were obtained, matched with schwertmannite, and the historical record was clarified (Schwertmann and Fojt 1996). Schwertmannite now stands as the accepted name for this poorly crystalline ferric hydroxysulfate.

Geochemical history. A multitude of laboratory studies have made some form of ferric hydroxide or hydrous ferric oxide (HFO) by numerous pathways (see Fox 1988a). A few of these are worth mentioning because they have a bearing on the formation of minerals such as schwertmannite. The first definitive chemical study on the solubility and stability relations of Fe hydroxysulfate minerals, for a range of sulfuric acid concentrations, was the classic paper of Posnjak and Merwin (1922). The solubility data in this study were for more soluble salts than schwertmannite and temperatures of 60° C and higher, but a supplemental report (Merwin and Posnjak 1937) made some extrapolations to 30° C. One of the first studies to clarify the solubility of freshly precipitated HFO was reported by Biedermann and Schindler (1957). They showed that a goethite equilibrium solubility behavior is obeyed ($Fe^{3+}/H^{+} = 1/3$) if ferric perchlorate solutions are used in a constant ionic medium of 3 M $NaClO_4$ and the precipitates are allowed to age for about 200 hours. When a NaCl medium of 0.5 M ionic strength is used, the goethite dissolution stoichiometry is not obeyed and a precipitate of composition $Fe(OH)_{2.7}Cl_{0.3}$ is formed (Biedermann and Chow 1966). Matijevic and Janauer (1966) noted the complexities of Fe colloid formation and were able to produce very uniform colloids of hydronium and other jarosites at 98° C (Matijevic et al. 1975). Several titration studies involving the hydrolysis of soluble Fe(III) salts indicated the incorporation of chloride into Fe(III) colloids (Feitknecht et al. 1973, Dousma and de Bruyn 1976, Dousma et al. 1978, 1979). Dousma and his colleagues titrated acid Fe(III) solutions with base and noted incorporation of anions into the precipitating phase when chloride, nitrate, or sulfate medium was used. Fox (1988a) recognized the change in the stoichiometry of precipitated HFO when chloride and nitrate media were used and derived a more appropriate stoichiometry of $Fe(OH)_{2.35}$ with the remainder of the charge balanced by chloride or nitrate or phosphate. He used this hypothesis to examine iron colloids in a river system and demonstrated its applicability (Fox 1988b, 1989).

Byrne and Luo (2000) have re-evaluated this issue by using a sensitive potentiometric technique similar to that employed by Biedermann and Chow (1966) to measure the stoichiometry for the HFO precipitation reaction over a wide pH range (3-7.5). It was concluded that, for the reaction:

$$Fe(OH)_n^{3-n} + nH^{+} \leftrightarrow Fe^{3+} + nH_2O \tag{7}$$

the solubility product constant should be

$$K^{*}_{SO} = [Fe^{3+}][H^{+}]^{-2.86} = 10^{4.28} \tag{8}$$

or in log form

$$\log [Fe^{3+}] = 4.28(\pm 0.05) - 2.86(\pm 0.009)\ pH \tag{9}$$

Biedermann and Schindler (1957) reported

$$\log [Fe^{3+}] = 3.96(\pm 0.10) - 3.0\ pH \quad (10)$$

The range of log K_{sp} values reported by Nordstrom et al. (1990) for ferrihydrite solubility range from 3.0 to 5.0 based on several other reported literature studies. These results and their implications for natural systems are discussed further in the section of this chapter that deals with geochemical controls on mineral formation.

Properties. Schwertmannite usually occurs in mixtures with other minerals that range from poorly crystalline (ferrihydrite) to moderately crystalline (goethite, lepidocrocite) to well crystalline (jarosite). Its presence in such mixtures complicates the processes of identification and characterization. The objective of this discussion is to define the properties of schwertmannite and to compare them with those of coexisting phases (Table 2).

Schwertmannite has the ideal formula $Fe_8O_8(OH)_6SO_4 \cdot nH_2O$, which implies an Fe/S molar ratio of 8 and a composition that is intermediate between those of jarosite (Fe/S = 1.5) and the common iron oxides (no S) with which it is generally associated. In fact, the sulfate content is somewhat variable, and natural samples are best described by the formula $Fe_8O_8(OH)_{8-2x}(SO_4)_x \cdot nH_2O$ where $1 \leq x \leq 1.75$ and Fe/S ranges from 8 to 4.6 (Bigham et al. 1996b). Slightly higher sulfate contents were recently reported for Korean samples (Yu et al. 1999). Available chemical data for both natural and synthetic schwertmannite are summarized in Table 3. The sulfate in schwertmannite may be partly or fully substituted by anions such as selenate, arsenate, and nitrate when co-precipitated (Waychunas et al. 1995). Therefore, sulfate deficient specimens and sulfate-free analogs are possible. Ferrihydrite can sorb enough sulfate to approximate the composition found for schwertmannite (Smith 1991), making it difficult to distinguish between HFO with sorbed sulfate and schwertmannite. Barham (1997) has suggested that the sulfate in schwertmannite can also be replaced through exchange reactions by equilibrating specimens with solutions containing other anions such as carbonate, oxalate, and chromate. These studies confirm that the exact character of sulfate in schwertmannite needs further investigation.

Synthesis studies have indicated that schwertmannite may have a structure similar to that of akaganéite, β-$FeO(OH)_{1-x}Cl_x$ (nominally β-FeOOH), which is composed of double chains of $FeO_3(OH)_3$ octahedra sharing corners to produce square tunnels extending parallel to the c axis (Bigham et al. 1990). The tunnels are actually a series of adjoining cavities created by framework oxygens/hydroxyls. In akaganéite, the structure is stabilized by Cl^- or F^- or OH^- occupying every second cavity (Childs et al. 1980), and it has been suggested that sulfate could play a similar role in schwertmannite. Because of size restrictions, sulfate ions could not occupy structural cavities without sharing the oxygen atoms with surrounding Fe atoms and without severe distortion of the structure. Although distortion is consistent with the poor crystallinity of schwertmannite, this model deserves further testing.

Perhaps the best physical evidence for structural sulfate in schwertmannite has been obtained from ^{57}Fe Mössbauer analyses (Murad et al. 1990). These data show the Fe in schwertmannite to be exclusively trivalent and in octahedral coordination. The mineral has a Néel temperature (temperature of transition from paramagnetic to ferrimagnetic behavior) of 75±5 K and a saturation magnetic hyperfine field of about 45.5 T. The former is intermediate to the Néel temperatures of commonly associated iron oxides and jarosite, and the magnetic hyperfine field is lower by about 1 T than those of even the most poorly crystalline ferrihydrite (Table 2). Presumably, the sulfate in schwertmannite

Table 2. Properties of Minerals† Encountered in Mine Drainage Ochres.

Mineral Name: Ideal Formula:	Goethite α-FeOOH	Lepidocrocite γ-FeOOH	Ferrihydrite ~ $Fe_5HO_8 \cdot 4H_2O$	Schwertmannite $Fe_8O_8(SO_4)(OH)_6$	Jarosite‡ $KFe_3(OH)_6(SO_4)_2$
Crystal system Cell dimensions (Å)	Orthorhombic a = 4.608 b = 9.956 c = 3.022	Orthorhombic a = 3.88 b = 12.54 c = 3.07	Trigonal a = 5.08 c = 9.4	Tetragonal a = 10.66 c = 6.04	Hexagonal a = 7.29 c = 17.16
Color (Hue)	Yellowish-brown (7.5YR - 10YR)	Orange (5YR - 7.5YR)	Reddish-brown (5YR - 7.5YR)	Yellow (10YR - 2.5Y)	Straw yellow (2.5Y - 5Y)
Crystal shape Crystallinity	Short rods Moderate	Laths Moderate	Spherical Poor	Pin-cushion Poor	Pseudocubic Good
Most intense XRD spacings (Å)	4.18, 2.45 2.69	6.26, 3.29 2.47, 1.937	2.54, 2.24, 1.97, 1.73, 1.47	4.86, 3.39, 2.55, 2.28, 1.66, 1.51	5.09, 3.11, 3.08
Major IR bands (cm^{-1})	890, 797	1161, 1026 753	Nil	1175, 1125, 1055, 975, 680, 615	1181, 1080, 1003, 628, 493, 472
Néel temp. (K)	400	77	28-115¶	75	55-60
DTA events (°C) En. = endotherm Ex. = exotherm	En. 280 - 400	En. 300 - 350 Ex. 370 - 500	En. 150	En. 100 - 300 Ex. 540 - 580 En. 680	En. 475, 740 - 800
Magnetic hyperfine field (T) at:					
295 K	38.2	----	----	----	----
77 K	50.0	----	≤ 45.1	----	----
4.2 K	50.6	46.0	46.5 - 50.0	45.4	47.0

† Data taken from:

Bigham et al. (1990); Bigham et al. (1992); Doner and Lynn (1989); Fanning et al., (1993); Murad (1988); Murad et al. (1988); Murad et al. (1994); Powers et al. (1975); Schwertmann (1993); Schwertmann and Fitzpatrick (1992); Schwertmann and Taylor (1989); Takano et al. (1968)

‡ Properties listed are specific to jarosite, but natrojarosite, hydronium jarosite or solid solutions may occur. ¶ Blocking temperature

Table 3. Chemical composition of natural and synthetic schwertmannites.

Element	*(1)*	*(2)*	*(3)*	*(4)*	*(5)*	*(6)*	*(7)*	*(8)*
Fe_2O_3 (%)	62.6	60.4–61.5	61.3–64.7	61.2–66.7	67.3	58.3–66.5	67.3	65.6
SO_3(%)	12.7	7.4–9.0	11.5–12.9	8.2–11.5	14.7	10.1–11.3	14.7	10.2
$H_2O\pm$ (%)	23.1	17.2	18.1–20.3	21.8–27.4	20.7	?	20.7	23.8
Fe/S	4.9	6.7–8.3	4.7–5.4	5.4–8.2	4.6	5.2–6.6	4.6	6.4

1. Type specimen, sample Py-4 from Finnish mine drainage (Bigham et al. 1994).
2. Samples Y1 and Y3b from Finnish mine drainage (Bigham et al. 1990).
3. Samples Bt-4, La-1, and Nb-1 from Ohio mine drainage (Bigham et al. 1990).
4. Five samples from Czech dripstone (Fojt 1975).
5. Sample PI3 from Korean mine drainage (Yu et al. 1999).
6. Samples MG1118 and DP4226 from Japanese lake sediments (Childs et al. 1998).
7. Synthetic sample Z510b formed by bacterial oxidation of ferrous sulfate (Bigham et al. 1990).
8. Synthetic sample B-2000s formed by hydrolysis of ferric nitrate in the presence of sulfate (Bigham et al. 1990).

inhibits magnetic exchange interactions between neighboring Fe atoms and is therefore responsible for the low ordering temperature and magnetic field. Spectra from both paramagnetic and magnetically ordered schwertmannite are asymmetric (Fig. 6), indicating multiple environments for Fe^{III} that could also reflect incorporation of SO_4 into the structure.

Schwertmannite is readily soluble in acidic (pH 3.0) solutions of ammonium oxalate (Brady et al. 1986) through a reaction that is catalyzed both by light (De Endredy 1963) and the presence of Fe^{2+} (Fischer 1972). This reagent has been widely employed for the selective dissolution of poorly crystalline Fe oxides (e.g. ferrihydrite) in soils by a 2- to 4-h extraction in the dark (Schwertmann 1964), and recent studies (Dold 1999) suggest that it may be equally efficient for partitioning schwertmannite from associated minerals of higher crystallinity in mine spoils and sediments. Studies of schwertmannite

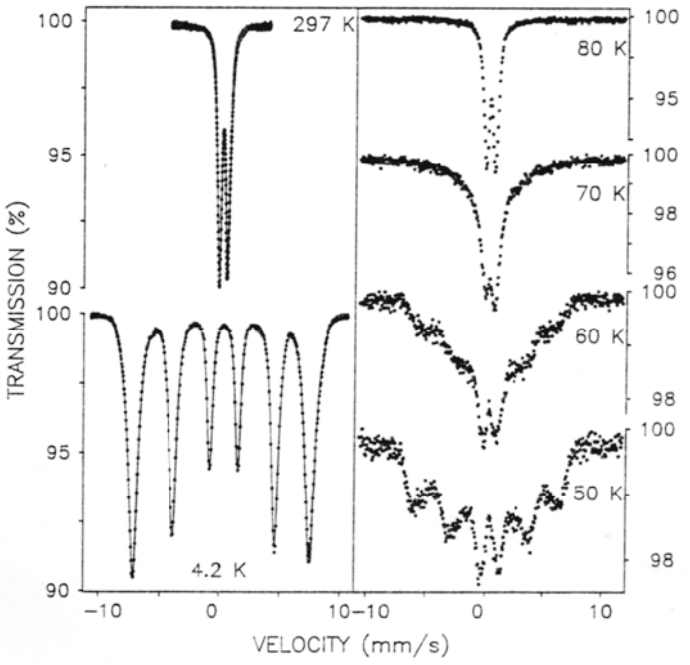

Figure 6. Mössbauer spectra of synthetic schwertmannite at 297 and 4.2 K and in the vicinity of the Néel temperature (modified from Bigham et al. 1990).

dissolution kinetics in 0.1 *M* HCl (Bigham et al. 1990) showed that about 15% of the total SO_4 was immediately released and was probably derived from surface sites. Half-reaction times for the remaining Fe and SO_4 were similar and indicated congruent dissolution of the bulk sample.

The thermal decomposition of schwertmannite yields a low-temperature endotherm between 100 and 300° C (Table 2) that is associated with a weight loss of 15 to 20% and is probably caused by the vaporization of sorbed water as well as structural OH/H_2O. This event is followed by an exotherm at 540-580° C that immediately gives way to a second endotherm at about 680° C. The exothermic event coincides with the formation of $Fe_2(SO_4)_3$ and may or may not be apparent in natural samples. The final endotherm can be attributed to the decomposition of $Fe_2(SO_4)_3$ to form hematite (α-Fe_2O_3) with release of SO_3. Volatilization of the latter produces a weight loss of 6 to 12%. The thermal characteristics of jarosite are similar except that the vaporization of structural hydroxyls occurs at a higher temperature (400-500° C) and the weight loss due to SO_3 evolution is greater (see Dutrizac and Jambor, this volume).

The infrared profile of schwertmannite has been examined in considerable detail (Lazaroff et al. 1985, Bigham et al. 1990, Bishop and Murad 1996) and is characterized by absorption features reflective of its composition. Four sulfate vibrational modes are possible. These modes and their approximate frequencies are υ_1 (symmetric stretch) at 983 cm^{-1}, υ_2 (symmetric bend) at 450 cm^{-1}, υ_3 (asymmetric stretch) at 1105 cm^{-1}, and υ_4 (asymmetric bend) at 611 cm^{-1} (Ross 1974). When the sulfate group exhibits symmetry lower than Td (isolated, tetrahedral SO_4^{2-}), the υ_2, υ_3, and υ_4 sulfate bending vibrations may be split into multiple vibrations. A typical schwertmannite spectrum (Table 2) exhibits a strong but degenerate υ_3 vibration near 1100 cm^{-1} with shoulders at about 1050 and 1170 cm^{-1}, a medium strength υ_4 vibration at about 610 cm^{-1}, a medium strength υ_1 vibration at 980 cm^{-1} and a probable, weak υ_2 vibration at 465 cm^{-1}. Additional features in the schwertmannite spectrum at about 850 and 700 cm^{-1} have been assigned to OH bending vibrations (Bishop and Murad 1996).

The color of schwertmannite is intermediate to those of goethite and jarosite (Table 2), and a recent study by Swayze et al. (2000) has suggested that the reflectance spectra of iron-bearing secondary minerals may provide a useful tool for mapping acidic mine wastes. Diffuse reflectance spectroscopy in the visible (400-700 nm) and extended visible range (400-1200 nm) has also been employed to identify secondary iron minerals in soils and sediments. Because of overlapping crystal-field band positions, it seems unlikely that this technique can be used to discriminate goethite, lepidocrocite, and schwertmannite (Scheinost et al. 1998). Visible color identification is inadequate to determine schwertmannite in the field because of high color variability and similar average colors to other hydrous Fe oxide minerals (Scheinost and Schwertmann 1999).

The crystal morphology of most minerals is variable and is not a reliable tool for identification purposes. This conclusion is particularly true of nanophase materials. Schwertmannite particles, by contrast, usually occur as fine needles that coalesce to form rounded aggregates that are 200 to 500 nm in diameter with electron-dense interiors (Fig. 7). This unique "pin-cushion" morphology is commonly observed in loose precipitates of both synthetic and natural samples but may not be apparent when materials are taken from consolidated sediments or surface crusts. The morphology of schwertmannite particles typically contrasts with those of associated jarosite or Fe-oxyhydroxides. Moreover, the morphology is responsible for high specific surface areas in the range of 100-200 m^2/g and should enhance the reactivity of schwertmannite in the environment.

The poor crystallinity of schwertmannite places limitations on the utility of

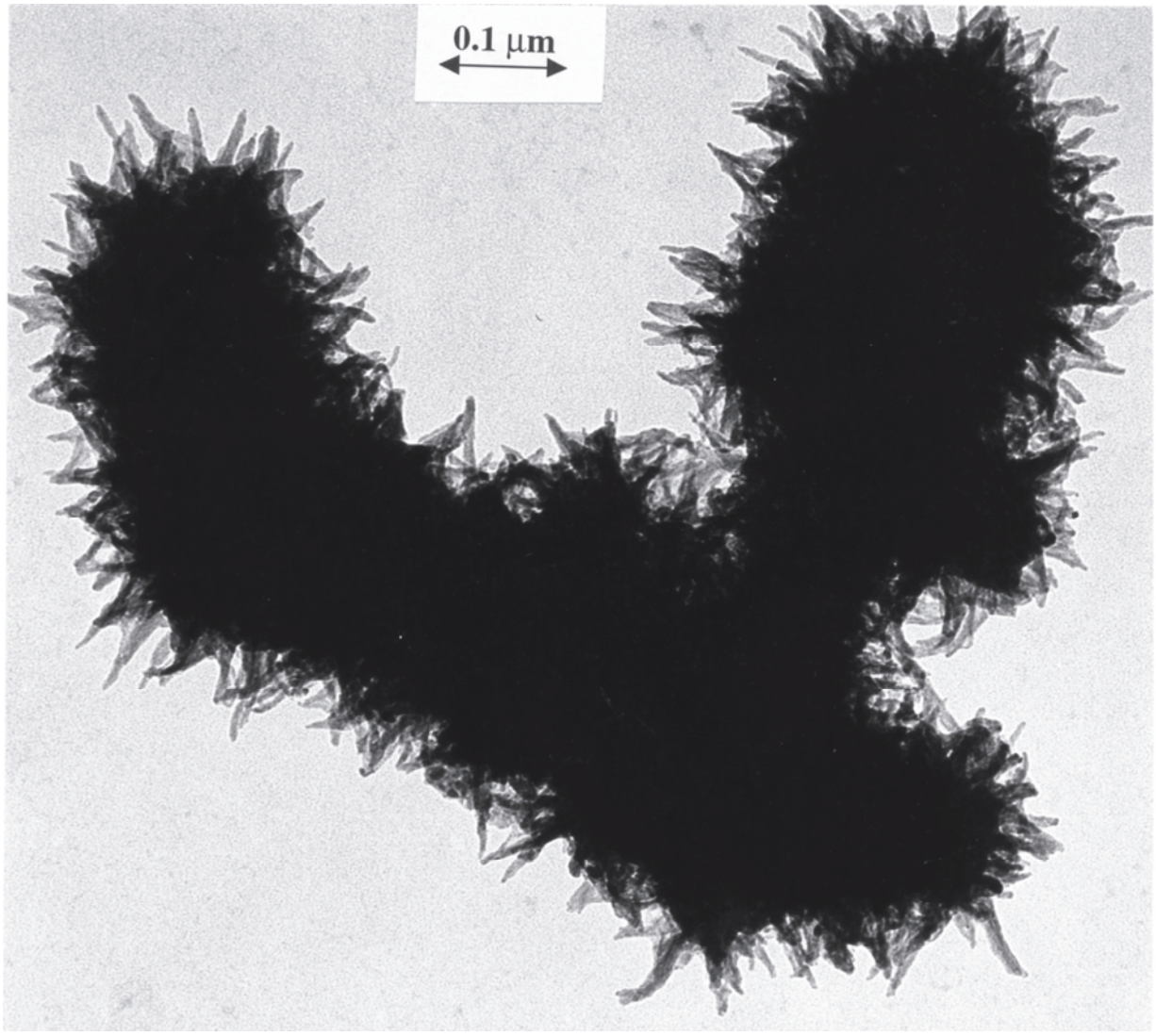

Figure 7. Transmission electron microscopy (TEM) photomicrograph of synthetic schwertmannite.

conventional X-ray diffraction (XRD) analysis, but the mineral has a unique XRD profile that can be readily distinguished from those of associated minerals if specimens are reasonably pure (Fig. 8). The powder diffraction pattern of schwertmannite consists of eight broad peaks for d > 1.4 Å and is perhaps most easily confused with that of well crystallized (6-line) ferrihydrite. The strongest peak for both minerals occurs at about 2.54 Å, but that of schwertmannite is characteristically more symmetrical. Both minerals exhibit reflections at 1.51 and 1.46 Å, but the intensity ratios are reversed. The 1.64 Å peak of schwertmannite is significantly displaced from that at 1.72 Å for ferrihydrite. Also, schwertmannite exhibits two additional reflections at about 3.31 and 4.95 Å. The detection of schwertmannite in mixed assemblage with other minerals may be difficult because of its poor crystallinity. When admixed with well crystalline minerals, such as jarosite, schwertmannite may be overlooked because its diffraction peaks become "lost" as background noise. Even when coarse-grained minerals are excluded, the diffraction patterns from mixtures may be difficult to evaluate. In such cases, the technique of differential X-ray diffraction, DXRD (Schulze 1981), may enable schwertmannite to be detected. For example, Figure 9 shows XRD patterns from a mine-drainage ochre before

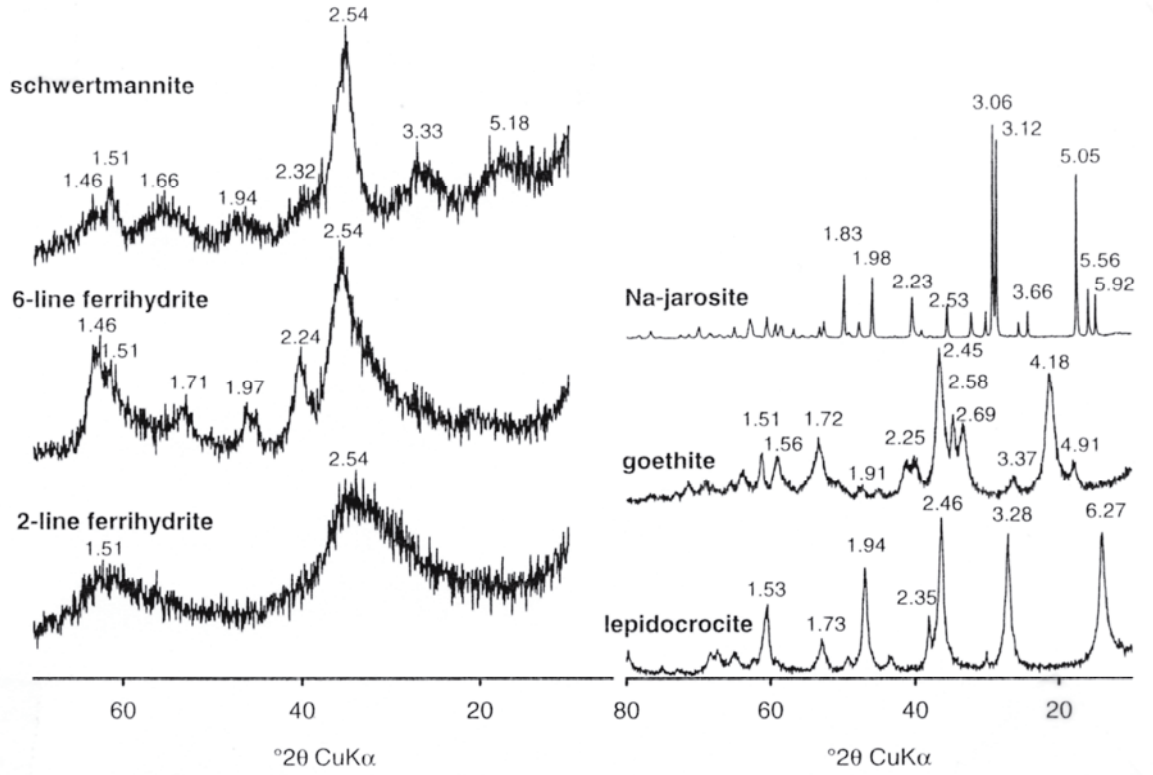

Figure 8. X-ray powder diffraction patterns for schwertmannite and commonly associated minerals; d values are in Å

and after a 15-min extraction with acid ammonium oxalate that left a residue of goethite and silicate minerals. Subtraction of the residue diffraction pattern from that of the original sample yields the diffraction profile of the component dissolved by acid ammonium oxalate. In this case, the pattern of schwertmannite is clearly recognizable.

Hydroxysulfates of Al

Several Al hydroxysulfates of poor crystallinity and low solubility are known to form in acid sulfate environments. A summary of these minerals and their properties is provided in Table 4a. These minerals occur as fine-grained materials with such small particle size and poor crystallinity that only a few have had crystal-structure studies and space group assignments. There are four distinct compositional sets of aluminum hydroxysulfate hydrates, characterized by their Al:SO_4 mole ratios. Hydrobasaluminite and basaluminite have the highest ratio (4:1), followed by zaherite (2.4:1), then aluminite and meta-aluminite (2:1), and finally jurbanite and rostite (1:1), which are well-crystallized and kept separate in Table 4b. These compositional changes must reflect the relative proportion of the dissolved Al to dissolved SO_4 (or sulfuric acid) in the aqueous solution, and, hence, the relative pH of the solution from which they precipitate. In other words, the basaluminite set (actually only hydrobasaluminite because basaluminite forms by dehydration of hydrobasaluminite) should precipitate at higher pH values than zaherite, and with decreasing pH the sequence should be zaherite to the aluminite set to the jurbanite set to alunogen [$Al_2(SO_4)_3 \cdot 17H_2O$, see Jambor et al., this volume]. Jurbanite and rostite (the jurbanite set) are not poorly ordered, insoluble precipitates. Rather, they crystallize as soluble salts with good crystallinity, and they will receive special mention in a later section.

Geochemical history. The chemistry of basic Al sulfates has been confusing because

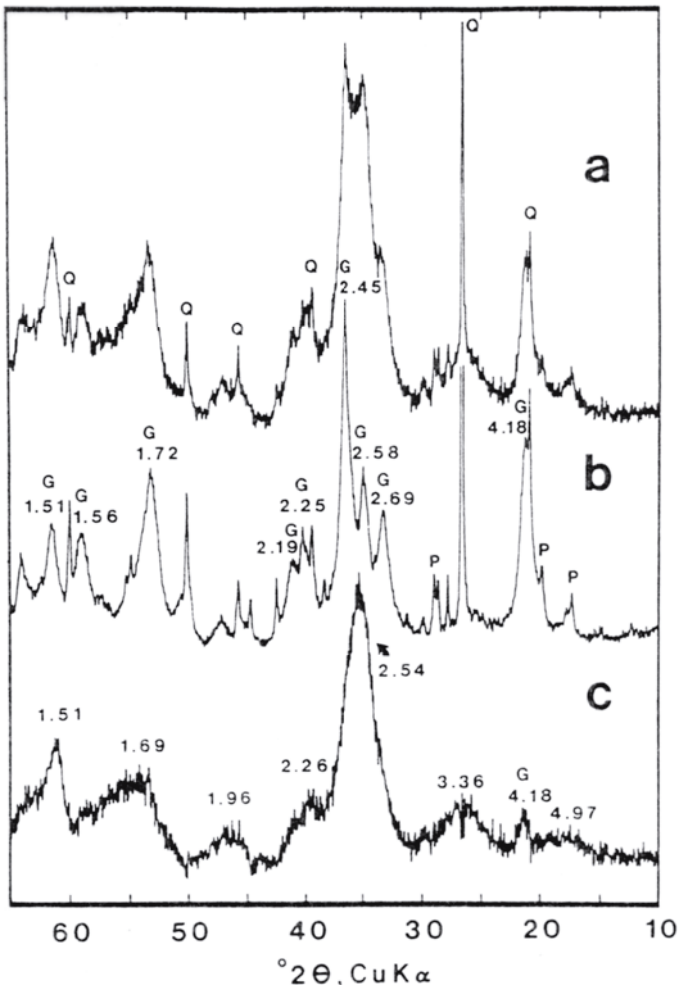

Figure 9. X-ray powder diffraction patterns from stream precipitate (a) untreated, (b) following 15-min oxalate extraction, and (c) after subtraction of (b) from (a) (DXRD) G = goethite, Q = quartz, P = Phyllosilicates (used with permission of the Clay Minerals Society; from Brady et al. 1986).

of the rapid formation of colloidal disequilibrium phases and mixtures of colloidal phases, similar to the formation of hydrous ferric oxides with substituted anions in the iron system. After the initial precipitation, slow transformations continue as the solution ages. For example, Singh (1982) showed that with sufficient aging, a 0.5 molar $Al_2(SO_4)_3$ solution will precipitate simultaneously gibbsite, böhmite, alumina, and alunite. Adams and Hajek (1978) formed both single-mineral precipitates and mixtures of gibbsite, basaluminite, and alunite when acid solutions of Al sulfate were aged for 18 weeks at 50° C. The existence of basic flocculants of Al sulfate was conjectural for many years; whereas some titration curves and chemical compositions supported the existence of such phases, the ease of displacement of the sulfate by washing seemed to suggest that sulfate was adsorbed (Weiser et al. 1941). Studies that combined XRD data with chemical compositions were most fruitful, and the identification of minerals with Al-hydroxysulfate composition provided inescapable evidence that such compounds exist (see next section).

The definitive study of Bassett and Goodwin (1949) combined phase-equilibria solubility data with careful XRD analysis and chemical composition of all precipitates that formed over a wide range of Al sulfate and sulfuric acid concentrations. Several striking results came from their 13-year study. First, they clearly defined the solubility range for alunogen and jurbanite before jurbanite was recognized as a mineral (Anthony and McLean 1976). Second, Bassett and Goodwin (1949) were unable to synthesize aluminite, basaluminite, hydrobasaluminite, zaherite, or rostite. Third, they showed a stable solubility range for a compound of composition $Al_{10}(SO_4)_6(OH)_{18}\cdot 37H_2O$ that has

Table 4a. Properties of Al hydroxysulfate minerals

Mineral Name *Formula*	Hydrobasaluminite $Al_4(OH)_{10}SO_4 \cdot 15H_2O$	Basaluminite $Al_4(OH)_{10}SO_4 \cdot 4H_2O$	Zaherite $Al_{12}(OH)_{26}(SO_4)_5 \cdot 20H_2O$	Aluminite $Al_2(OH)_4SO_4 \cdot 7H_2O$	Meta-Aluminite $Al_2(OH)_4SO_4 \cdot 5H_2O$
Crystal System	Monoclinic	Monoclinic	Triclinic	Monoclinic	Monoclinic
Space Group	?	$P2_1$	$P1$ or $P\bar{1}$	$P2_1/c$	?
Cell Dimension	a = 14.911 b = 9.993 c = 13.640 β = 112.24°	a = 12.954 b = 10.004 c = 11.064 β = 104.1°	a = 18.475 α = 95.24° b = 19.454 β = 91.48° c = 3.771 γ = 80.24°	a = 7.440 b = 15.583 c = 11.700 β = 110.18°	a = 7.930 b = 16.879 c = 7.353 β = 106.73°
Color	White to light yellow-brown	White	Chalk-white, to light bluish green when contains Cu	White	Silky white
Texture and Crystallinity	Clay-like Usually moist and plastic	Clay-like Conchoidal fracture	Densely-packed aggregates of micro- to cryptocrystalline	Clay-like, friable, nodular masses of minute fibers	Nodular microcrystal-line aggregates and concretions
Most intense XRD spacings (Å)	12.6, 6.18, 5.29, 4.70	9.39, 4.73, 3.69, 1.438	18.1	8.98, 7.79, 4.70	8.46, 4.52, 4.39, 3.54
Stability	Dehydrates to basaluminite	Formed from hydro-basaluminite	Dehydrates under ambient conditions		Dehydrates to aluminite at 55°C

Table 4b. Properties of jurbanite and rostite.

Mineral Name	Jurbanite	Rostite
Formula	$Al(OH)SO_4 \cdot 5H_2O$	$Al(OH)SO_4 \cdot 5H_2O$
Crystal System	Monoclinic	Orthorhombic
Space Group	$P2_1/n$ or $P2_1/c$	*Pcab*
Cell dimensions	a = 8.396 b = 12.479 c = 8.155 β = 101.92°	a = 11.175 b = 13.043 c = 10.878
Color and texture	Colorless	Chalky mass
Most intense XRD spacings (Å)	6.75, 5.73, 4.48, 4.00, 3.99, 3.90	4.26, 4.19, 3.91

not yet been identified as a mineral. Johansson (1962) made relatively large crystals of jurbanite from which he was able to determine the crystal structure.

Another study by Johansson (1963) demonstrated that $Al_{13}O_{40}$ units form the building blocks for several, if not all, Al hydroxysulfates. Although the occurrence and proportion of mononuclear versus polynuclear species in titrations and other lab studies has been debated considerably in the literature, these Al_{13} polynuclear units have been recognized as rapidly forming, metastable colloids, that do not decompose easily (Bertsch and Parker 1996). Furthermore, anions such as sulfate usually decrease the pH of maximum precipitation and increase the rate of precipitation and coagulation (Bertsch and Parker 1996). The $13Al_2O_3 \cdot 6SO_3 \cdot xH_2O$ compound synthesized by Bassett and Goodwin (1949) and for which the crystal structure was determined by Johansson (1963), has compositional similarities to hydrobasaluminite/basaluminite but the XRD data do not bear a resemblance. This observation would suggest that there are other minerals, not yet identified, that might form in these systems.

Mineralogy and genesis. The most common Al hydroxysulfate minerals are hydrobasaluminite and basaluminite. Hydrobasaluminite seems to be the precipitate that forms when acid rock drainage is neutralized by mixing with a neutral, buffered water or by reaction with carbonate minerals such that the resultant pH is nearly 5.0 or higher. Examples of such precipitates and their compositions are given in Table 5. Theoretical compositions of hydrobasaluminite along with that for hydronium alunite and the analyzed compositions of two basaluminite samples (one of which is well-characterized, Clayton 1980) are provided for comparison. Samples C and E of Table 5 precipitated in cold, mountain-stream waters upon mixing of acid mine water with neutral-pH water. A typical TEM photograph of sample C (but also similar to sample E) in Figure 10 shows the lack of any crystal morphology and the appearance of aggregation of spherical colloids. Sample D of Table 5 is unusual in that it precipitated by mixing of an acid mine water with a highly carbonated, warm (20°C), mineral spring with elevated concentrations of chloride (700-800 mg/L). These conditions probably enhanced the

Table 5. Composition (wt %) of aluminous precipitates relative to theoretical and analyzed compositions of Al hydroxysulfate minerals.

	Hydronium alunite	Basaluminite	Basaluminite Sussex, UK	Basaluminite Dorset, UK	Hydro-basaluminite		C		D	E	F
	(Theoretical)	(Theoretical)	A	B	(Theoretical)	(1)	(2)	(3)	(4)	(5)	(6)
Al_2O_3	38.80	45.8	46.4	44.75	31.7	36.2	42.8	47.0	39.0	40.1	44.1
CaO				0.30		0.4	0.77	1.5			
Na_2O						0.0	0.05	0.18	1.2	0.1	
K_2O						0.0	0.04	0.00	0.5	0.0	0.0
H_2O	20.57	36.3	33.4	35.60	55.9	46.9	40.8	39.5	46.0	45.6	35.0
SO_3	40.63	17.9	17.4	18.10	12.4	10.7	12.4	8.7	17.4	11.6	22.3
Sum	100.00	100.00	97.2	98.75	100.00	94.2	96.9	96.9	104.2	97.4	101.4
X-ray diffr.	----	----	Basaluminite	Basaluminite	----	Amorphous	Amorphous	Amorphous	Alunite	Amorphous	Amorphous
Electron diffr.	----	----		Basaluminite	----	Amorphous	Amorphous	Amorphous	crystalline	Amorphous	Basaluminite

A: Bannister and Hollingworth (1948a,b)
B: Clayton (1980)
C: Precipitates 1, 2, and 3 from Paradise portal drainage, San Juan Mountains, CO (Nordstrom et al., 1984)
D: Precipitate from Doughty Springs, Delta County, CO (Headden, 1905; Cunningham et al., 1996)
E: Precipitate from Leviathan mine drainage, Alpine County, CA (Ball and Nordstrom, 1989)
F: Precipitate synthesized in laboratory from aluminum sulfate solution, pH = 4.1 (Charles Roberson and John Hem, USGS, unpublished data)

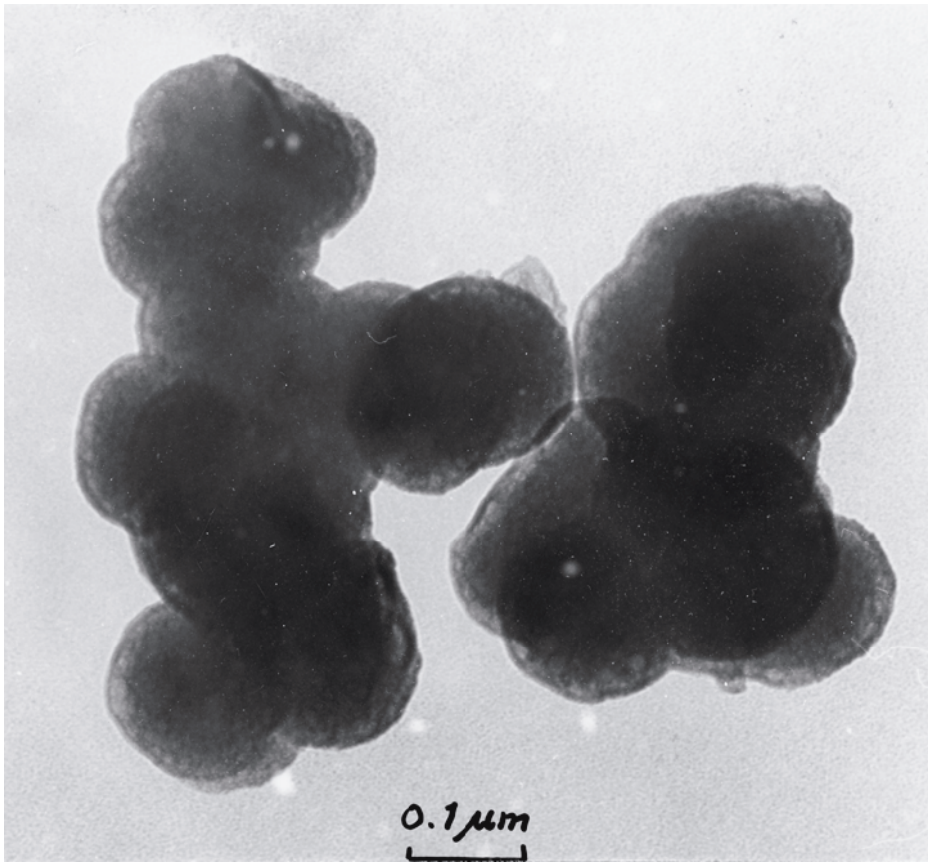

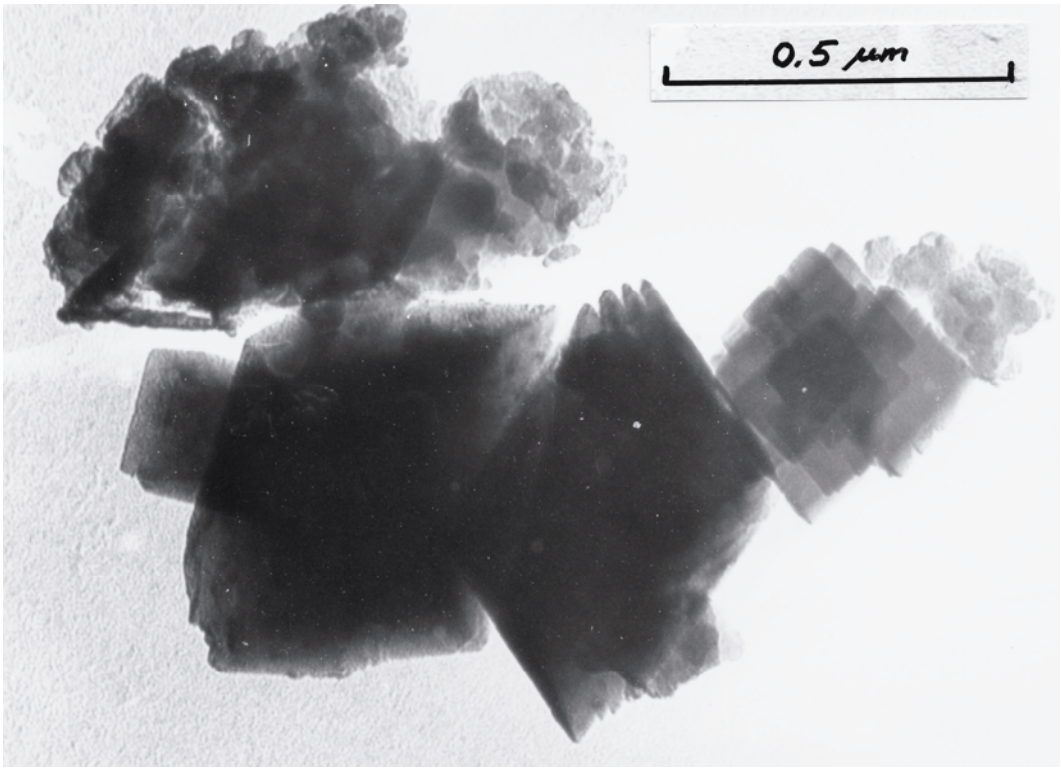

Figure 10 (top). TEM photograph of Al-hydroxysulfate precipitate C (hydrobasaluminite/basaluminite) in Table 5.

Figure 11 (bottom). TEM photograph of Al-hydroxysulfate precipitate D (alunite) in Table 5.

formation of alunite at this site. A TEM photograph of sample D (Fig. 11) clearly shows crystal faces and both electron diffraction and XRD show the presence of alunite. The elevated water content of some of the "amorphous" precipitates may reflect the hydrated character of hydrobasaluminite relative to basaluminite. All of the analyzed precipitates fall within the range of composition between the theoretical values for hydrobasaluminite and basaluminite. The analyses that are short of 100% probably reflect admixed silica. Frequently, quartz fragments can be seen mixed with the basaluminite when observed with a microscope.

Bannister and Hollingworth (1948a,b) first identified basaluminite and hydrobasaluminite in the Northampton Ironstone, near Wellingsborough, UK. One or both of these minerals have since been found in the caves of the Guadalupe Mountains, New Mexico (Polyak and Provencio 1998), in the Flysch formations of the Carpathian Mountains (Wieser 1974), near Brno, Czech Republic (Batik and Hruskova 1971), associated with a Middle Pennsylvanian coal bed in southeastern Kansas, USA (Tien 1968), in several prefectures in Japan (Matsubara et al. 1990, Minakawa et al. 1996), in Jurassic strata, Namana, Yakutia, Russia (Lizalek et al. 1989), in the bauxite deposit of Csordut, Hungary (Toth et al. 1984), near Newhaven, Sussex, UK (Wilmot and Young 1985), and in the black schist of Karatau, Kazakhistan (Zazubina and Ankinovich 1982). Formation of the minerals occurs by the reaction of acid sulfate solutions (from pyrite oxidation) with Al-rich clays, or by mixing of acid, Al-rich sulfate waters with dilute neutral waters, or through the neutralization of acid sulfate solutions, rich in Al, by carbonate minerals. The most detailed study was reported by Clayton (1980) on hydrobasalumunite and basaluminite from Chickerell, Dorset, UK and includes transmission electron microscopy with electron-diffraction data, XRD data, chemical analysis, thermogravimetric analysis (TGA), and differential thermal analysis (DTA). Crystal structure determinations of felsőbanyaite (thought to be a dimorph of basaluminite) and basaluminite have demonstrated that these two minerals are identical (Farkas and Pertlik 1997, Jambor et al. 1998).

Zaherite was first described by Ruotsala and Babcock (1977) as a white, massive, fine-grained mineral from the Salt Range, Pakistan. A second occurrence has been found in South Africa in a biotite schist near Pofadder (Beukes et al. 1984) and new XRD, IR, DTA, and compositional data was obtained. However, the XRD data gave incorrect cell dimensions that were corrected later (de Bruiyn et al. 1985).

Aluminite and meta-aluminite have been found in similar types of environments as those with basaluminite and hydrobasaluminite. Aluminite has been found in the mineral deposits of the southern Donbass area of the Ukraine (Chernitsyna et al. 1999), in the oxidized zone of the Deputatsk tin ore deposit in Yakutia, Russia (Zhdanov and Solov'ev 1998), in the oxidized zone of a silver ore deposit in the Magadan area, Russia (Oycollonov et al. 1994), in Paleozoic and Mesozoic carbonates of Siberia (Lizalek and Filatov 1986), in shales and sandstones at the contact between Cambrian and lower Jurassic rocks at Namansk, near Yakutsk, Siberia (Sokolov et al. 1985), with alunite in clay deposits near Buenos Aires, Argentina (Zalba 1982), with basaluminite and gibbsite in Carboniferous and Permian limestones and dolostones (Van'shin and Gutsaki 1982), in pyritized Proterozoic sericitic schists near Lake Baikal, Siberia (Dombrovskaya et al. 1976), in the bauxite deposits of Montenegro, Yugoslavia (Lukovic 1970), and in the Bshlybel copper deposits, Kelbadzhar area, Azerbaijan (Mamedov et al. 1969) and at several other localities (France, Germany, Italy, England, and USA). Meta-aluminite was first described by Frondel (1968) in association with basaluminite and gypsum at the Fuemrole mine in Emery County, Utah. It appears to have formed by reaction of acidic Al-rich waters with clays and carbonates. Meta-aluminite also occurs in the upper

Proterozoic schists of the Greater Goloustan area, Siberia (Mazilov et al. 1975) in a similar setting to the Utah occurrence. Sizia (1966) reported on the IR spectra of 9 sulfate minerals including aluminite.

Although numerous geochemical modeling studies have reported acidified waters in equilibrium with jurbanite (van Breeman 1973 1976; Kram et al. 1995; Monterroso et al. 1994; Alvarez et al. 1993), the only two known occurrences of the mineral are at the San Manuel copper mine, Pinal County, Arizona, USA (Anthony and McLean (1976) and the Cetine mine in Tuscany, Italy (Sabelli 1984, Brizzi et al. 1986). Sabelli (1985) refined the crystal structure for jurbanite. Rostite has had an eventful history because of the difficulty in characterizing it. Rost (1937) originally found it on burning coal heaps in Czechoslovakia, but reliable crystallographic data were not available until Cech (1979). However, there was found to be considerable F-OH substitution and it is now recognized that rostite refers to the compositional range OH>F, whereas khademite refers to F > OH.

The reason for apparent solubility equilibrium with respect to jurbanite for acid sulfate waters with pH generally less than 4.5 originated with the publications of van Breemen (1973) and Nordstrom (1982b). Van Breemen (1973) found good agreement between ion-activity products calculated from speciation computations of acid sulfate waters and an unidentified mineral that had the equilibrium stoichiometry of $Al(OH)SO_4$. Nordstrom (1982b), noting that there was a mineral with the same stoichiometry, whose solubility had been measured by Bassett and Goodwin (1949), reduced the solubility data to a solubility-product constant. Many investigators have used this information for chemical speciation modeling and the calculation of saturation indices. The agreement between the ion-activity product (IAP) for jurbanite and the solubility-product constant (K_{sp}), however, should be considered fortuitous and not indicative of solubility equilibrium for the following reasons. Jurbanite is a rare and very soluble efflorescent mineral. Bassett and Goodwin (1949) found that it was at equilibrium with a solution containing 15-20 wt % sulfate which would be equivalent to pH values of 0.0 or less, not pH values of 1 to 4.5. There must be some error in the K_{sp} value reported by Nordstrom (1982b) that shows its stability in pH values of 4 or less depending on sulfate concentrations. The solubility data of Bassett and Goodwin (1949) needs to be re-evaluated with the Pitzer. The fortuitous coincidence between the IAP and the K_{sp} most likely reflects the well-behaved correlation of increasing sulfate with increasing Al and with decreasing pH for pH < 4.5, the pH below which Al behaves conservatively (Nordstrom and Ball 1986). In other words, for pH values below the first hydrolysis constant for Al (pK = 5.0), Al remains predominately dissolved and any changes in concentration are caused by dilution in an identical manner as changes in sulfate concentration (see later section on Geochemical controls on formation and transformation: The Al system).

FORMATION AND DECOMPOSITION OF FE- AND AL-HYDROXYSULFATES OF LOW CRYSTALLINITY

Biological influences on mineral formation

The important role played by acidophilic bacteria in the aqueous oxidation of pyrite and related sulfide minerals was discussed previously. The $Fe^{2+}_{(aq)}$ released during this microbially catalyzed process is ultimately oxidized, hydrolyzed and precipitated as ferric oxyhydroxides or hydroxysulfates. At pH values <3.5, there is no doubt that the enzymatic oxidation of $Fe^{2+}_{(aq)}$ as an energy source for acidophilic organisms, such as *T. ferrooxidans* and *L. ferrooxidans*, is an essential requirement for the formation of secondary Fe^{III} minerals. Because little energy is produced by the oxidation reaction

(ΔG = 6.5 kcal/mol with O_2 as the electron acceptor at pH 2.5), these bacteria must oxidize large quantities of $Fe^{2+}_{(aq)}$ to sustain metabolic processes (Lees et al. 1969). Ehrlich (1996) has estimated that a "consumption" of 90.1 mol of $Fe^{2+}_{(aq)}$ is required to assimilate 1.0 mol of C. As a result, even a modest bacterial population is capable of oxidizing large quantities of $Fe^{2+}_{(aq)}$.

The extended role of microorganisms in guiding the actual "mineralization" of Fe, Al, and other dissolved species has been a topic of considerable debate. Mineral precipitates of Fe have been observed in direct contact with bacterial cells that grew in acid mine drainage (Ferris et al. 1989a,b; Clarke et al. 1997). Electron microscope images commonly show cells partly to completely encapsulated with Fe-rich epicellular material. This material has usually been identified as ferrihydrite (Ferris et al. 1989a) or goethite (Konhauser and Ferris 1996) but, in at least one case (Clarke et al. 1997), energy dispersive X-ray analyses have indicated the presence of ferric hydroxysulfates with Fe:S ratios ranging from 3.5:1 to 1.9:1. Bacterial surfaces have also been shown to enhance the immobilzation of other cations, especially Al (Urrutia and Beveridge 1995). Bacterial slimes may thus facilitate the undesirable accumulation of Al-hydroxysulfate precipitates and clogging of anoxic limestone drains designed for treating acid mine drainage (Robbins et al. 1999).

The formation of epicellular precipitates is related to the character of bacterial surfaces. The cell walls of both Gram-positive and Gram-negative bacteria contain functional groups, such as carboxylates and phosphates, that impart a negative surface charge and provide reactive sites for sorption of metal cations from the surrounding solution (Schultze-Lam et al. 1996). In natural environments, bacteria produce an extracellular sheath or capsule composed of polysaccharides with molecular components that are also capable of accumulating metals from around the cell. Once a metal is complexed, it effectively reduces the activation energy for nucleation of solid phases. In this way, the bacterial surface may function as a template for heterogenous nucleation (Konhauser 1998, Warren and Ferris 1998). Precipitates grow rapidly and incorporate available counter-ions from the surrounding solution to form mineral aggregates that may approach the mass of the cell. These initial precipitates are usually poorly crystalline because such phases have lower interfacial free energies than more crystalline products (Steefel and van Cappellen 1990).

It is tempting to conclude that surface-mediated mineralization is responsible for the formation of all poorly crystalline hydroxysulfates and oxyhydroxides of Fe and Al associated with acid sulfate waters and that mineral speciation is somehow biologically controlled, however, evidence suggests otherwise. There is probably little, if any, active genetic control on the process because mineralization can develop on the remains of dead cells (Ferris et al. 1989b) and occurs independently of cell morphology or physiological condition. Moreover, mineral phases can form spontaneously under conditions of rapid flow where acid sulfate waters are mixed with solutions of higher pH in the field. Geochemical parameters such as pH, SO_4, and HCO_3 must direct the ultimate mineralogical fate of Fe and Al compounds precipitated from acid sulfate waters, even when mineralization is bacterially induced. For example, Bigham et al. (1996a) identified mineral precipitates obtained by oxidizing 0.1 M $FeSO_4 \cdot 7H_2O$ solutions at room temperature and pH values of 2.3, 2.6, 3.0, 3.3 and 3.6 using a stirred bioreactor and a strain of *T. ferrooxidans* (Fig. 12). Measured oxidation rates were similar across the pH range studied. Schwertmannite formed at pH 3.0. Jarosite increased in abundance with decreasing pH, whereas goethite appeared at pH 3.3 and 3.6. These results indicate that pH is a master variable influencing the speciation of secondary Fe minerals under conditions typical of acid sulfate waters.

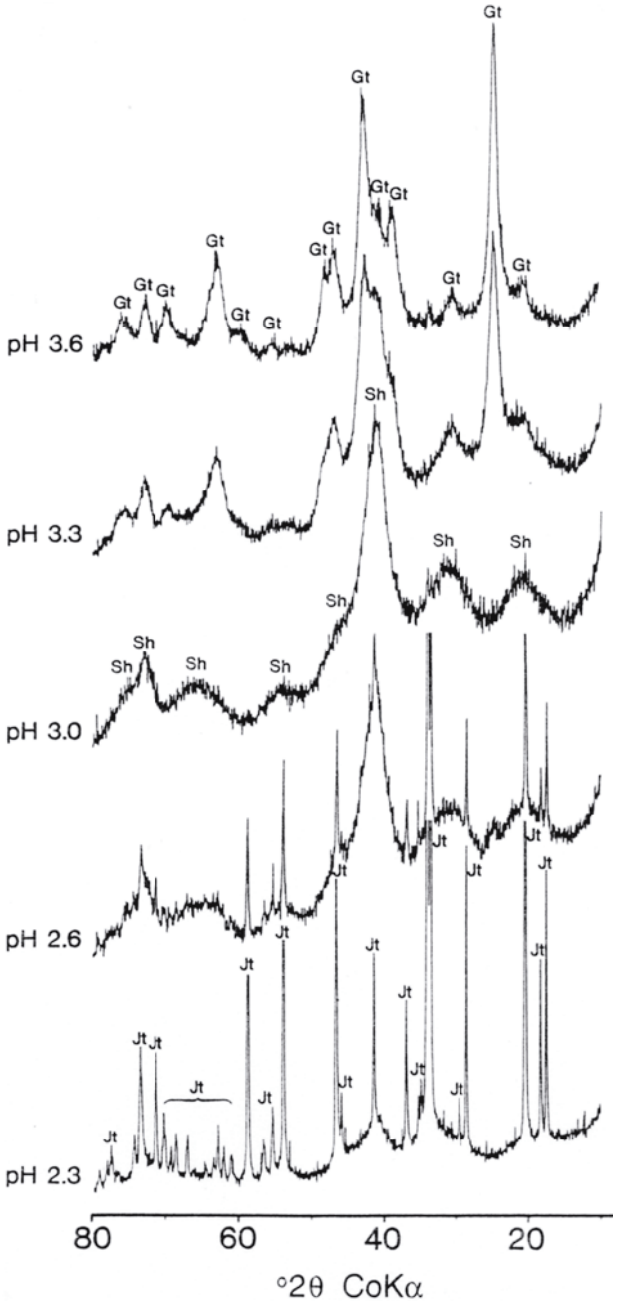

Figure 12. X-ray powder diffraction patterns from bioreactor precipitates at various pH values.
Gt = goethite; Sh = schwertmannite; Jt = jarosite
Modified from Bigham et al. (1996a).

GEOCHEMICAL CONTROLS ON MINERAL FORMATION AND TRANSFORMATION

If complete and reliable solution analyses have been obtained, geochemical speciation computations can be performed to determine the state of saturation of an aqueous system with respect to any particular mineral (provided that thermodynamic data for mineral solubility reactions are available, see Nordstrom et al. 1990, Nordstrom and May 1996). The usual goal of such computations is to understand the control of dissolved

major elements in terms of mineral solubilities. Such computations can be used to predict the formation of various mineral species on the basis of saturation indices (SI):

$$SI = \log (IAP/K_{sp}) \quad (11)$$

where IAP is the ion-activity product determined from observed solution concentrations after appropriate activity and speciation calculations are performed, and K_{sp} is the solubility-product constant (Nordstrom and Munoz 1994). Positive SI values indicate supersaturation and negative SI values indicate undersaturation. SI values plotted as a function of a relevant compositional variable, such as pH, should show a linear, horizontal trend close to zero when equilibrium saturation is reached with respect to the stoichiometry of a given mineral. SI calculations (and geochemical modeling in general) require reliable thermodynamic data and certain assumptions regarding chemical equilibrium. Both factors may be of concern when attempting to understand the formation of poorly crystalline Fe and Al hydroxysulfates from acid sulfate waters.

The Fe System

Numerous solutions from mines, mine tailings, and cat clays have been subjected to speciation calculations (van Breeman 1973, Nordstrom 1982a, Chapman et al. 1983, Nordstrom and Ball 1986, Karathanasis et al. 1988, Sullivan et al. 1988a,b; Blowes and Jambor 1990, Winland et al. 1991, Blowes et al. 1998, Nordstrom and Alpers 1999). In most instances, jarosite and ferrihydrite have been assumed to be the phases controlling Fe^{III} activities over relevant pH ranges. Saturation-index plots typically indicate supersaturation with respect to ferrihydrite at pH values above 4 for both surface and ground waters. An example of ferrihydrite supersaturation for about 200 samples collected from Wightman Fork and the Alamosa River system near Summitville, Colorado (Nordstrom et al. 2000) is shown in Figure 13. Supersaturation may be explained either by colloidal Fe particles that were not removed by filtering prior to conducting solution analyses, by incorrect identification of the solid phase, or by sampling artifacts.

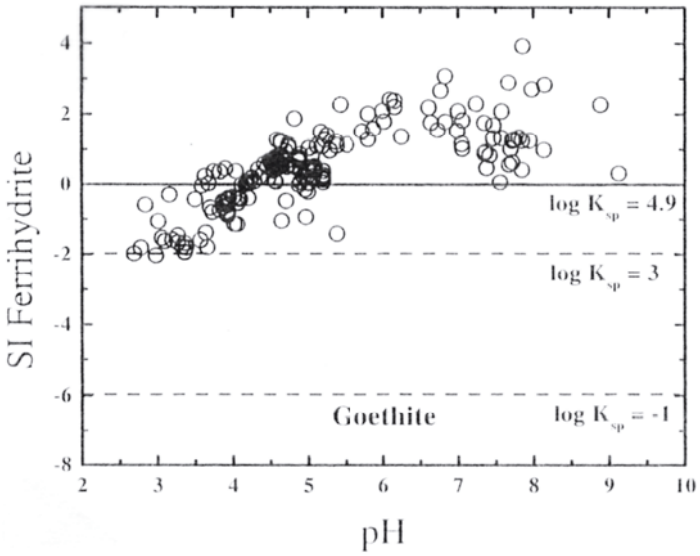

Figure 13. About 200 saturation indices for ferrihydrite plotted against pH for samples from the Summitville-Wightman Fork-Alamosa River system, Colorado.

The stoichiometry of the phase controlling the solubility of Fe can be predicted from an appropriate ion-activity plot. For example, if ferrihydrite is the phase controlling the solubility of Fe^{3+}, the reaction

$$Fe(OH)_{3(s)} + 3H^{+}_{(aq)} \leftrightarrow Fe^{3+}_{(aq)} + 3H_2O_{(l)} \quad (12)$$

and its log equilibrium constant expression

$$\log K = \log a_{Fe}^{3+} - 3\log a_{H}^{+} + 3\log a_{H2O} \quad (13)$$

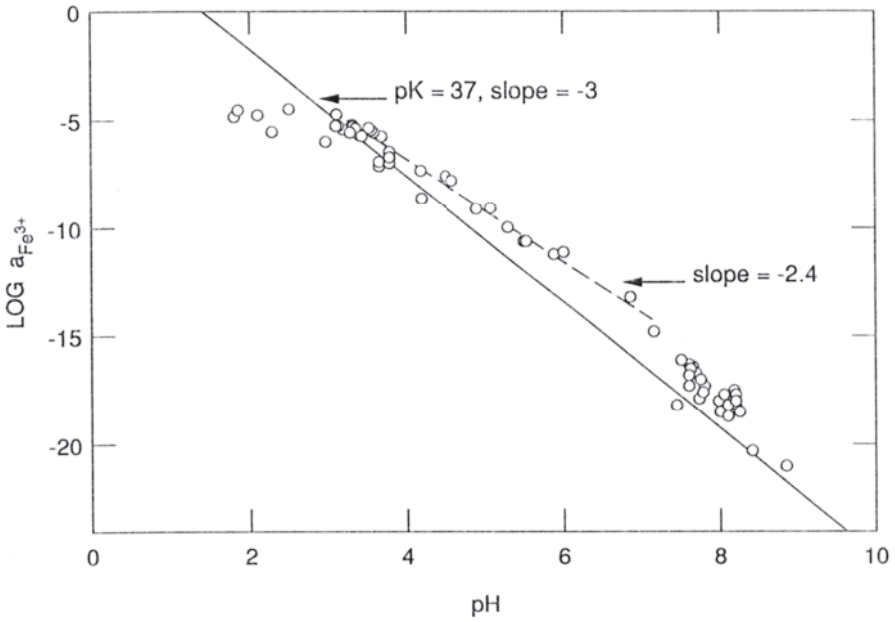

Figure 14. Plot of Fe^{3+} activity against pH for Leviathan mine waters (from Nordstrom 1991, Nordstrom and Alpers 1999). Thesolid line is equilibrium solubility for freshly precipitated ferrihydrite (log K_{sp} = 5.0) and the dashed line shows best fit of data between pH of 3.5 and 7.0 with a slope of -2.4.

would indicate that a plot of Fe^{3+} activity versus pH should have a slope of -3.0. Nordstrom (1991) reported a slope of -2.4 for Fe^{3+} data from mine waters at the Leviathan mine, CA, (Fig. 14). Similar results for mine drainage from St. Kevin Gulch, CO (Kimball et al. 1994), Korea (Yu et al. 1999) and numerous streams in Ohio (Bigham et al. 1996b) suggest that the relationship is fairly universal. The observed slope indicates that another anion, such as SO_4^{2-}, is replacing OH^- in the suspended mineral phase. This would be the case if schwertmannite is controlling the aqueous solubility of Fe^{3+} (Nordstrom 1991); however, the proposed compositional range for schwertmannite [$Fe_8O_8(OH)_{8-2x}(SO_4)_x \cdot nH_2O$ where $1 \le x \le 1.75$] should yield greater slopes, in the range of -2.75 to -2.56. A more likely scenario to explain solubility discrepancies is that mixtures of different Fe minerals, including schwertmannite, precipitate over the pH range represented by acid sulfate waters, and the slope is not clearly resolvable into a particular reaction.

On the basis of mineralogical and chemical analyses of ochreous precipitates and associated waters from Ohio mine drainage, Bigham et al. (1996b) proposed a solubility "window" of log IAP_{sh} = 18.0±2.5 for schwertmannite dissolution according to the reaction:

$$Fe_8O_8(OH)_x(SO_4)_{y(s)} + (24 - 2y)\ H^+_{(aq)} \leftrightarrow 8\ Fe^{3+}_{(aq)} + y\ SO_4^{2-}{}_{(aq)} + (24 - 2y + x)/2\ H_2O_{(l)} \quad (14)$$

and the log equilibrium expression

$$\log K_{sh} = 8 \log a_{Fe^{3+}} + y \log a_{SO_4^{2-}} + (24 - 2y)\ pH \quad (15)$$

Bigham et al. (1996b) also suggested that the discrepancy between observed and calculated slopes in pH vs. log $a_{Fe^{3+}}$ plots for acid sulfate waters was because the data define at least three slopes corresponding to the precipitation of different minerals over the full pH range examined. Mineralogical analyses of the precipitates indicated that those data in the pH range of 1.5 to 2.5 were influenced by the formation of jarosite, those above pH 5.5 by ferrihydrite, and those at intermediate pH values by

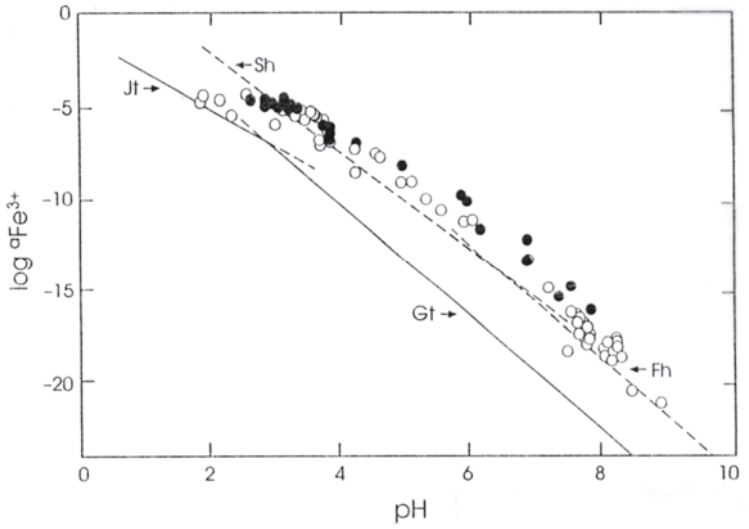

Figure 15. Plot of Fe^{3+} activity against pH for combined data from Ohio (closed circles) and Leviathan mine drainage waters (open circles) with solubility lines for Gt = goethite (log $a_{Fe^{3+}}$ = 1.40 – 3pH), Jt = K-jarosite (log $a_{Fe^{3+}}$ = -0.30 – 2pH), Fh = ferrihydrite (log $a_{Fe^{3+}}$ = 5.0 – 3pH), and Sh = schwert-mannite (log $a_{Fe^{3+}}$ = 2.67 – 2.60pH). Solubility lines calculated using an average log $a_{SO_4^{2-}}$ = -2.32, an average log a_{K^+} = -3.78 (from Nordstrom and Alpers 1999 and used with permission of Elsevier Science from Bigham et al. 1996b).schwertmannite (Fig. 15). Both schwertmannite and ferrihydrite were assumed to be metastable with respect to goethite.

The instability of schwertmannite with respect to goethite was confirmed in a long-term (1740 d) aqueous equilibrium study wherein a pure, synthetic specimen of schwertmannite was completely transformed to goethite over a period of 543 days via the overall reaction:

$$Fe_8O_8(OH)_{5.5}(SO_4)_{1.25(s)} + 2.5\ H_2O_{(l)} \leftrightarrow\ 8\ FeOOH_{(s)} + 2.5\ H^+_{(aq)} + 1.25\ SO_4^{2-}{}_{(aq)} \quad (16)$$

Solution measurements corroborated a decrease in pH and an increase in soluble SO_4^{2-} (Fig. 16). Levels of dissolved $Fe^{3+}_{(aq)}$ temporarily peaked at concentrations that were 0.5 to 1.0 orders of magnitude higher than those represented by the proposed equilibrium situation associated with goethite formation. This phenomenon may also contribute to the frequently reported supersaturation of acid sulfate waters with respect to Fe minerals.

Because the precipitation of schwertmannite may be controlled by not only the activities of H^+ and Fe^{3+}, but also of SO_4^{2-}, Yu et al. (1999) rewrote the dissolution reaction for schwertmannite as:

$$Fe_8O_8(OH)_{8-2x}(SO_4)_{x(s)} + (8 + 2x)\ H_2O_{(l)} \leftrightarrow 8\ Fe^{3+}_{(aq)} + 24\ OH^-_{(aq)} + x\ SO_4^{2-}{}_{(aq)} + 2x\ H^+_{(aq)} \quad (17)$$

so that the solubility relation becomes:

$$(pFe + 3pOH) = -x/8\ (pSO_4 + 2pH) + 1/8\ (pK_s + 24pK_w) \quad (18)$$

where K_w is the dissociation constant for water and K_s is the equilibrium constant for Reaction (17). Equation (18) then generates a line on a plot of (pFe + 3pOH) against (pSO_4 + 2pH) (Fig. 17).

The aqueous geochemistry of Fe is further complicated by the fact that Fe is a reduction–oxidation (redox) active species. The traditional method for delineating the

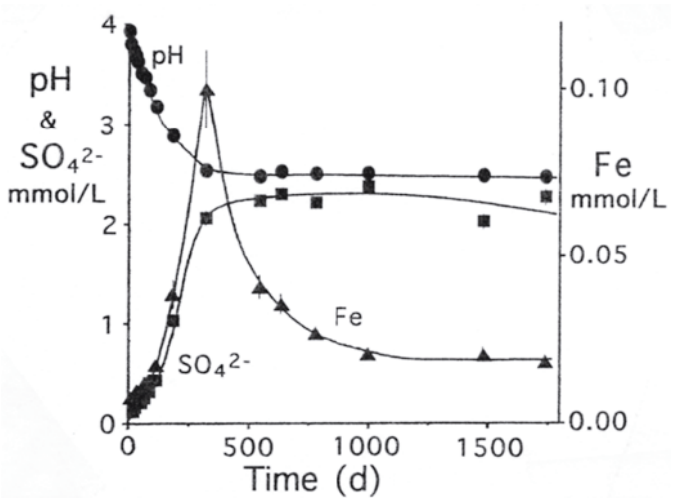

Figure 16. Changes in pH, SO_4 and Fe with time for a beginning suspension of synthetic schwertmannite in water. Goethite with log K_{Gt} = 1.40±0.01 was the final mineral product (modified from Bigham et al. 1996b).

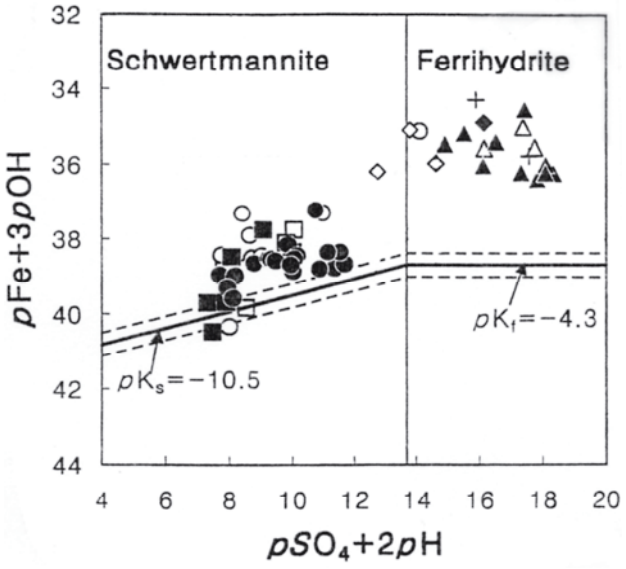

Figure 17. Plot of (pFe + 3pOH) vs. (pSO_4 + 2pH) for mine drainage waters from Korea (filled symbols) and Ohio (open symbols); pK_s and pK_f indicate proposed solubility products for schwert-mannite and ferrihydrite, respectively. Dashed lines indicate proposed error term (±2.5) in the solubility product for schwertmannite (modified from Yu et al. 1999).

stabilities of such species in geochemical systems has been through the use of Eh–pH (or pe–pH) diagrams. Although such diagrams can be very useful for showing general stability relationships among minerals containing redox-sensitive ions, they are also subject to many limitations, as described by Nordstrom and Alpers (1999).

Iron speciation in acid sulfate waters is typically described using diagrams for the Fe–S–K–O_2–H_2O system in which fields for jarosite, goethite, and water are stable phases over relevant pe–pH ranges. It is important to note that stability boundaries between minerals can vary significantly with crystallinity, particle size, and composition (as is reflected in the range of the solubility products reported for both jarosite and goethite). In addition, metastable phases such as schwertmannite and ferrihydrite may form more readily than stable phases, thereby imparting kinetic controls to the system. Using reported log K_{sp} values for jarosite and ferrihydrite, a measured log K_{sp} for goethite, and an apparent log K_{sp} for schwertmannite, Bigham et al. (1996b) proposed a pe–pH diagram for acid sulfate waters with fields of metastability for schwertmannite and

ferrihydrite (Fig. 18). As is often the case, this diagram places constraints on the total log activities of Fe^{2+}, Fe^{3+}, K^+, and SO_4^{2-}. According to Figure 18, jarosite and goethite ultimately control the solubility of Fe in high-pe, acid sulfate waters, and schwertmannite is unstable relative to goethite over the pH range 2 to 6. At higher pH values, ferrihydrite precipitation is kinetically favored, but ferrihydrite is also unstable with respect to goethite.

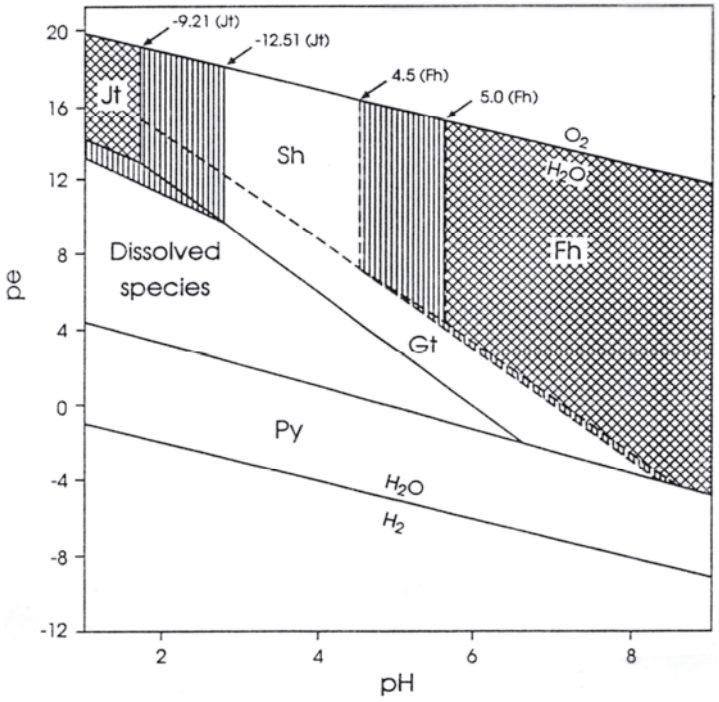

Figure 18. pe-pH diagram for Fe–S–K–O–H system at 25° C where pe = Eh(mV)/59.2, total log activities of $Fe^{2+} = -3.47$, $Fe^{3+} = -3.36$ or -2.27, $SO_4^{2-} = -2.32$, $K^+ = -3.78$. log K_{sp} values are given in Figure 13. Jt = K-jarosite, Sh = schwertmannite, Fh = ferrihydrite, Gt = goethite, and Py = pyrite. Line equations are: Gt (pe = 17.9 – 3pH), Jt (pe = 16.21 – 2pH), Fh (pe = 21.50 – 3pH), Sh (pe = 19.22 – 2.6pH), and Py (pe = 5.39 – 1.14pH). Fields of metastability shown by dashed lines. Single-hatched areas demonstrate expansion of K-jarosite and ferrihydrite fields if lower log K values are chosen from available literature. (used with permission of Elsevier Science from Bigham et al. 1996b).

Field data supporting a paragenetic relationship between jarosite, schwertmannite, ferrihydrite, and goethite have been obtained from a naturally acid alpine stream originating as a spring in talus from a pyritic schist (Schwertmann et al. 1995). Although the spring water (pH 2.3–2.8) was visibly clear, the saturated talus was laden with jarosite, indicating that its precipitation was limited by the release of K^+ from micas occurring in the schist. Downslope, the spring water merged with multiple, non-acid tributaries and produced a strong geochemical gradient. At the first confluence (pH 3.0), schwertmannite precipitated with some goethite. Further dilution down the watercourse eventually raised the solution pH to 7.0 and produced a gradual increase in the proportions of goethite and ferrihydrite in the sediments.

In addition to the Fe^{III} minerals represented in Figure 18, lepidocrocite has been reported as a product of acid sulfate weathering (e.g. Blowes et al. 1991, Milnes et al. 1992). Whereas most Fe^{III}oxides can be synthesized from either Fe^{II} or Fe^{III} salts, lepidocrocite appears to form almost entirely by oxidation of Fe^{II}. It has been identified as a direct pseudomorph after pyrite (Romberg 1969) and pyrrhotite (Jambor 1986), but its formation from Fe^{2+} solutions seems normally to pass through the blue-green (Fe^{II}, Fe^{III})-hydroxy compounds known as green rusts (Schwertmann and Fechter 1994, Lewis 1997). The green rusts have a pyroaurite structure consisting of sheets of $Fe^{II}(OH)_6$ octahedra in which some of the Fe^{II} is replaced by Fe^{III} thereby creating a positive layer charge that is balanced by anions (primarily SO_4^{2-}, Cl^-, and CO_3^{2-}) located between the octahedral sheets. Green rusts are common corrosion products of steel, but they have rarely been identified as occurring in soils (Trolard et al. 1997) or sediments (Bender Koch and Mørup 1991) because they rapidly oxidize to form either goethite or

lepidocrocite through competing reactions that are strongly influenced by solution parameters. Factors that appear to suppress lepidocrocite in favor of goethite formation under laboratory conditions are low pH (<5) and the presence of excess dissolved SO_4^{2-}, HCO_3^-, or Al^{3+} (Schwertmann and Thalmann 1976, Taylor and Schwertmann 1978, Carlson and Schwertmann 1990). If similar factors affect natural systems, the precipitation of lepidocrocite from acid sulfate waters seems unlikely under most conditions.

The Al system

An approach similar to that for Fe has been used for interpreting the behavior of Al in acid sulfate systems, but with somewhat different results. Several plots have been made for log $a_{Al^{3+}}$ against pH with results indicating a solubility control by microcrystalline gibbsite (e.g. Driscoll et al. 1984, Hendershot et al. 1996) for waters having a pH greater than about 4.5. At lower pH values, a clear deviation from this trend is observed (e.g. Losno et al. 1993). Using water samples over a wide range of pH, Al concentrations, and sulfate concentrations from a single watershed in speciation calculations Nordstrom and Ball (1986) showed that two trends are apparent, with a change in slope close to the first hydrolysis constant for Al ($pK_1 = 5.0$) as shown in Figure 19. When the pH is significantly less than pK_1 then Al hydrolysis is insignificant; the Al is little affected by geochemical reactions, and it travels in surface-water systems as if it were a conservative constituent. Once the pH of the water reaches the pK_1, hydrolysis causes the Al to become insoluble and precipitate. Although Neal (1988) has argued that plots of log $a_{Al^{3+}}$ against pH are autocorrelated because pH is used to calculate the activity of free Al so that the plot looks better than it should, this argument is flawed. It is clear from a plot of dissolved Al against dissolved sulfate that the correlation (indicative of conservative solute transport) is excellent for pH values <4.5 and that for higher pH values a sudden decrease in Al concentrations is observed (Nordstrom and Ball 1986). Plotting the saturation indices against specific conductance

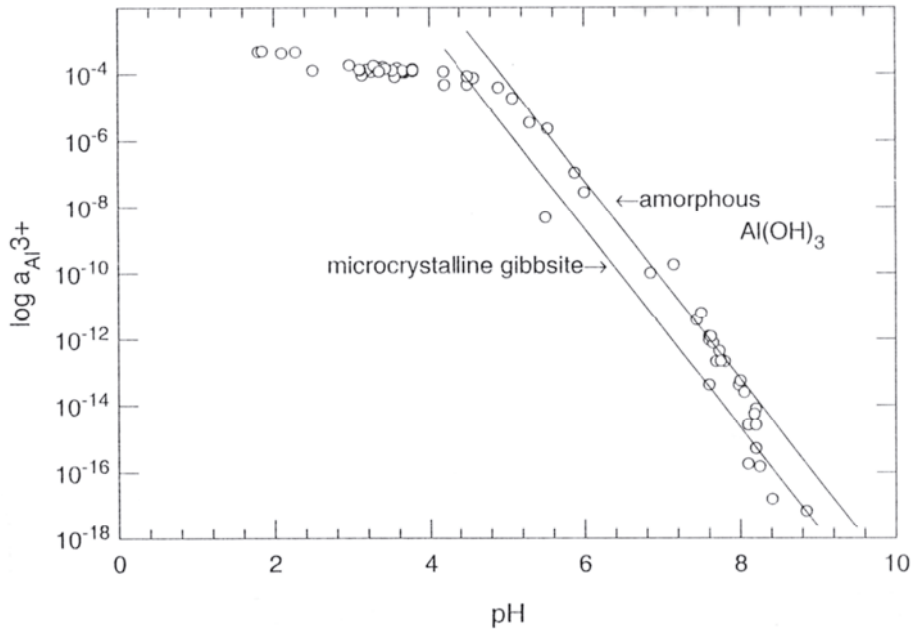

Figure 19. Plot of the log Al^{3+} activity against pH for Leviathan mine waters (from Nordstrom and Alpers 1999). Solid lines show equilibrium solubilities of microcrystalline and amorphous $Al(OH)_3$ to which the data fits well, suggesting an equilibrium solubility control.

or sulfate concentrations or viewing a histogram plot (Nordstrom and Ball 1989) results in the same conclusion. A similar trend can be seen in dilute acid sulfate waters from other watersheds; a distinct change is seen in the behavior of Al from conservative to non-conservative at the same pH value and a similar slope but with a different intercept (May and Nordstrom 1991). It is well known that the first hydrolysis constant greatly affects the chemical behavior and separation of metals (Hem and Roberson 1990, Baes and Mesmer 1976, Rubin 1974), which also explains the tendency for the separation of Al ($pK_1 = 5.0$) and Fe^{III} ($pK_1 = 2.2$).

Solubility data and solubility-product constants for alunite ($\log K_{sp} = -85.4$), crystalline basaluminite ($\log K_{sp} = 117.7$), and amorphous basaluminite ($\log K_{sp} = -116.0$) at 25° C have been determined by Adams and Rawajfih (1977) and seem reasonably consistent with other data (Nordstrom 1982b).

ENVIRONMENTAL IMPLICATIONS OF TRACE ELEMENT SORPTION

Mining activities usually involve ore or coal deposits that have accumulations of such elements as Ag, As, Au, Cd, Co, Cu, Hg, Mo, Ni, Pb, Se, Sb, Tl, and Zn in either economic or sub-economic quantities. These elements occur as mineral sulfides or sulfosalts (sometimes as solid solution impurities) or in gangue minerals. When acid drainage waters are produced by oxidation of mining residues, these elements may be mobilized and transported offsite at concentrations that are sufficiently elevated to be of environmental concern. In such cases, the precipitation of hydroxysulfates and oxyhydroxides of Fe and Al may attenuate the problem by scavenging associated trace elements through processes of adsorption and/or coprecipitation (hereafter referred to collectively as sorption). Although cleansing of attendant drainage waters is a desirable effect, the sediments have a potential for pollution through changing redox conditions and their long-term stability in downstream environments may be a concern.

A substantial body of information has accumulated on the chemical and microbial composition of waters and sediments affected by acid mine drainage, and the reader is referred to recent reviews by Singh et al. (1997), Nordstrom and Southam (1997), Plumlee et al. (1999), Nordstrom and Alpers (1999), and Nordstrom (2000) for a summary of this literature. Smith (1999) has reviewed sorption, especially as it pertains to metal attenuation in mine waste environments. It can generally be concluded that most trace elements, including both cations and oxyanions, tend to accumulate in mine drainage sediments at the expense of associated solutions. Concentration factors vary widely depending on local geochemical and hydrologic conditions. Fuge et al. (1994) examined water and ochre deposits from several metal-sulfide mines in Wales and concluded that As, Mo, Ag, Sn, Sb, Hg, Ba, Tl, Pb, and Bi were strongly concentrated into the solid phase, whereas, other common trace metals (e.g. Mn, Co, Ni, Cu, Zn, Cd) showed less segregation (Fig. 20). In the case of Ba and Pb, metal solubilities may have been controlled by the precipitation of barite ($BaSO_4$) and anglesite ($PbSO_4$), respectively. Other elements were thought to have accumulated primarily by sorption to Fe compounds comprising the ochreous precipitates.

Compared to drainage waters from ore bodies like those in Wales, most drainage waters from coal mines are substantially lower in ionic strength and have lower concentrations of trace contaminants. Nevertheless, significant partitioning of trace elements into Fe and Al precipitates from these waters also occurs. For example, Winland et al. (1991) examined trace-element distributions between solid and aqueous phases at 28 sites in the Ohio coalfield by the use of distribution coefficients (K_d) calculated as:

$$K_d = (\text{mol } X \text{ kg}^{-1} \text{ solid})/(\text{mol } X \text{ L}^{-1} \text{ stream water}) \quad (19)$$

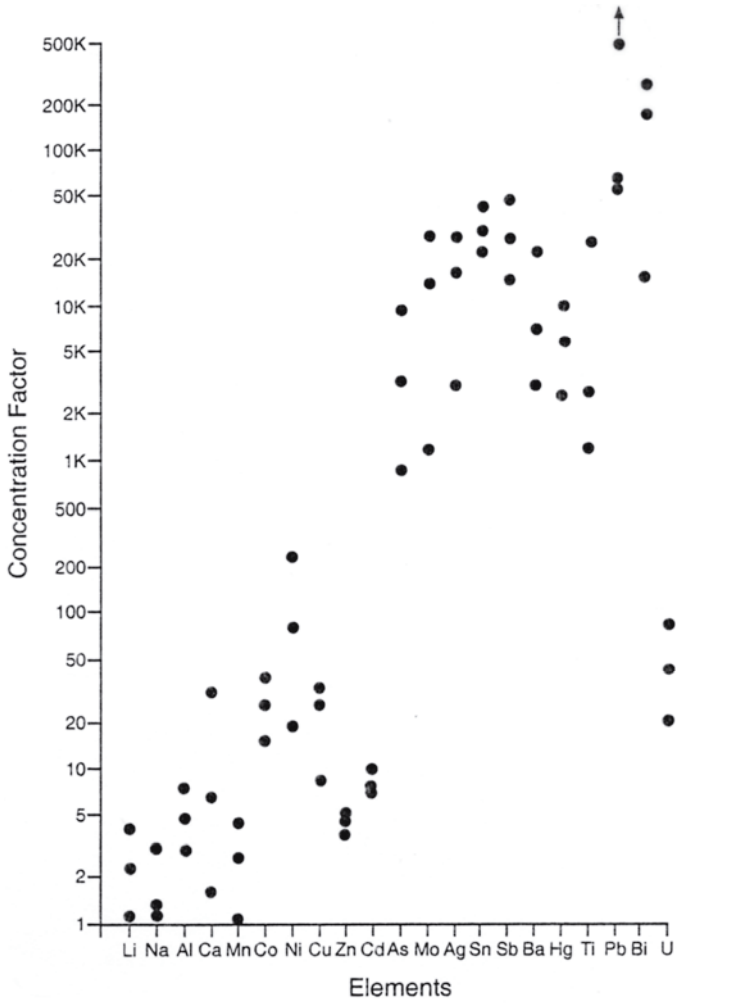

Figure 20. Relationship between ochre and water chemistry in acid mine drainage from Wales; concentration factor = [element conc. in ochre (mg/kg) / element conc. in water (mg/L)] (modified from Fuge et al. 1994).

Table 6. Mean, minimum, and maximum distribution coefficients (K_d) [†] for trace elements from 28 coal mine drainage sites in Ohio[‡].

Element	*Min K_d*	*Max K_d*	*Mean K_d*	*SD*[*]	*N*[**]
As	5.8	6.7	6.3	6.1	9
B	1.8	4.0	3.5	3.3	27
Ba	3.3	5.9	4.9	5.2	27
Co	0.2	3.1	2.3	2.5	21
Cu	2.2	3.4	2.9	2.8	15
Cr	2.5	3.3	3.1	2.8	10
Mn	0.1	4.1	2.9	3.4	28
P	3.0	5.2	4.6	4.6	28
Zn	1.2	3.7	2.9	3.1	27

[†] modified from Winland et al. (1991)
[‡] K_d = (mol *X* kg^{-1} solid)/(mol *X* L^{-1} drainage water)
*SD = standard deviation
**n = number of samples included in the analysis

where *X* is the trace element of interest. As in Fuge et al. (1994), the mean distribution coefficients were determined to be highest for As and Ba and lowest for Co, Cu, Mn and Zn (Table 6).

Bulk chemical analyses of mine drainage waters and sediments are valuable, but they provide little insight into either geochemical factors that control trace-element sorption or the behavior of specific mineral sorbents that may be involved in this process. Relatively few attempts have been made to sort out such interactions in mine drainage environments because of the heterogeneous character of both the mine effluents and the associated chemical precipitates of Fe and Al. An understanding of relevant processes must be based primarily on studies of well-defined systems through experiments completed under controlled conditions. To that end, the adsorption of foreign species at metal-oxide surfaces, especially the Fe and Al oxides, is a subject of widespread interest because of industrial applications and the environmental implications of this process. Consequently, a huge literature has accumulated on this topic over the past few decades. The reader is referred to a number of comprehensive texts and reviews for general information on this subject (e.g. Sposito 1984, Hochella and White 1990, Dzombak and Morel 1990, Stumm 1992, Brown et al. 1999).

Interest in the interfacial chemistry of Fe and Al oxides stems largely from the fact that their surface charge is pH-dependent. Thus, H^+ and OH^- are potential-determining ions whose exchange at the surface is responsible for establishing the net surface charge. Each surface also has a characteristic point of zero charge (pzc), the pH value at which the net surface charge is zero. The net surface charge is positive at pH values below the pzc but becomes negative at pH values higher than the pzc. Experimentally determined pzc values of the Fe and Al oxides, hydroxides, and oxyhydroxides typically range between 5.0 and 9.0 (Parks 1965, 1967; Stumm 1992).

Sorption of metal cations

The development of surface complexes between foreign metal cations and the surface of a hydrous Fe or Al oxide involves coordination of the foreign ion with oxygen donor atoms to form either monodentate or bidentate complexes, with the release of protons as per:

$$\equiv Fe{-}OH + Pb^{2+} \leftrightarrow \equiv Fe{-}OPb^{+} + H^{+} \qquad (20)$$

or

$$\begin{matrix} \equiv Fe{-}OH & & \equiv Fe{-}O \\ \quad | & + Pb^{2+} \leftrightarrow & \quad | \quad \diagdown \\ \equiv Fe{-}OH & & \equiv Fe{-}O \quad \diagup \end{matrix} \quad Pb + 2\,H^{+} \qquad (21)$$

The complexes are considered to be inner-sphere if a mostly covalent bond is formed between the metal and the electron-donating oxygen ions. Otherwise, the complex is outer-sphere, with solute molecules providing separation between the metal and oxide surface. As might be expected, the attraction and binding of a foreign metal ion to an oxide surface is strongly pH dependent and is favored by pH values that produce a net negative surface charge (above the pzc). The formation of inner-sphere complexes with foreign metal ions effectively shifts the pzc of the oxide surface to higher pH values. As shown by Dzombak and Morel (1990), there is a narrow interval of 1-2 pH units where the extent of sorption for each metal on a hydrous iron oxide (ferrihydrite) surface rises from zero to almost 100%, thereby defining a sorption "edge" (Fig. 21a).

Evidence for the pH-dependence of metal sorption to mine-drainage precipitates and for the existence of metal-specific sorption edges is shown in Figure 22 and Table 7. The former (Karlsson et al. 1987) presents the distribution of Pb, Cu, Cd, and Zn between suspended particles and the solution phase in a stream receiving leachates from a deposit

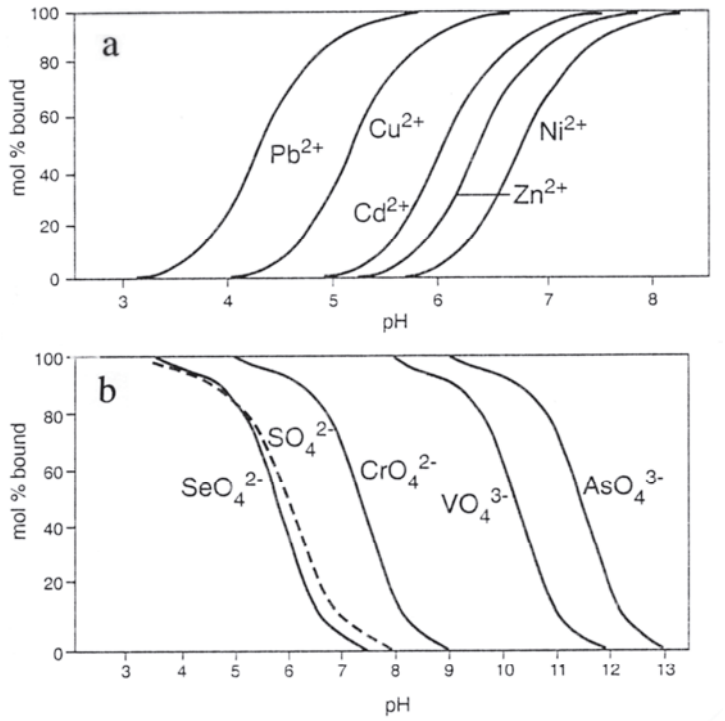

Figure 21. Binding of (a) metal ions and (b) oxyanions to ferrihydrite as a function of pH (modified from Dzombak and Morel 1990).

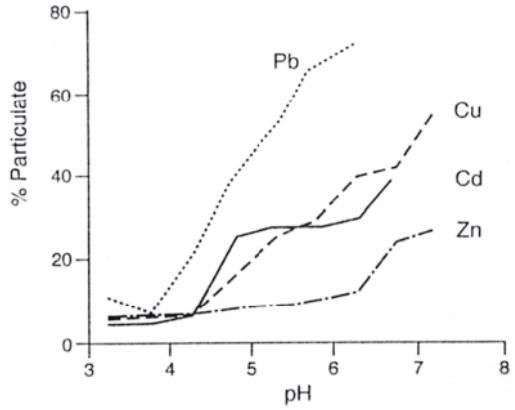

Figure 22. Distribution of metals between suspended precipitates and the solution phase as a function of pH in a stream affected by mine drainage (modified from Karlsson et al. 1987).

Table 7. Concentration factors[†] for selected metals in Welsh ochre deposits as a function of solution pH (modified from Fuge et al. 1994).

Locality[‡]	*1*	*2*	*3*	*4*	*5*	*6*
pH	5.0	3.5	2.9	2.5	2.4	2.3
	----------Concentration factor----------					
Mn	200	51	275	4.3	1.1	2.7
Cu	307,000	19,500	7,380	384	169	111
Zn	382	160	14	3.8	5.2	4.6
Cd	381	333	34	7.6	10	7.6

[†] Concentration factor = [conc. of element in ochre (mg/Kg) / conc. in water (mg/L)].
[‡] Localities: 1 = Y Fan mine; 2 = Gwynfynedd mine; 3 = Cwmrheidol mine; 4,5,6 = Parys Mountain.

of mine tailings. The data show a significant transfer of contaminant species from the solution phase to suspended particulates with increasing downstream pH in the order Pb > Cu ≃ Cd > Zn. The data in Table 7, from Fuge et al. (1994), give concentration factors for selected metals (Mn, Cu, Zn, Cd) in ochre and water samples collected at different pH values from a number of mining localities in Wales. Note that the concentration factors for all metals increase with increasing pH and that the concentration factor for Cu at pH 5 is significantly higher than for Cd and Zn, as would be predicted from the sorption edges in Figure 20a. A number of additional studies (e.g. Filipek et al. 1987, Rampe and Runnels 1989, Webster et al. 1994, Schemel et al. 2000) have demonstrated that Mn and Zn behave as conservative ions at pH < 6 in surface waters affected by mine drainage.

At this point, no information is available concerning the surface-charge properties of schwertmannite or a theoretically corresponding Al hydroxysulfate precipitate from acid sulfate waters. Recently, however, Webster et al. (1998) compared the adsorption of Cu, Pb, Zn, and Cd on synthetic specimens of schwertmannite and 2-line ferrihydrite, as well as a natural mine drainage precipitate composed mostly of goethite. They found that the adsorption edges of all four metals occurred at a lower pH with the natural precipitate; that edges for Pb and Cd were similar for the two synthetic materials; and that the edges for Zn and Cu occurred at a lower pH for schwertmannite as compared to ferrihydrite. Removal of adsorbed sulfate from schwertmannite and the AMD precipitate by titration with $Ba(NO_3)_2$ before conducting the sorption experiments generally decreased the sorption of Pb, Cu, and Zn indicating that adsorbed sulfate may alter electrostatic conditions at the mineral surface or lead to the formation of ternary surface complexes. In another study, it was found that Al precipitates had little effect on metal removal, attenuating Cu slightly and Zn and Ni not at all (Rothenhofer et al. 1999). The only known significant uptake on Al colloids seems to be rare-earth elements (Auque et al. 1993, Gimeno et al. 1994, Nordstrom et al. 1995, Landa et al. 2000).

Sorption of oxyanions

The process of oxyanion accumulation at oxide surfaces can also be described in terms of sorption edges (Dzombak and Morel 1990). Unlike metal cations, however, the sorption of oxyanions decreases with increasing pH because of competition with OH^- and electrostatic repulsion by the negatively-charged oxide surface at pH values above the pzc (Fig. 21b). As with metal cations, the surface complexes formed by oxyanion sorption may be inner-sphere or outer-sphere in character. Inner-sphere sorption may result in both monodentate and bidentate surface complexes, and the latter may be bidentate mononuclear or bidentate binuclear as per:

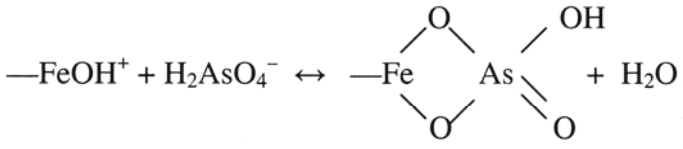

(22)

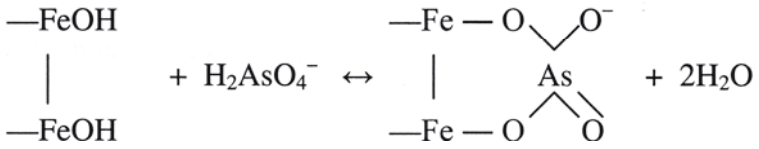

(23)

Trivalent oxyanions, such as PO_4^{3-}, AsO_4^{3-}, and VO_4^{3-}, are much more aggressive in forming inner-sphere complexes as compared to their divalent counterparts (e.g. SO_4^{2-} and SeO_4^{2-}). As a result, the trivalent species yield sorption edges that are non-reversible.

Sulfate is clearly the dominant anion in most acid sulfate waters; therefore, its behavior at the mineral–water interface is important to an understanding of surface-mediated reactions in these systems. There has been considerable controversy regarding the inner-sphere vs. outer-sphere character of sorbed SO_4 (see Myneni, this volume). Macroscopic experiments involving SO_4 sorption on reference minerals and soils have generally been consistent with the formation of outer-sphere complexes because little retention occurs above the mineral pzc, and the ionic strength of the aqueous phase has a large effect on the amount of SO_4 accumulated (e.g. Charlet et al. 1993). Studies involving spectroscopic techniques have generally been less conclusive. For example, early transmission IR studies of SO_4 sorption on iron oxides (e.g. Parfitt and Smart 1978, Harrison and Berkheiser 1982) supported the formation of binuclear bridging surface complexes. More recently, Persson and Lövgren (1996) concluded that the adsorption of SO_4 on goethite was outer-sphere on the basis of results from diffuse reflectance infrared (DRIFT) spectroscopy. In contrast, Hug (1997) identified mainly monodentate, inner-sphere complexes of SO_4 on hematite surfaces between pH 3 and 5 by using *in situ* attenuated total reflection (ATR)-FTIR methods. Peak et al. (1999), employing similar techniques, concluded that SO_4 formed both outer-sphere and inner-sphere surface complexes on goethite at pH < 6. At higher pH values, SO_4 adsorption was entirely outer-sphere.

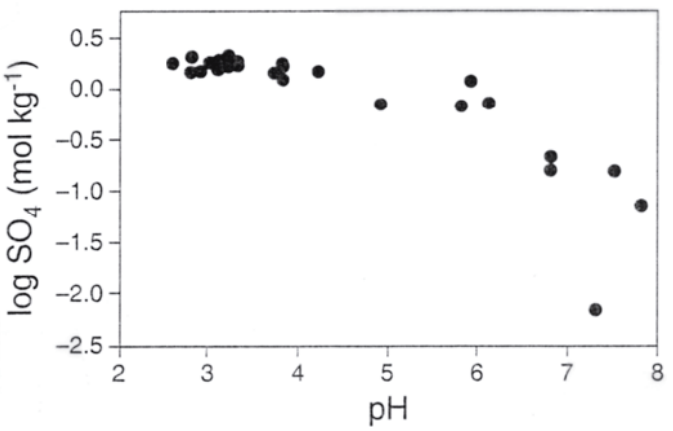

Figure 23. Relationship between solution pH and the concentration of SO_4 in mine drainage precipitates from Ohio (modified from Winland et al. 1991).

Ochreous precipitates from coal-mine drainage in Ohio contain 0.1 to 20 wt % SO_4, and a general decrease in solid-phase SO_4 content was noted with increasing pH of the source waters (Fig. 23) (Winland et al. 1991). Molar Fe/S ratios for mine drainage ochres formed at pH < 5 in the Appalachian region have been reported to range between 3.5 and 10 (Karathanasis and Thompson 1995, Bigham et al. 1996b). Rose and Ghazi (1997) examined the release of SO_4 from such materials in batch experiments involving equilibration of sediments with solutions of various pH values and containing a variety of exchange ligands (nitrate, chloride, bicarbonate, oxalate, phosphate). A significant portion of the total SO_4 load was determined to be labile; at neutral pH (with OH^- as the only exchange ligand), 33-50% of the total was released to solution. Similar results were obtained at neutral pH in the presence of nitrate and chloride, but higher quantities (50-68%) were mobilized when bicarbonate and phosphate were present. The overall results indicated that about 70% of the total sulfate was associated with specific binding sites; that is, as inner-sphere complexes on mineral surfaces or as a structural component in minerals such as schwertmannite and jarosite. Because of similarities in size and valence, the binding characteristics of SeO_4^{2-} should be similar to those of SO_4^{2-} (Waychunas et al. 1995).

Next to SO_4, the most common oxyanions in acid sulfate waters are probably

arsenate (AsO_4^{3-}) and arsenite (AsO_3^{3-}) because of the common occurrence of As as an impurity in pyrite and as a stoichiometric component of such minerals as arsenopyrite (FeAsS) and cobaltite (CoAsS). Accumulations of As have been noted in numerous acid sulfate soils (Dudas 1987, Bowell 1994, Bowell et al. 1994), mine tailings (Moore and Luoma 1990), and mine drainage precipitates (Chapman et al. 1983, Johnson and Thornton 1987, Webster et al. 1994, Bowell and Bruce 1995, Kimball et al. 1995, Hudson-Edwards et al. 1999). Arsenic is extremely toxic to humans, it is a known carcinogen, and it may cause severe health effects even at low concentrations (Morton and Dunnette 1994). Consequently, its bioavailability in soils, sediments and acid leach waters is a major environmental concern.

At pH values <2.0 and AsO_4 concentrations >0.01 molal, the aqueous solubility of AsO_4 may be controlled by the precipitation of scorodite [$FeAsO_4 \cdot 2H_2O$] (Robbins 1990) or its "amorphous" counterpart ($FeAsO_4 \cdot xH_2O$) (Krause and Ettel 1988, Tuovinen et al. 1994). At higher pH values and in solutions with lower AsO_4 activity, the sorption of AsO_4^{3-} at oxide surfaces is thought to be a more important mechanism controlling dissolved As levels. Consequently, As sorption has been widely studied in relation to pH, background electrolyte, and oxidation state (arsenate vs. arsenite) as major experimental variables (e.g. Anderson et al. 1976, Pierce and Moore 1982, Goldberg 1986, Raven et al. 1998). Co-precipitation phenomena involving As and Fe have also been examined by hydrometallurgists as a means of removing As from process wastewaters (e.g. Robins et al. 1988, Papassiopi et al. 1988). Coprecipitation of AsO_4 and Fe^{III} to form ferrihydrite apparently yields smaller particles and higher As site densities than when AsO_4 is adsorbed on pre-formed ferrihydrite (Waychunas et al. 1993, Fuller et al. 1993). By contrast, coprecipitation of AsO_4 destabilizes the structure of schwertmannite and poisons crystal growth (Waychunas et al. 1995).

Mineral instability and possible effects on sorbed species

Laboratory studies of the aging of schwertmannite have shown it to be unstable with respect to goethite (Bigham et al. 1996b), and similar instability has recently been demonstrated under field conditions (Brill 1999, Peine et al. 2000). The transformation gives rise to increased proton and sulfate activities in associated solutions and would presumably have a dramatic effect on sorbed contaminants. However, data to this effect are currently lacking. Variations in dissolved arsenate in a contaminated stream have been coupled to diurnal fluctuations in pH arising from changes in photosynthetic activity as evidenced by the coincidence of pH, arsenate concentrations, and light-intensity maxima (Fuller and Davis 1989). Increases of up to 0.5 pH units during daylight hours apparently caused desorption of arsenate from iron oxyhydroxides in the streambed. The photoreduction of dissolved Fe^{3+} and colloidal Fe minerals may also have a significant impact on the concentrations of Fe^{2+} in oxygenated surface waters. McKnight et al. (1988) found that dissolved Fe^{2+} in a stream impacted by mine drainage reached a maximum during midday. Daytime production of Fe^{2+} occurred at rates that were nearly four times faster than the night–time oxidation of Fe^{2+}. An opposite effect has been observed in mine drainage wetlands, where Fe^{2+} concentrations reached a minimum during daylight hours, apparently due to daytime oxygenation by algae (Wieder 1994). In either case, exposure of acid sulfate waters to the sun could promote cycling of Fe between dissolved and particulate phases with a release of sorbed contaminant species. Alternatively, the generation of fresh mineral surfaces might provide an increased opportunity for sorption of trace elements (McKnight and Bencala 1989).

SUMMARY

Acid sulfate waters provide a complex biogeochemical stage for numerous reactions

involving the weathering, formation, and transformation of minerals. Important secondary precipitates from such waters include hydroxysulfates of Fe (schwertmannite) and Al (primarily hydrobasaluminite). The environmental significance of these compounds stems from the fact that they (1) form spontaneously under pH regimes that are common to most acid sulfate waters; (2) have very short-range structural order which translates to high specific surface area and chemical reactivity with respect to dissolved contaminants; and (3) are metastable with respect to more common oxyhydroxides of Fe and Al. Because of their poor crystallinity, much remains to be learned concerning both their properties and occurrence. When admixed with other minerals commonly found in secondary precipitates from acid sulfate waters, the hydroxysulfates of Fe and Al can be difficult to identify. Considering pH as a master variable, schwertmannite seems to form primarily over the pH range of 2.5-4.5, whereas Al hydroxysulfate is strongly linked to pH values in the range of 4.5-5.5 (Fig. 24). For this reason, aluminous precipitates form as colloids separate from the Fe precipitates and there is little, if any, mutual substitution of Fe in the Al hydroxysulfates and vice versa. Minerals in the jarosite group generally form at lower pH (less than 2.5), and ferrihydrite (perhaps with microcrystalline gibbsite) is a common component of ochreous precipitates formed in the pH range of 6-8. Both schwertmannite and ferrrihydrite are metastable with respect to goethite. Minerals such as hydrobasaluminite and aluminite are metastable with respect to alunite and gibbsite.

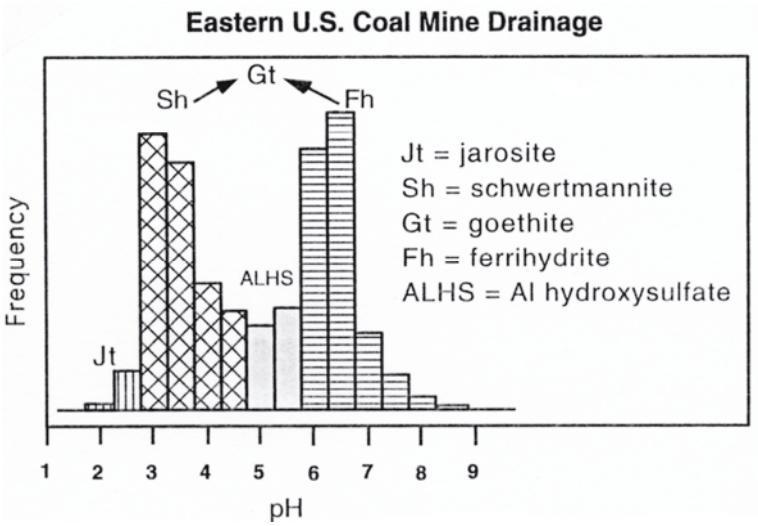

Figure 24. Schematic showing the distribution of common minerals in mine drainage precipitates as a function of pH (modified from Cravotta et al. 1999).

More research is needed to define/refine the chemical and mineralogical properties of schwertmannite and Al hydroxysulfates. The formation of both consumes substantial amounts of sulfate, but the structural role of sulfate has not been rigorously defined in either. Almost nothing is known about the surface characteristics of these minerals or how surface reactivity may vary with changes in environmental parameters. Relevant thermodynamic data have been developed to only rudimentary levels, and information regarding the possiblity of structural solid solution by other metals or oxyanions is lacking. More research is needed to understand better the processes of biomineralization as they relate to both the formation and transformation of schwertmannite and Al hydroxysulfate.

REFERENCES

Adams F, Hajek BF (1978) Effects of solution sulfate, hydroxide, and potassium concentrations on the crystallization of alunite, basaluminite, and gibbsite from dilute aluminum solutions. Soil Sci 126:169-173

Adams F, Rawajfih Z (1977) Basaluminite and alunite: a possible cause of sulfate retention by acid soils. Soil Sci Soc Am J 41:686-692

Alpers CN, Rye RO, Nordstrom DK, White LD, King BS (1992) Chemical, crystallographic, and isotopic properties of alunite and jarosite from acid hypersaline Australian lakes. Chem Geol 96:203-226

Alpers CN, Blowes DW, Nordstrom DK, Jambor JL (1994) Secondary minerals and acid mine-water chemistry. *In* The Environmental Geochemistry of Sulfide Mine-Wastes. Jambor JL, Blowes DW (Eds) Mineral Assoc Canada Short Course 22:249-270

Alvarez E, Perez A, Calvo R (1993) Aluminum speciation in surface waters and soil solutions in areas of sulfide mineralization in Galicia. Sci Total Environ 133:17-37

Anderson MA, Ferguson JF, Gavis J (1976) Arsenate adsorption on amorphous aluminum hydroxide. J Colloid Interface Sci 54:391-399

Anthony JW, McLean WJ (1976) Jurbanite, a new post-mine aluminum sulfate mineral from San Manuel, Arizona. Am Mineral 61:1-4

Ash SH, Felegy EW, Kennedy DO, Miller PS (1951) Acid Mine Drainage Problems—Anthracite Region of Pennsylvania. US Bur Mines Bull 508

Auqué LF, Tena JM, Gimeno MJ, Mandado J, Zamora A, Ló pez-Julian P (1993) Distribució n de tierras raras en soluciones y coloides de un sistema natural de aguas ácidas (Arroyo del Val, Zaragoza). Est Geol 49:41-48

Baes CF Jr, Mesmer RE (1976) The Hydrolysis of Cations. Wiley-Interscience, New York

Ball JW, Nordstrom DK (1989) Final revised anaylyses of major and trace elements from acid mine waters in the Leviathan mine drainage basin, California and Nevada—October 1981 to October 1982. US Geol Survey Water-Res Invest Peport 89-4138, 49 p

Bannister FA, Hollingworth SE (1948a) Two new British minerals. Nature 162:565

Bannister FA, Hollingworth SE (1948b) Basaluminite hydrobasaluminite. Am Mineral 33:787

Barham RJ (1997) Schwertmannite: A unique mineral, contains a replaceable ligand, transforms to jarosites, hematite, and/or basic iron sulfate. J Mater Res 12:2751-2758

Barnhisel RI, Daniels WL, Darmondy RG (2000) Reclamation of Drastically Disturbed Lands. Am Soc Agron Monograph No 41. Am Soc Agron, Madison, Wisconsin

Barton P (1978) The acid mine drainage. *In* Sulfur in the Environment, Part II. Ecological Impacts. Nriagu JO (Ed) John Wiley and Sons, New York, p 313-358

Batik P, Hruskova J (1971) Hydrobasaluminite and basaluminite from Nikolcice near Brno. Czech Sb Nar Muz Praze Rada B 27:9-16

Bassett H, Goodwin TH (1949) The basic aluminum sulphates. J Chem Soc:2239-2279

Bender Koch C, Mørup S (1991) Identification of green rust in an ochre sludge. Clay Minerals 26:577-582

Bertsch PM, Parker BR (1996) Aqueous polynuclear aluminum species. *In* The Environmental Chemistry of Aluminum. Sposito G (Ed) CRC/Lewis Publishers, Boca Raton, Florida, p 117-168

Beukes GJ, Schoch AE, De Bruiyn H, Van der Westhuizen WA, Bok LDC (1984) A new occurrence of the hydrated aluminum sulfate zaherite, from Pofadder, South Africa. Mineral Mag 48:131-135

Bhatti TM, Bigham JM, Carlson L, Tuovinen OH (1993) Mineral products of pyrrhotite oxidation by *Thiobacillus ferrooxidans.* Appl Environ Microbiol 59:1984-1990

Bhatti TM, Bigham JM, Vuorinen A, Tuovinen OH (1994) Alteration of mica and feldspar associated with the microbial oxidation of pyrrhotite and pyrite. *In* The Environmental Geochemistry of Sulfide Oxidation. Alpers CN, Blowes DW (Eds) Am Chem Soc Symp Series 550: 90-105

Biedermann G, Chow TJ (1966) Studies on the hydrolysis of metal ions 57. The hydrolysis of the iron (III) ion and the solubility product of $Fe(OH)_{2.7}Cl_{0.3}$ in 0.5 M $(Na^+)Cl^-$ medium. Acta Chem Scand 20:1376-1388

Biedermann G, Schindler P (1957) On the solubility product of precipitated iron (III) hydroxide. Acta Chem Scand 11:731-740

Bigham JM (1994) Mineralogy of ochre deposits formed by sulfide oxidation. *In* The Environmental Geochemistry Of Sulfide Mine-Wastes. Jambor JL, Blowes DW (Eds) Mineral Assoc Canada Short Course 22:103-132

Bigham JM, Schwertmann U, Carlson L, Murad E (1990) A poorly crystallized oxyhydroxysulfate of iron formed by bacterial oxidation of Fe(II) in acid mine waters. Geochim Cosmochim Acta 54:2743-2758

Bigham JM, Schwertmann U, Carlson L (1992) Mineralogy of precipitates formed by the biogeochemical oxidation of Fe(II) in mine drainage. *In* Biomineralization Processes of Iron And Manganese—Modern

and Ancient Environments. Skinner HCW, Fitzpatrick RW (Eds) Catena Supplement 21:219-232, Cremlingen-Destedt
Bigham JM, Carlson L, Murad E (1994) Schwertmannite, a new iron oxyhydroxysulfate from Pyhä salmi, Finland, and other localities. Mineral Mag 58:641-64
Bigham JM, Schwertmann U, Pfab G (1996a) Influence of pH on mineral speciation in a bioreactor simulating acid mine drainage. Appl Geochem 11:845-849
Bigham JM, Schwertmann U, Traina SJ, Winland RL, Wolf M (1996b) Schwertmannite and the chemical modeling of iron in acid sulfate waters. Geochim Cosmochim Acta 60:2111-2121
Bishop JL (1998) Biogenic catalysis of soil formation on Mars. Origins Life Evol Biosphere 28:449-459
Bishop JL, Murad E (1996) Schwertmannite on Mars? Spectroscopic analyses of schwertmannite, its relationship to other ferric minerals, and its possible presence in the surface material on Mars. *In* Mineral Spectroscopy: A Tribute to Roger G Burns. Dyar MD, McCammon C, Schaefer MW (Eds) Geochemical Society Spec Publ No 5:337-358
Bloomfield C (1972) The oxidation of iron sulphides in soils in relation to the formation of acid sulphate soils, and of ochre deposits in field drains. J Soil Sci 23:1-16
Bloomfield C, Coulter JK (1973) Genesis and management of acid sulfate soils. Adv Agron 25:265-326
Blowes DW, Jambor JL (1990) The pore-water geochemistry and the mineralogy of the vadose zone of sulfide tailings, Waite Amulet, Quebec, Canada. Appl Geochem 5:327-346
Blowes DW, Reardon EJ, Jambor J, Cherry JA (1991) The formation and potential importance of cemented layers in inactive sulfide mine tailings. Geochim Cosmochim Acta 55:965-978
Blowes DW, Al T, Lortie L, Gould WD, Jambor JL (1995) Microbiological, chemical, and mineralogical characterization of the Kidd Creek mine tailings impoundment, Timmins area, Ontario. Geomicrobiol J 13:13-21
Blowes DW, Jambor JL, Hanton-Fong CJ, Lortie L, Gould WD (1998) Geochemical, mineralogical and microbiological characterization of a sulphide-bearing carbonate-rich gold-mine tailings impoundment, Joutel, Qué bec. Appl Geochem 13:687-705
Bowell RJ (1994) Sorption of arsenic by iron oxides and oxyhydroxides in soils. Appl Geochem 9:279-286
Bowell RJ, Bruce I (1995) Geochemistry of iron ochres and mine waters from Levant Mine, Cornwall. Appl Geochem 10:237-250
Bowell RJ, Morley NH, Din VK (1994) Arsenic speciation in soil porewaters from the Ashanti Mine, Ghana. Appl Geochem 9:15-22
Brizzi G, Ciselli I, Santucci A (1986) Geology of the Cetine mine, Siena, Italy. Riv Mineral Ital:145-155
Brady KS, Bigham JM, Jaynes WF, Logan TJ (1986) Influence of sulfate on Fe-oxide formation: Comparisons with a stream receiving acid mine drainage. Clays Clay Minerals 34:266-274
Brill MR (1999) Sediment mineralogy and geochemistry in a constructed mine drainage wetland. MS Thesis, The Ohio State University, Columbus, Ohio
Brodie GA, Hammer DA, Tomljanovich DA (1988) Constructed wetlands for acid drainage control in the Tennessee Valley. *In* Mine Drainage and Surface Mine Reclamation. US Bur Mines Inf Circ 9183: 325-331
Brown GE Jr, Henrich VE, Casey WH, Clark DL, Eggleston C, Felmy A, Goodman DW, Grä tzel M, Maciel G, McCarthy MI, Nealson KH, Sverjensky DA, Toney MF, Zachara JM (1999) Metal oxide surfaces and their interactions with aqueous solutions and microbial organisms. Chem Rev 99: 77-174
Burns RG (1988) Gossans on Mars. Proc 18th Lunar Planet Sci Conf LPI, Houston, p 713-721
Burns RG (1994) Schwertmannite on Mars: Deposition of this ferric oxyhydroxysulfate mineral in acidic saline meltwaters Lunar Planet Sci 25:203-204 (abstr)
Byrne RH, Luo Y-R (2000) Direct observations of nonintegral hydrous ferric oxide solubility products. Geochim Cosmochim Acta 64:1873-1877
Carlson L, Schwertmann U (1990) The effect of CO_2 and oxidation rate on the formation of goethite versus lepidocrocite from an Fe(II) system at pH 6 and 7. Clay Minerals 25:65-71
Caruccio FT (1975) Estimating the acid potential of coal mine refuse. *In* The Ecology of Resource Degradation and Renewal, Chadwick MJ, Goodman GT (Eds) Blackwell Science, London:197-203
Cathles LM (1994) Attempts to model the industrial-scale leaching of copper-bearing mine waste. *In* The Environmental Geochemistry of Sulfide Oxidation. Alpers CN, Blowes DW (Eds) Am Chem Soc Symp Ser 550:123-131
Cech F (1979) A new name for orthorhombic $Al(SO_4)(OH)\cdot 5H_2O$. N Jahrb Mineral Monatsch:193-196
Cesbron FP, Bayliss P (1988) Mineral nomenclature: Khademite. Mineral Mag 52:133-134
Chapman BM, Jones DR, Jung RF (1983) Processes controlling metal ion attenuation in acid mine drainage streams. Geochim Cosmochim Acta 47:1957-1973
Charlet L, Dise N, Stumm W (1993) Sulfate adsorption on a variable charge soil and on reference minerals. Agric Ecosys Environ 47:87-102

Chernitsyna OM, Artemenko VM, Artemenko OV, Ponomarev VE (1999) Aluminite from gold-mercury ores in terrigenous-carbonate complex of southern Donbass. Mineral Zh 21: 29-32

Childs CW, Goodman BA, Paterson E, Woodhams FWD (1980) The nature of iron in akaganéite (β-FeOOH). Aust J Chem 33:15-26

Childs CW, Inoue K, Mizota C (1997) Natural and anthropogenic schwertmannites from Towada-Hachimantai National Park, Honshu, Japan. Chem Geol 144:81-86

Clark BC, Baird AK, Weldon RJ, Tsusaki DM, Schnabel L, Candelaria MP (1982) Chemical composition of martian fines. J Geophys Res 87:10059-10067

Clark BC, Van Hart D (1981) The salts of Mars. Icarus 45:370-378

Clarke W, Konhauser KO, Thomas J, Bottrell SH (1997) Ferric hydroxide and ferric hydroxysulfate precipitation by bacteria in an acid mine drainage lagoon. FEMS Microbiol Rev 20:351-361

Clayton T (1980) Hydrobasaluminite and basaluminite from Chickerell, Dorset. Mineral Mag 43:931-937

Cornell R, Schwertmann U (1996) The Iron Oxides. VCH Publishers, Weinheim

Cornu F (1909) Über die Verbreitung gelartiger Körper im Mineralbereich, ihrre chemisch-geologische Bedeutung und ihre systematische Stellung. Zbl Mineral Geol 12:324-326

Cravotta CA III, Brady KBC, Rose AW, Douds JB (1999) Frequency distribution of the pH of coal-mine drainage in Pennsylvania. *In* U.S. Geological Survey Toxic Substances Hydrology Program—Proc Technical Meeting. Morganwalp DW, Buxton H (Eds) US Geol Surv Water-Res Invest Rep 99-4018A:313-324

Cunningham KM, Wright WG, Nordstrom DK, Ball JW (1996) Water-quality data for Doughty Springs, Delta County, Colorado, 1903-1994, with emphasis on sulfur redox species. US Geol Survey Open-File Rep 96-619, 69 p

De Bruiyn H, Schoch AE, Beukes GJ, Bok LDC, Van Der Westhuizen WA (1985) Note on cell parameters of zaherite. Mineral Mag 49:145-146

De Endredy A S (1963) Estimation of free iron oxides in soils and clays by a photolytic method. Clay Minerals 5:209-217

Dent DL, Pons LJ (1995) A world perspective on acid sulphate soils. Geoderma 67:263-276

Dold B (1999) Mineralogical and geochemical changes of copper flotation tailings in relation to their original composition and climatic setting: Implications for acid mine drainage and element mobility. PhD Thesis #3125, Université de Genève, Switzerland

Dombrovskaya ZV, Yashina RS, Piloyan GO (1976) Aluminite from the zone of oxidation of pyritized schists in the Lake Baikal region. Kora Vyvetrivaniya 15:162-167

Doner HE, Lynn WC (1989) Carbonate, halide, sulfate and sulfide minerals. *In* Minerals in Soil Environments. 2nd edition. Dixon JB, Weed SB (Eds) Soil Sci Soc Am, Madison, Wisconsin, p 279-330

Dousma J, de Bruyn PL (1976) Hydrolysis-precipitation studies of iron solutions I. Model for hydrolysis and precipitation from Fe(III) nitrate solutions. J Colloid Interface Sci 56:527-539

Dousma J, van den Hoven TJ, de Bruyn PL (1978) The influence of chloride ions on the formation of iron(III) oxyhydroxide. J Inorg Nucl Chem 40:1089-1093

Dousma J, den Ottelander D, de Bruyn PL (1979) The influence of sulfate ions on the formation of iron(III) oxides. J Inorg Nucl Chem 41:1565-1568

Driscoll CT, Baker JP, Bisogni JJ, Schofield CL (1984) Aluminum speciation and equilibria in dilute acidic surface waters of the Adirondack region of New York State. *In* Geological Aspects of Acid Deposition, 4:55-75. Bricker OP (Ed) Ann Arbor Science, Boston

Dudas MJ (1987) Accumulation of native arsenic in acid sulphate soils in Alberta. Can J Soil Sci 67: 317-331

Dzombak DA, Morel FMM (1990) Surface Complexation Modeling: Hydrous Ferric Oxide. John Wiley, New York

Edwards KJ, Bond PL, Gihring TM, Banfield F (2000) An archaeal iron-oxidizing extreme acidophile important in acid mine drainage. Science 287:1796-1799

Ehrlich HL (1996) Geomicrobiology (3rd Edition) Marcel Dekker, New York

Fanning DS, Burch SN (1997) Acid sulphate soils and some associated environmental problems. *In* Soils and Environment: Soil Processes from Mineral to Landscape Scale. Auerswald K, Stanjek H, Bigham JM (Eds) Adv. Geoecol 30:145-158, Reiskirchen, Catena Verlag

Fanning DS, Rabenhorst MC, Bigham JM (1993) Colors of acid sulfate soils. *In* Soil color. Bigham JM, Ciolkosz EJ (Eds) Soil Sci Soc Am Spec Publ 31:91-108 Soil Sci Soc Am, Madison, WI.

Farkas L, Pertlik F (1997) Crystal structure determinations of felsőbányaite and basaluminite, $Al_4(SO_4(OH)_{10} \cdot 4H_2O$. Acta Mineral-Petrogr 38:5-15

Feitknecht W, Giovanoli R, Michaelis W, Müller M (1973) Über die Hydrolyse von Eisen (III) Salzlösungen. I. Die Hydrolyse der Lösungen von Eisen (III) Chlorid. Helv Chim Acta 56:2847-2856

Fennessy MS, Mitsch WJ (1989) Treating coal mine drainage with an artificial wetland. Res J Water Pollut Cont Fed 61:1691-1701

Ferris FG, Tazaki K, Fyfe WS (1989a) Iron oxides in acid mine drainage environments and their association with bacteria. Chem Geol 74:321-330

Ferris FG, Schultze S, Witten TC, Fyfe WS, Beveridge TJ (1989b) Metal interactions with microbial biofilms in acidic and neutral pH environments. Appl Environ Microbiol 55:1249-1257

Filipek LH, Nordstrom DK, Ficklin WH (1987) Interaction of acid mine drainage with waters and sediments of West Squaw Creek in the West Shasta Mining District, California. Environ Sci Technol 21:388-396

Fischer WR (1972) Die Wirkung von zweiwertigem Eisen auf Lösung un Umwandlung von Eisen(III)-hydroxiden. *In* Pseudogley und Gley. Schlichting E, Schwertmann U (Eds) Weinheim, Verlag Chemie, p 37-44

Fitzpatrick RW, Self PG (1997) Iron oxyhydroxides, sulfides and oxyhydroxysulfates as indicators of acid sulfate weathering environments. *In* Soils and Environment: Soil Processes from Mineral to Landscape Scale. Auerswald K, Stanjek H, Bigham JM (Eds) Adv. Geoecol 30:227-240, Reiskirchen, Catena Verlag

Fitzpatrick R W, Naidu R, Self PG (1992). Iron deposits and microorganisms in saline sulfidic soils with altered soil water regimes in South Australia. *In* Biomineralization Processes of Iron and Manganese—Modern and Ancient Environments. Skinner HCW, Fitzpatrick RW (Eds) Catena Supplement 21: 263-286, Cremlingen-Destedt

Fitzpatrick R. W, Fritsch E, Self PG (1996) Interpretation of soil features produced by ancient and modern processes in degraded landscapes: V. Development of saline sulfidic features in non-tidal seepage areas. Geoderma 69:1-29

Flynn CM Jr (1990) Dense hydrolysis products from iron (III) nitrate and sulfate solutions. Hydrometall 25:257-270

Fojt B (1975) On the problem of glockerite as a secondary mineral of ore deposits. Scripta Fac Sci Nat UJEP Brunensis, Geologia I. 5:5-20

Fox LE (1988a) Solubility of colloidal ferric hydroxide. Nature 333:442-444

Fox LE (1988b) The solubility of colloidal ferric hydroxide and its relevance to iron concentrations in river water. Geochim Cosmochim Acta 52:771-777

Fox LE (1989) A model for inorganic control of phosphate concentrations in river waters. Geochim Cosmochim Acta 53:417-428

Frondel C (1968) Meta-aluminite, a new mineral from Temple Mountain, Utah. Am Mineral 53:717-721

Fuge R, Pearce FM, Pearce NJ, Perkins WT (1994) Acid mine drainage in Wales and influence of ochre precipitation on water chemistry. *In* The Environmental Geochemistry of Sulfide Oxidation. Alpers CN, Blowes DW (Eds) Am Chem Soc Symp Series 550:261-274

Fuller CC, Davis JA (1989) Influence of coupling of sorption and photosynthetic processes on trace element cycles in natural waters. Nature 340:52-54

Fuller CC, Davis JA, Waychunas GA (1993) Surface chemistry of ferrihydrite: Part 2. Kinetics of arsenate adsorption and coprecipitation. Geochim Cosmochim Acta 57:2271-2282

Furniss G, Hinman NW, Doyle GA, Runnells DD (1999) Radiocarbon-dated ferricrete provides a record of natural acid rock drainage and paleoclimatic changes. Environ Geol 37:102-106

Gimeno MJ, Tena JM, Auqué LF, Mandado J (1994) Caracterización geoquímica del sistema de agues ácidas del Arroyo del Val (Zaragoza). Bol R Soc Esp Hist Nat (Sección Geología) 89:5-17

Glocker EF (1853) Über einen neuen Eisensinter von Obergrund bie Zuckmantel. Poggendorff's Annalen Physik Chemie 89:482-488

Glocker EF (1858) Über den sulphatischen Eisensinter von Obergrund bei Zuckmantel. Acta Nova Leopold Carol 26:189-220

Godin E (Ed) (1991) Canadian Minerals Yearbook—Review and Outlook. Energy, Mines and Resources, Ottawa, Canada

Goldberg S (1986) Chemical modeling of arsenate adsorption on aluminum and iron oxide minerals. Soil Sci Soc Amer J 50:1154-1160

Gould WD, Bé chard G, Lortie L (1994) The nature and role of microorganisms in the tailings environment. *In* The Environmental Geochemistry of Sulfide Mine-Wastes. Jambor JL, Blowes DW (Eds) Mineral Assoc Canada Short Course 22:185-200

Hammack RW, Lau RW, Diehl JR (1988) Methods for determining fundamental chemical differences between iron disulfides from different geologic provenances. US Bur Mines Inf Circ IC-9183:136-146

Harrison JB, Berkheiser VE (1982) Anion interactions with freshly prepared hydrous iron oxides. Clays Clay Minerals 30:97-102

Headden WP (1905) Mineralogical notes, no. II. Proc Colorado Sci Soc 8:62-66

Hem JD, Roberson CE (1990) Aluminum hydrolysis reactions and products in mildly acidic aqueous systems. *In* Chemical modeling in aqueous systems II. Melchior DC, Bassett RL (Eds) Am Chem Soc Symp Series 416:429-446

Hemley JJ, Hostetler PB, Gude AJ, Mountjoy WT (1969) Some stability relations of alunite. Econ Geol 64:599-612

Hendershot WH, Courchesne F, Jeffries DS (1996) Aluminum geochemistry at the catchment scale in watersheds influenced by acidic precipitation. *In* The Environmental Chemistry of Aluminum. 2nd Edition. Sposito G (Ed) CRC Press/Lewis Publishers, Boca Raton, Florida, p 419-449

Hochella MF Jr, White AF (Eds) (1990) Mineral-Water Interface Geochemistry. Rev Mineral 23, Mineral Soc Am, Washington, DC, 603 p

Hudson-Edwards KA, Schell C, Macklin MG (1999) Mineralogy and geochemistry of alluvium contaminated by metal mining in the Rio Tinto area, southwest Spain. Appl Geochem 14:1015-1030

Hug SJ (1997) *In situ* Fourier transform infrared measurements of sulfate adsorption on hematite in aqueous solutions. J Colloid Interface Sci 188:415-422

Jambor JL (1986) Detailed mineralogical examination of alteration products in core WA-20 from Waite Amulet tailings. CANMET Div Rep MSL 86-137(IR). Dep Energy Mines Res Canada.

Jambor JL (1994) Mineralogy of sulfide-rich tailings and their oxidation products. *In* The Environmental Geochemistry of Sulfide Mine-Wastes. Jambor JL, Blowes DW (Eds) Mineral Assoc Canada Short Course Vol. 22:59-102

Jambor JL Dutrizac JE (1998) Occurrence and consititution of natural and synthetic ferrihydrite, a widespread iron oxyhydroxide. Chem Rev 98:2549-2585

Jambor JL, Grew ES, Roberts AC (1998) New mineral names. Am Mineral 83:1347-1352

Johansson G (1962) The crystal structure of $[Al_2(OH)_2(H_2O)_8](SO_4)_2 \cdot 2H_2O$ and $[Al_2(OH)_2(H_2O)_8](SeO_4)_2 \cdot 2H_2O$. Acta Chem Scand 16:403-420

Johansson G (1963) On the crystal structure of the basic aluminum sulfate $13Al_2O_3 \cdot SO_3 \cdot xH_2O$. Arkiv Kemi 20:321-342

Johnson CA, Thornton I (1987) Hydrological and chemical factors controlling the concentrations of Fe, Cu, Zn and As in a river system contaminated by acid mine drainage. Water Res 21:359-365

Karathanasis AD, Evangelou VP, Thompson, YL (1988) Aluminum and iron equilibria in soil solutions and surface waters of acid mine watersheds. J Environ Qual 17:534-543

Karathanasis AD, Thompson YL (1995) Mineralogy of iron precipitates in a constructed acid mine drainage wetland. Soil Sci Soc Am J 59:1773-1781

Karlsson S, Sandén P, Allard B (1987) Environmental impacts of an old mine tailings deposit—metal adsorption by particulate matter. Nordic Hydrol 18:313-324

Kimball BA, Broshears RA, McKnight DM, Bencala KE (1994) Effects of instream pH modification on transport of sulfide-oxidation products. *In* The Environmental Geochemistry of Sulfide Oxidation. Am Chem Soc Symp Series 550:224-243, Am Chem Soc, Washington, DC

Kimball BA, Callender E, Axtmann EV (1995) Effects of colloids on metal transport in a river receiving acid mine drainage, upper Arkansas River, Colorado, U.S.A. Appl Geochem 10:285-306

Kirby CS, Decker SM, Macander NK (1999) Comparison of color, chemical and mineralogical compositions of mine drainage sediments to pigment. Environ Geol 37:243-254

Kleinmann RLP (1989) Acid mine drainage in the United States: Controlling the impact on streams and rivers. *In* 4th World Congress on the Conservation of Built and Natural Environments, Univ Toronto, p 1-10

Kleinmann RLP, Crerar DA, Pacelli RR (1981) Biogeochemistry of acid mine drainage and a method to control acid formation. Mining Eng 33:300-303

Konhauser KO (1998) Diversity of bacterial iron mineralization. Earth Sci Rev 43:91-121

Konhauser KO, Ferris FG (1996) Diversity of iron and silica precipitation by microbial mats in hydrothermal waters, Iceland: Implications for Precambrian iron formations. Geology 24:323-326

Kram P, Hruska J, Driscoll CT, Johnson CE (1995) Biogeochemistry of aluminum in a forest catchment in the Czech Republic impacted by atmospheric inputs of strong acids. Water Air Soil Pollut 85:1831-1836

Krause E, Ettel VA (1988) Solubility and stability of scorodite, $FeAsO_4 \cdot H_2O$: New data and further discussion. Am Mineral 73:850-854

Landa ER, Cravotta CA III, Naftz DL, Verplanck PL, Nordstrom DK, and Zielinski RA (2000) Geochemical investigations by the U.S. Geological Survey on uranium mining, milling, and environmental restoration. Tech 7:381-396

Lazaroff N, Sigal W, Wasserman, A (1982) Iron oxidation and precipitation of ferric hydroxysulfates by resting *Thiobacillus ferrooxidans* cells. Appl Environ Microbiol 43:924-938

Lazaroff N, Melanson L, Lewis E, Santoro N, Pueschel C (1985) Scanning electron microscopy and infrared spectroscopy of iron sediments formed by *Thiobacillus ferrooxidans*. Geomicrobiol J 4:231-268

Lees H, Kwok SC, Suzuki I (1969) The thermodynamics of iron oxidation by ferrobacilli. Can J Microbiol 15:43-46

Letterman RD, Mitsch WJ (1978) Impact of mine drainage on a mountain stream in Pennsylvania. Environ Pollut 17:53-73

Lewis DG (1997). Factors influencing the stability and properties of green rusts. *In* Soils and Environment: Soil Processes from Mineral to Landscape Scale. Auerswald K, Stanjek H, Bigham JM (Eds) Adv Geoecol 30:345-372, Reiskirchen, Catena Verlag

Linnaeus C (1735) Systema Natural XII, vol. 111, Gen 52:11

Lizalek NA, Filatov VF (1986) Geology and origin of aluminites of Siberia. Sov Geol, p 41-49

Lizalek NA, Ivlev NF, Madaras A, and Speshilova MA (1989) The Namana occurrence of secondary sulfates in Yakutia [USSR]. Sov Geol, p 46-52.

Long DT, Fegan NE, McKee JD, Lyons WB, Hines ME and Macumber PG (1992) Formation of alunite, jarosite and hydrous iron oxides in a hypersaline lake system: Lake Tyrrell, Victoria, Australia. Chem Geol 96:183-202

Losno R, Colin JL, Le Bris N, Bergametti G, Jickells T, Lim B (1993) Aluminum solubility in rainwater and molten snow. J Atmosph Chem 17:29-43

Lukovic SM (1970) Weathering processes and formation of secondary aluminite and gibbsite in boehmite-kaolin bauxite of Montenegro, Yugoslavia. Zb Rad Rud-Geol Fak, Univ Beogradu 11-12:55-63

Luther GW II (1990) The frontier-molecular-orbital theory approach in geotechnical processes. *In* Aquatic chemical kinetics. W Stumm (Ed) John Wiley and Sons, Inc., New York, p 173-198

Lyon JS, Hilliard TJ, Bethell TN (1993) Burden of Guilt. Mineral Policy Center, Washington, DC, 68 p

Mamedov AI, Makhmudov SA, Babaev IA (1969) Aluminite from the Kelbadzhar area (Azerbaidzhan SSR). Uch Zap Aerb Gos Univ, Ser Geol-Geogr Nauk, p 136-142

Mazilov VN, Kashik SA, Kashaeva GM (1975) First finding of meta-aluminite in the USSR. Zap Vses Mineral Obshch 104:202-203

Margulis EV, Savchenko LA, Shokarev MM, Beisekeeva LI, Vershinina FI (1975) The amorphous basic sulphate $2Fe_2O_3 \cdot SO_3 \cdot mH_2O$. Russ J Inorg Chem 20:1045-1048

Margulis EV, Getskin LS, Zapuskalova NA, Beisekeeva LI (1976) Hydrolytic precipitation of iron in the $Fe_2(SO_4)_3$--KOH--H_2O system. Russ J Inorg Chem 21:996-999

Mast MA, Verplanck PL, Yager DB, Wright WG, Bove DJ. (2000) Natural sources of metals to surface waters in the upper Animas River watershed, Colorado. ICARD 2000, Proc. 5th Internat Conf Acid Rock Drainage, Vol. 1. Soc Mining Metall Explor, Littleton, CO, p 513-522

Matijevic E, Janauer GE (1966) Coagulation and reversal of charge of lyophobic colloids by hydrolyzed metal ions. II. Ferric nitrate. J Colloid Interface Sci 21:197-223

Matijevic E, Sapieszko RS, Melville JR (1975) Ferric hydrous oxide sols I. Monodispersed basic iron (III) sulfate particles. J Colloid Interface Sci 50:567-581

Matsubara S, Kato A, Hashimoto E (1990) Basaluminite in fissure of the Takanuki metamorphic rocks, [Fukushima prefecture], northeast Japan. Chigaku Kenkyu 39:165-169

May HM, Nordstrom DK (1991) Assessing the solubilities and reaction kinetics of aluminous minerals in soils. *In* Soil Acidity. Ulrich B, Sumner ME (Eds) Springer-Verlag, Berlin, p 125-148

McKibben MA, Barnes HL (1986) Oxidation of pyrite in low temperature acidic solutions: Rate laws and surface textures. Geochim Cosmochim Acta 50:1509-1520

McKnight DM, Bencala KE (1989) Reactive iron transport in an acidic mountain stream in Summit County, Colorado: A hydrologic perspective. Geochim Cosmochim Acta 53:2225-2234

McKnight DM, Kimball BA, Bencala KE (1988) Iron photoreduction and oxidation in an acidic mountain stream. Science 240:637-640

Merwin HE, Posnjak E (1937) Sulphate encrustations in the Copper Queen mine, Bisbee, Arizona. Am Mineral 22:567-571

Milnes AR, Fitzpatrick RW, Self PG, Fordham AW, McClure SG (1992) Natural iron precipitates in a mine retention pond near Jabiru, Northern Territory, Australia. *In* Biomineralization Processes of Iron and Manganese—Modern and Ancient Environments. Skinner HCW, Fitzpatrick RW (Eds) Catena Supplement 21:233-261, Cremlingen-Destedt

Minikawa T, Inaba S, Tamura Y (1996) A few occurrences of basaluminite in Japan. Chigaku Kenkyu 44:193-197

Monterroso C, Alvarez E, Macias F (1994) Speciation and solubility control of Al and Fe in minesoil solutions. Sci Total Environ 158:31-43

Moore JN and Luoma SN (1990) Hazardous wastes from large-scale metal extraction: A case study. Environ Sci Technol 24:1278-1285

Morris RV, Golden DC, Bell JF III, Shelfer TD, Scheinost AC, Hinman NW, Furniss G, Mertzman SA, Bishop J, Ming DW, Allen CC, Britt DT (2000) Mineralogy, composition, and alteration of Mars Pathfinder rocks and soils: Evidence from multispectral, elemental, and magnetic data on terrestrial analogue, SNC meteorite, and Pathfinder samples. J Geophys Res 105:1757-1817

Morton WE, Dunnette DA (1994) Health effects of environmental arsenic. *In* Arsenic in the Environment. Part II: Human Health and Ecosystem Effects. Nriagu JO (Ed) John Wiley, New York, p 17-34

Murad E (1988a) The Mössbauer spectrum of "well" crystallized ferrihydrie. J Magnet Magnetic Mat 74: 155-157.

Murad E (1988b) Properties and behavior of iron oxides as determined by Mössbauer spectroscopy. *In* Iron in Soils and Clay Minerals. Stucki JW, Goodman BA, Schwertmann U (Eds) NATO Am Soils Inst Series C 217:309-350, D. Reidel, Dordrecht

Murad E, Bowen LH, Long GJ, Quin TG (1988) The influence of crystallinity on magnetic ordering in natural ferrihydrites. Clay Minerals 23:161-173

Murad E, Bigham JM, Bowen LH, Schwertmann U (1990) Magnetic properties of iron oxides produced by bacterial oxidation of Fe^{2+} under acid conditions. Hyperfine Interactions 58:2373-2376

Murad E, Schwertmann U, Bigham JM, Carlson L (1994) The mineralogical characteristics of poorly crystalline precipitates formed by oxidation of Fe^{2+} in acid sulfate waters. *In* The Environmental Geochemistry of Sulfide Oxidation. Alpers CN, Blowes DW (Eds) Am Chem Soc Symp Series 550: 190-200

Naumann CF (1855) Elemente der Mineralogie, 4 Aufl. V.W. Engelmann, Leipzig.

Neal C (1988) Aluminum solubility relationships in acid waters–A practical example of the need for a radical reappraisal. J Hydrol 194:141-159

Ninteman DJ (1978) Spontaneous Oxidation and Combustion of Sulfide Ores in Underground Mines, a Literature Survey. US Bur Mines Inf Circ 8775

Nordstrom D K (1982a) Aqueous pyrite oxidation and the consequent formation of secondary iron minerals. *In* Acid Sulfate Weathering. Kittrick JA, Fanning DS, Hossner LR (Eds) Soil Sci Soc Am Spec Publ 10:37-56

Nordstrom DK (1982b) The effect of sulfate on aluminum concentrations in natural waters: some stability relations in the system Al_2O_3-SO_3-H_2O at 298 K. Geochim Cosmochim Acta 46:681-692

Nordstrom DK (1991) Chemical modeling of acid mine waters in the western United States. US Geol Survey Water Res Invest Rep No 91-4034:534-538

Nordstrom DK (2000) Advances in the hydrogeochemistry and microbiology of acid mine waters. Internat Geol Rev 42:499-515

Nordstrom DK, Alpers CN (1999). Geochemistry of acid mine waters. *In* The Environmental Geochemistry of Mineral Deposits. Part A. Processes, methods and health issues. Plumlee GS, Logsdon MJ (Eds) Rev Econ Geol 6A:133-160

Nordstrom DK, Ball JW (1986) The geochemical behavior of aluminum in acidified surface waters. Science 232:54-56

Nordstrom DK, Ball JW (1989) Mineral saturation states in natural waters and their sensitivity to thermodynamic and analytic errors. Sci Gé ol Bull 42:269-280

Nordstrom DK, May HM (1996) Aqueous equilibrium data for mononuclear aluminum species. *In* The Environmental Chemistry of Aluminum. Sposito G (Ed) 2nd edition. CRC Press/Lewis Publishers, Boca Raton, Florida, p 39-80

Nordstrom DK, Munoz JL (1994) Geochemical Thermodynamics, 2nd edition. Blackwell Science, Boston

Nordstrom DK, Southam G (1997) Geomicrobiology of sulfide mineral oxidation. *In* Geomicrobiology: Interactions between Microbes andMinerals. Banfield JF, Nealson KH (Eds) Rev Mineral 35:361-390

Nordstrom DK, Ball JW, Roberson, CE, Hanshaw BB (1984) The effect of sulfate on aluminum concentrations in natural waters. II. Field occurrences and identification of aluminum hydroxysulfate precipitates. Proc Geol Soc Am Ann Mtg 16:611

Nordstrom DK, Plummer LN, Langmuir D, Busenberg E, May HM, Jones BF, Parkhurst DL (1990) Revised chemical equilibrium data for major water-mineral reactions and their limitations. *In* Chemical Modeling of Aqueous Systems II. Melchior DC, Bassett RL (Eds) Am Chem Soc Symp Series 416:398-413

Nordstrom DK, Carson-Foscz V, Oreskes N (1995) Rare earth element (REE) fractionation during acidic weathering of San Juan tuff, Colorado. Proc Geol Soc Am Ann Mtg, New Orleans, p A-199 (abstr)

Nordstrom DK, Ball JW, Southam G, Donald R (1997) Biogeochemistry of natural elemental sulur oxidation and derivative acidic waters at Brimstone Basin, Yellowstone National Park, Wyoming: I. Chemical and isotopic results.

Nordstrom DK, Ball JW, McClesky RB (2000) On the interpretation of saturation indices for iron colloids in acid mine waters. Abstracts with Programs Geol Soc Am Ann Mtg, p A-78

Olson GJ (1991) Rate of pyrite bioleaching by *Thiobacillus ferrooxidans*: Results of an interlaboratory comparison. Appl Environ Microbiol 57:642-644

Öborn I, Berggren D (1995). Characterization of jarosite-natrojarosite in two northern Scandinavian soils. Geoderma 66:213-225

Oycollonov VN, Dolinina YV, Ogovodova LP, Sokolov VN (1994) Aluminite from the oxidation zone of sulfide-poor silver ore deposit. Vestn Mosk Univ Ser 4 Geol, p 58-61

Palache C, Berman H, Frondel C (1951) The System of Mineralogy, Vol. 2. John Wiley and Sons, New York

Papassiopi N, Stefanakis M, Kontopoulos A (1988) Removal of arsenic from solutions by precipitation as ferric arsenates. *In* Arsenic Metallurgy Fundamentals and Applications. Reddy RG, Hendrix JL, Queneau PB (Eds) Symp Proc TMS-AIME Ann Mtg, Phoenix, AZ, p 321-334

Parfitt RL, Smart R StC (1978) The mechanism of sulfate adsorption on iron oxides. Soil Sci Soc Am J 42:48-50

Parks GA (1965) The isoelectric points of solid oxides, solid hydroxides, and aqueous hydroxo complex systems. Chem Rev 65:177-198

Parks GA (1967) Aqueous surface chemistry of oxides and complex oxide minerals. *In* Equilibrium Concepts in Natural Water Systems. Stumm W (Ed) Am Chem Soc. Adv Chem Series 67:121-160

Peak D, Ford RG, Sparks DL (1999) An *in situ* ATR-FTIR investigation of sulfate bonding mechanisms on goethite. J Colloid Inter Sci 218:289-299

Persson P, Lövgren L (1996) Potentiometric and spectroscopic studies of sulfate complexation at the goethite–water interface. Geochim Cosmochim Acta 60:2789-2799

Peine A, Tritschler A, Küsel K, Peiffer S (2000) Electron flow in an iron-rich acidic sediment–evidence for an acidity-driven iron cycle. Limnol Oceanogr 45:1077-1087

Pierce ML, Moore CB (1982) Adsorption of arsenite and aresenate on amorphous iron hydroxide. Water Res 16:1247-1253

Plumlee GS, Smith KS, Montour MR, Ficklin WS, Mosier E (1999) Geologic controls on the composition of natural waters and mine waters draining diverse mineral-deposit types. *In* The Environmental Geochemistry of Mineral Deposits. Part B. Case studies and research topics. Filipek LH, Plumlee GS (Eds) Rev Econ Geol 6B:373-432

Polyak VJ, Provencio P (1998) Hydrobasaluminite and aluminite in caves of the Guadalupe Mountains, New Mexico. J Cave Karst Stud 60:51-57

Pons LJ (1973) Outline of the genesis, characteristics, classification and improvement of acid sulphate soils. *In* Acid Sulphate Soils. Dost H (Ed) Proc 1st Internat Symp Land Reclamation Institute Publ 18, 1:3-27, Wageningen, The Netherlands

Posey HH, Renkin ML, Woodling J (2000) Natural acidic drainage in the upper Alamosa River watershed, Colorado. ICARD 2000 Proc 5th Internat Conf Acid Rock Drainage 1:485-498 Soc Mining Metall Explor, Littleton, CO

Posnjak E, Merwin HE (1922) The system Fe_2O_3-SO_3-H_2O. J Am Chem Soc 44:1965-1994

Powers DA, Rossman GR, Schugar HJ, Gray HB (1975) Magnetic behavior and infrared spectra of jarosite, basic iron sulfate, and their chromate analogs. J Solid State Chem 13:1-13

Rampe JJ, Runnells DD (1989) Contamination of water and sediment in a desert stream by metals from an abandoned gold mine and mill, Eureka District, Arizona, U.S.A. Appl Geochem 4:445-454

Raven KP, Jain A, Loeppert RH (1998) Arsenite and arsenate adsorption on ferrihydrite: kinetics, equilibrium, and adsorption envelopes. Environ Sci. Technol 32:344-349

Rawlings EE, Tributsch H, Hansford GS (1999) Reasons why *'Leptospirillum'*-like species rather than Thiobacillus ferrooxidans are the dominant iron-oxidizing bacteria in many commercial processes for the biooxidation of pyrite and related ores. Microbiol 145:5-13

Raymahashay BC (1968) A geochemical study of rock alteration by hot springs in the Paint Pot Hill area, Yellowstone Park. Geochim Cosmochim Acta 32:499-522

Rieder RT, Ecomomou T, Wanke H, Turkevich A, Crisp J, Bruckner J, Drebus G, McSween HY Jr (1997) The chemical composition of Martian soil and rock returned by the mobile alpha proton X-ray spectrometer: Preliminary results from the x-ray mode. Science 278:1771-1774

Ritchie AIM (1994) The waste-rock environment. *In* The Environmental Geochemistry of Sulfide Mine-Wastes. Jambor JL, Blowes DW (Eds) Mineral Assoc Canada Short Course 22:131-161

Robbins EI, Cravotta CA III, Savela CE, Nord GL Jr (1999) Hydrobiogeochemical interactions in 'anoxic' limestone drains for neutralization of acidic mine drainage. Fuel 78:259-270

Robins, RG (1990) The stability and solubility of ferric arsenate: An update. *In* EPD Congress, Gaskell DR (Ed) TMS Ann Mtg, Feb 18-22, 1990, Anaheim, California, p 93

Robins RG, Huang JCY, Nishimura T, Khoe GH (1988) The adsorption of arsenate ion by ferric hydroxide. *In* Arsenic Metallurgy: Fundamentals and Applications. Reddy RG, Hendrix JL, Queneau PB (Eds) Symp Proc TMS-AIME Ann Mtg, Phoenix, AZ, p 99-112

Romberg IB (1969) Lepidocrocite at Rossvatn, north-Norway, an example of pseudomorphism after pyrite cubes. Norsk Geol Tidsskr 49:251-256

Rose AW, Cravotta CA III (1998) Geochemistry of coal mine drainage. p 1-1 to 1-22. *In* Coal Mine Drainage Prediction and Prevention in Pennsylvania. Brady KBC, Smith MW, Schueck J (Eds) Pennsylvania Dept Environ Protection, Harrisburg, PA

Rose S, Ghazi AM (1997) Release of sorbed sulfate from iron oxyhydroxides precipitated from acid mine drainage associated with coal mining. Environ Sci Technol 31:2136-2140

Rose S, Elliott WC (2000) The effects of pH regulation upon the release of sulfate from ferric precipitates formed in acid mine drainage. Appl Geochem 15: 27-34

Ross (1972) Inorganic Infrared and Raman Spectra. McGraw-Hill, New York

Rost R (1937) The minerals forming on burning coal heaps in the coal basin of Kladno. Bull Internat Acad Sci Bohême 1937:1-7

Rothenhofer P, Sahin H, Peiffer S (1999) Attenuation of heavy metals and sulfate by aluminum precipitates in acid mine drainage. Acta Hydrochim Hydrobiol 28:136-144

Rowe GL Jr, Ohsawa S, Takano B, Brantley SL, Fernandez JF, Barquero J (1992) Using crater lake chemistry to predict volcanic activity at Poas Volcano, Costa Rica. Bull Volcanol 54:494-503

Rubin AJ (Ed) (1974) Aqueous-Environmental Chemistry of Metals. Ann Arbor Science, Ann Arbor, Michigan.

Runnells DD, Shepherd TA, Angino EE (1992) Estimation of natural background concentrations of metals in water in mineralized regions after disturbance by mining. Environ Sci Technol 26:2316-2323

Ruotsala AP, Babcock LL (1977) Zaherite, a new hydrated aluminum sulfate. Am Mineral 62:1125-1128

Sabelli C (1984) On the mineralogy of the Cetine mine of Cotorniano: The sulfate dimorphs jurbanite and rostite. Per Mineral (Roma), p 53-65

Sabelli C (1985) Refinement of the crystal structure of jurbanite, $Al(SO_4)(OH)\cdot 5H_2O$. Z Kristallogr 173:33-39

Sand W, Rhode K, Zenneck C (1992) Evaluation of *Leptospirillum ferrooxidans* for leaching. Appl Environ Microbiol 58:85-92

Scheinost AC, Schwertmann U (1999) Color identification of iron oxide and hydroxysulfates: Use and limitations. Soil Sci Soc Am J 63:1463-1471

Scheinost AC, Chavernas A, Barrón V, Torrent J (1998) Use and limitations of second-derivative diffuse reflectance spectroscopy in the visible to near-infrared range to identify and quantify Fe oxide minerals in soils. Clays Clay Minerals 46:528-536

Schemel LE, Kimball BA, Bencala KE (2000) Colloid formation and metal transport through two mixing zones affected by acid mine drainage near Silverton, Colorado. Appl Geochem 15:1003-1018

Schrenk MO, Edwards KJ, Goodman RM, Hamers RJ, Banfield JF (1998) Distribution of *Thiobacillus ferrooxidans* and *Leptospirillum ferrooxidans*: Implications for generation of acid mine drainage. Science 279:1519-1522

Schulze DG (1981) Identification of soil iron oxide minerals by differential x-ray diffraction. Soil Sci Soc Am J 45:437-440

Schultze-Lam S, Fortin D, Davis BS, Beveridge TJ (1996) Mineralization of bacterial surfaces. Chem Geol 132:171-181

Schwertmann U (1961) Über das Vorkommen und die Enstehung von Jarosit in Marschboden (Maibolt). Naturwiss 45:159-160

Schwertmann U (1964) Differenzierung der Eisenoxide des Bodens durch Extraktion mit Ammoniumoxalat-Lösung. Z Pflanzenern. Bodenkunde 105:194-202

Schwertmann U (1993) Relations between iron oxides, soil color, and soil formation. *In* Soil color. Bigham JM, Ciokosz EJ (Eds) Soil Sci Soc Am Spec Publ No 31:51-69, Soil Sci Soc Am, Madison, Wisconsin

Schwertmann U, Taylor RM (1989) Iron oxides. *In* Minerals in Soil Environments. 2nd edition. Dixon JB, Weed SB (Eds) Soil Sci Soc Am, Madison, Wisconsin

Schwertmann U, Thalmann H (1976) The influence of [Fe (II)], [Si], and pH on the formation of lepidocrocite and ferrihydrite during oxidation of aqueous $FeCl_2$ solutions. Clay Minerals 11:189-200

Schwertmann U, Fechter H (1994) The formation of green rust and its transformation to lepidocrocite. Clay Minerals 29:87-92

Schwertmann U, Fojt B (1996) Schwertmannit–ein neues Mineral und seine Geschichte. Lapis, p 33-34

Schwertmann U, Bigham JM, Murad E (1995) The first occurrence of schwertmannite in a natural stream environment. Eur J Mineral 7:547-552

Singer PC, Stumm W (1968) Kinetics of the oxidation of ferrous iron. 2nd Symp Coal Mine Drainage Res National Coal Assoc Bitum Coal Res, p 12-34

Singer PC, Stumm W (1970) Acid mine drainage: The rate-determining step. Science 167:1121-1123

Singh B, Harris PJ, Wilson MJ (1997). Geochemistry of acid mine waters and the role of micro-organisms in such environments: a review. *In* Soils and Environment: Soil Processes from Mineral to Landscape

Scale. Auerswald K, Stanjek H, Bigham JM (Eds) Adv Geoecol 30:159-192, Reiskirchen, Catena Verlag
Singh SS (1982) The formation and coexistence of gibbsite, boehmite, alumina and alunite at room temperature. Can J Soil Sci 62:327-332
Sizia R (1966) Infrared spectra of some sulfates. Rend Semin Fac Sci Univ Cagliari 36:82-91
Smith KS (1991) Factors Influencing Metal Sorption onto Iron-Rich Sediment in Acid-Mine Drainage. PhD thesis T-3925, Colorado School of Mines, Golden, Colorado
Smith KS (1999) Metal sorption on mineral surfaces: An overview with examples relating to mineral deposits. *In* The Environmental Geochemistry of Mineral Deposits. Part A. Processes, methods and health issues. Plumlee GS, Logsdon MJ (Eds) Rev Econ Geol 6A:161-182
Sokolov PN, Korobov YI, Kosukhina IG, Kolotova LV (1985) Mineralogy of water-soluble sulfates in the Namansk manifestation of aluminite (Yakutsk ASSR). Morfol Genezis Zakonomern Razmeshcheniya Mineral Obraz Altae-Sayan Skladchatoi Obl Sib Platformy, p 120-124
Sposito G (1984) The Surface Chemistry of Soils. Oxford Univ Press, New York
Steefel CI, van Cappellen P (1990) A new kinetic approach to modeling water-rock interaction: the role of nucleation, precursors, and Ostwald ripening. Geochim Cosmochim Acta 54:2657-2677
Stumm W (1992) Chemistry of the Solid-Water Interface: Processes at the Mineral-Water and Particle-Water Interface in Natural Systems. John Wiley, New York
Sullivan PJ, Yelton JL, Reddy KJ (1988a). Solubility relationships of aluminum and iron minerals associated with acid mine drainage. Environ Geol Water Sci 11:283-287
Sullivan PJ, Yelton JL, Reddy KJ (1988b). Iron sulfide oxidation and the chemistry of acid generation. Environ Geol Water Sci 11:289-295
Swayze GA, Smith KS, Clark RN, Sutley SJ, Pearson RM, Vance JS, Hageman PL, Briggs PH, Meier AL, Singleton MJ, Roth S (2000) Using imaging spectroscopy to map acidic mine waste. Environ Sci Techno 34:47-54
Takano M, Shinjo T, Kiyama M, Takada T (1968) Magnetic properties of jarosites, $RFe_3(OH)_6(SO_4)_2$ (R = NH_4, Na or K). J Phys Soc Japan 25:902
Taylor RM and Schwertmann U (1978) The influence of aluminum on iron oxides. Part I. The influence of Al on Fe oxide formation from the Fe(II) system. Clays Clay Minerals 26:373-383
Theobald PK, Lakin HW, Hawkins DB (1963) The precipitation of aluminum, iron, and manganese at the junction of Deer Creek with the Snake River in Summit County, Colorado. Geochim Cosmochim Acta 27:121-132
Tien P-L (1968) Hydrobasaluminite and basaluminite in Cabaniss Formation (Middle Pennsylvanian), southeastern Kansas. Am Mineral 53:722-732
Tkachenko RI, Zotov AV (1982) Ultra-acidic therms of volcanic origin as mineralizing solutions. *In* Hydrothermal Mineral-Forming Solutions in the Areas of Active Volcanism. Naboko SI (Ed) Nauka Publishers, Novosibirsk, p 126-131
Toth A, Gecse E, Popity J (1984) Aluminite and basaluminite in the bauxite of Csordakut [Hungary]. Magy All Foldt Intez. Evi Jel 1982:423-430
Trafford BD, Bloomfield C, Kelso WI, Pruden G (1973) Ochre formation in field drains in pyritic soils. J Soil Sci 24:453-460
Trolard F, Génin J-MR, Abdelmoula M, Bourrié Humbert B, Herbillon A (1997) Identification of a green rust mineral in a reductomorphic soil by Mössbauer and Raman spectroscopies. Geochim Cosmochim Acta 61:1107-1111
Tuovinen OH, Bhatti TM, Bigham JM, Hallberg KB, Garcia O Jr, Lindström EB (1994) Oxidative dissolution of arsenopyrite by mesophilic and moderately thermophilic acidophiles. Appl Environ Microbiol 60:3268-3274
Urrutia MM, Beveridge TJ (1995) Formation of short-range ordered aluminosilicates in the presence of a bacterial surface (Bacillus subtilis) and organic ligands. Geoderma 65:149-165
Van Breemen N (1973) Dissolved aluminum in acid sulfate soils and in acid mine waters. Soil Sci Soc Am Proc 37:694-697
Van Breemen N (1976) Genesis and solution chemistry of acid sulfate soils in Thailand. Agric Res Rep 848, PhD thesis, Wageningen Univ, The Netherlands
Van Breeman N (1980) Acid sulphate soils. *In* Land Reclamation and Water Management. ILRI Publ 27, Wageningen, The Netherlands, p 53-57
Van Breemen N, Harmsen K (1975) Translocation of iron in acid sulfate soils: I. Soil morphology, and the chemistry and mineralogy of iron in a chronosequence of acid sulfate soils. Soil Sci Soc Am Proc 39:1140-1148
Van Mensvoort MEF, Dent DL (1998) Acid Sulfate Soils. *In* Lal R, Blum WH, Valentine C, Stewart BA (Eds) Methods for assessment of soil degradation. Advances in Soil Science, CRC Press, Boca Raton, p 301-335

Van'shin YV, Gutsaki VA (1982) Occurrence of aluminum minerals in the lower Volga River region. Dokl Akad Nauk SSSR 262:160-162

Warren LA, Ferris FG (1998) Continuum between sorption and precipitation of Fe(III) on microbial surfaces. Environ Sci Technol 32:2331-2337

Waychunas GA, Rea BA, Fuller CC, Davis JA (1993) Surface chemistry of ferrihydrite: Part I. EXAFS studies of the geometry of coprecipitated and adsorbed arsenate. Geochim Cosmochim Acta 57:251-2269

Waychunas GA, Xu N, Fuller CC, Davis, JA, Bigham JM (1995) XAS study of AsO_4^{3-} and SeO_4^{2-} substituted schwertmannites. Physica B 208/209:481-483

Webster JG, Nordstrom DK, Smith KS (1994) Transport and natural attenuation of Cu, Zn, As, and Fe in the acid mine drainage of Leviathan and Bryant Creeks. *In* The environmental geochemistry of sulfide oxidation, Alpers CN, Blowes DW (Eds) Am Chem Soc Symp Series 550:244-260

Webster JG, Swedlund PJ, Webster KS (1998). Trace metal adsorption onto an acid mine drainage(III) oxy-hydroxy sulfate. Environ Sci Technol 32:1361-1368

Westerveld GJW, van Holst AF (1973) Detailed survey and its application in areas with actual and potential acid sulphate soils in the Netherlands. p 243-262. *In* Acid Sulphate Soils. Dost H (Ed) Proc 1st Internat Symp Land Reclamation Institute Publ 18, 1:243-262, Wageningen, The Netherlands

Wieder RK (1994) Diel changes in iron(III)/iron(II) in effluent from constructed acid mine drainage treatment wetlands. J Environ Qual 23:730-738

Weiser HB, Milligan WO, Purcell WR (1941) Composition of floc formed at pH values below 5.5. Ind Eng Chem 33:669-672

Wieser T (1974) Basaluminite in the weathering zone of Carpathian Flysch deposits. Mineral Pol 5:55-66

Williamson MA, Rimstidt JD (1993) The rate of decomposition of ferric-thiosulfate complex in acidic aqueous solutions. Geochim Cosmochim. Acta 57:3555-3561

Wilmot RD, Young B (1985) Alunite and other aluminum minerals from Newhaven, Sussex. Proc Geol Assoc 96:47-52

Winland RL, Traina SJ, Bigham JM (1991) Chemical composition of ochreous precipitates from Ohio coal mine drainage. J Environ Qual 20:452-460

Wright LT (1906) Controlling and extinguishing fires in pyritous mines. Eng Mining J 81:171-172

Xu Y, Schoonen MAA (1995) The stability of thiosulfate in the presence of pyrite in low-temperature aqueous solutions. Geochim Cosmochim Acta 59:4605-4622

Yager DB, Mast MA, Verplanck PL, Bove DJ, Wright WG, Hageman PL (2000) Natural versus mining-related water quality degradation to tributaries draining Mount Moly, Silverton, Colorado. ICARD 2000 Proc 5th Internat Conf Acid Rock Drainage 1:535-550. Soc Mining Metall Explor, Littleton, CO

Yu J-Y, Heo B, Cho I-K, Chang H-W (1999) Apparent solubilities of schwertmannite and ferrihydrite in natural stream waters polluted by mine drainage. Geochim Cosmochim Acta 63:3407-3416

Zalba PE (1982) Scanning electron micrographs of clay deposits of Buenos Aires Province, Argentina. Dev Sedimentol 35th Internat Clay Conf 1981:513-528

Zazubina IS, Ankinovich EA(1982) Basaluminite from black-schist strata of northwestern Karatau Vopr Metall Strukt Osob Veshchestv Sostava Mestorozhd Kaz, p 3-8

Zhdanov Y, Solov'ev LI (1998) Geology and mineralogical composition of the oxidized zone in the Deputatsk tin ore deposit. Otechestvennaya Geol, p 77-79

Zodrow FL and McCandlish K (1978) Hydrated sulfates in the Sydney coalfield, Cape Breton, Nova Scotia. Can Mineral 16:17-22